Communications of the LUNAR AND PLANETARY LABORATORY

Volume 2 Numbers 31–35

THE UNIVERSITY OF ARIZONA

1964

Communications of the Lunar and Planetary Laboratory

These *Communications* contain the shorter publications and reports by the staff of the Lunar and Planetary Laboratory. They may be either original contributions, reprints of articles published in professional journals, preliminary reports, or announcements. Tabular material too bulky or specialized for regular journals is included if future use of such material appears to warrant it. The *Communications* are issued as separate numbers, but they are paged and indexed by volumes.

The *Communications* are mailed to observatories and to laboratories known to be engaged in planetary, interplanetary or geophysical research in exchange for their reports and publications. The University of Arizona Press can supply at cost copies to other libraries and interested persons.

The University of Arizona
Tucson, Arizona

GERARD P. KUIPER, *Director*
Lunar and Planetary Laboratory

Published with the support of the National Aeronautics and Space Administration

Library of Congress Catalog Number 62-63619

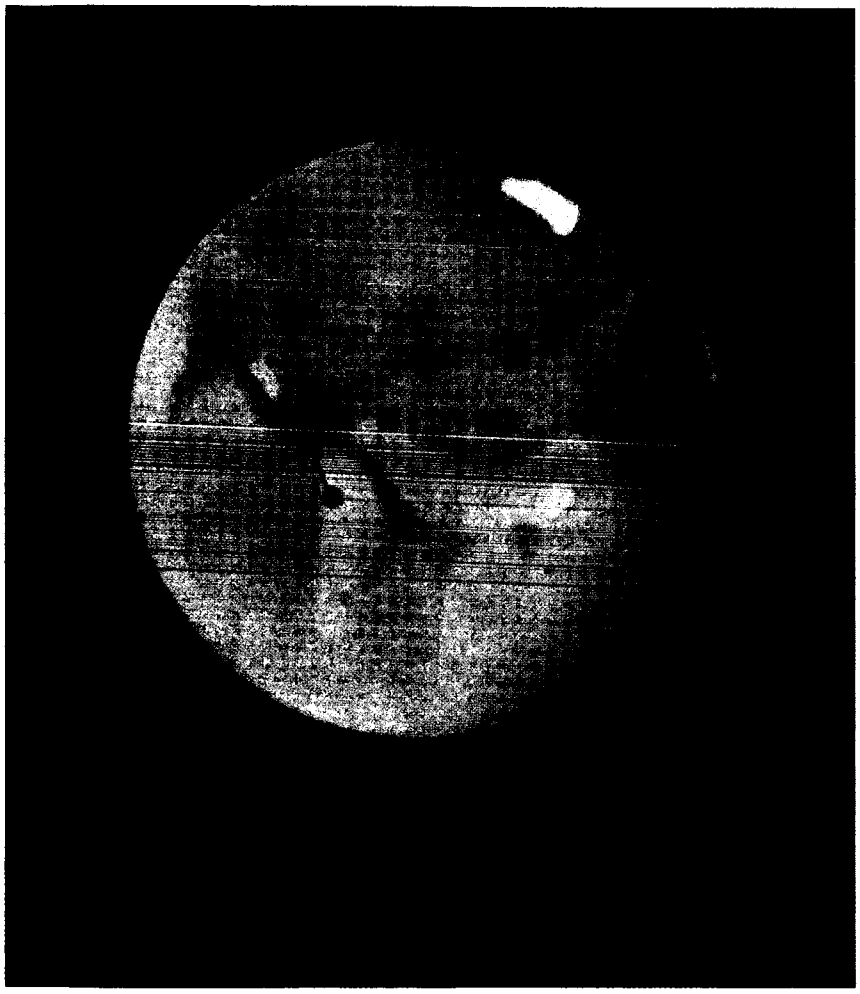

MARS

Reproduction of Mars drawing in pastel by E. M. Antionadi, 83 cm refractor, Meudon, Paris, 1909, October 11, $\omega = 76°$; presented to Professor E. E. Barnard of Yerkes Observatory, University of Chicago, late 1909; reproduced by permission of Miss M. R. Calvert.

NO. 31. INFRARED SPECTRA OF STARS AND PLANETS, IV: THE SPECTRUM OF MARS, 1-2.5 MICRONS, AND THE STRUCTURE OF ITS ATMOSPHERE*

by GERARD P. KUIPER

July 4, 1964

ABSTRACT

Spectra of the planet Mars obtained from the 82″ telescope of the McDonald Observatory are presented for the interval 1-2.5μ, together with lunar comparisons and a limited set of laboratory calibrations. A full discussion of the CO_2 content of the Martian atmosphere and the surface pressure is given in the following two *Communications*. In this paper the IR spectra are examined for the presence of constituents other than CO_2 (CO, CH_4, NH_3, H_2S, NO, N_2O, HCHO, and COS), and for the presence of isotopic bands of CO_2. The O^{18} isotopic band at λ 2.15μ is definitely present in the Martian spectra and allows a provisional determination of the O^{18}/O^{16} ratio relative to the Earth. The evidence is strong, though not yet conclusive, that this ratio is larger on Mars than on the Earth. The other gases listed are all below the threshold of detection, with the upper limits found given in the text. The Martian spectral intensities are also expressed in terms of those derived for the Moon; the ratio spectra so obtained for Mars are summarized in Figure 25. In the introductory parts of the paper a discussion is given of the types of atmospheric particles detected in the Martian atmosphere and the information that may be derived therefrom. A rough value of the atmospheric pressure 10-20 mb is thus derived.

1. The Martian Atmosphere

The *presence* of a Martian atmosphere is shown by several well-known phenomena among which are: The variable and often local obscuration of surface detail; the variable appearance of the limb, including the occasional presence of clouds; the presence and seasonal variations of the polar caps and associated cloud phenomena; the occasional occurrence of white clouds and of yellow dust storms on the disk; the general veil observed in blue and ultraviolet light; and irregular polarization changes, correlated with the presence of varying haze. Two gases, CO_2 and H_2O, have been detected spectroscopically.

The *density* of this atmosphere has been uncertain. It has been widely held that a fair estimate was at hand from the interpretation of visual polarization measurements, notably by A. Dollfus. On the basis of all published data, de Vaucouleurs (1954, p. 125) concluded that the atmospheric surface pressure is 64 $\pm$ 3 mm or 85 $\pm$ 4 millibars (corresponding to an atmospheric mass of 0.20 terrestrial atmospheres or 1.6 $\times$ 10^5 cm NPT). Dollfus (1961, p. 387) similarly concluded that the pressure is near 90 millibars. This result, by the nature of its derivation, must actually be an *upper limit*. The violet layer that at all times surrounds the planet has been interpreted as due to particles because of its variable opacity

*Paper presented in outline at NASA Conference, Washington, D.C., October 1-2, 1963. The IR spectra were reviewed at the Liège Conference on Astrophysics, June 24-26, 1963 (Kuiper 1963).

near $\lambda = 0.45\ \mu$ (e.g., de Vaucouleurs, 1954, p. 55); and these particles must scatter in visual light also in a manner that would make it difficult to distinguish them from molecules.

We shall first examine what may be derived regarding the density of the Martian atmosphere from the presence of atmospheric particles and thereafter, from infrared spectroscopy.

2. *Atmospheric Particles: the Blue-Violet Haze*

The geometric albedo of Mars (measuring the brightness at opposition) is 0.154 in visual light ($\lambda = 0.554\ \mu$; Harris, 1961, p. 307) and 0.052 in the accessible ultraviolet (Harris, *loc. cit.;* effective wavelength: 0.353 μ). From the center-to-limb effect it may be estimated that the *atmospheric* contribution to the visual albedo does not exceed 0.02-0.03, whereas the absence of surface detail in the UV indicates that the atmospheric contribution to the UV albedo is 0.04 ± 0.01.

Dollfus's visual polarization data have been interpreted as due to an air mass of 0.2 terrestrial atmospheres in a vertical column, or 0.4 atm for the integrated disk. Since the back scattering of a tenuous gaseous atmosphere is $\frac{3}{8}\ \tau$, and at $\lambda = 0.55\ \mu$ the value of τ for the terrestrial atmosphere is 0.08 (Van de Hulst, 1952, p. 53), the computed atmospheric contribution to the visual albedo would be $\frac{3}{8} \times 0.08 \times 0.4 = 0.012$. The ratio of the assumed atmospheric scattering powers, UV to V, is then $(0.04 \pm 0.01)/0.012 = 3.3 \pm 1$, whereas molecular scattering would make the ratio $(.554/.353)^4 = 6.0$. However, the atmospheric component of the UV albedo cannot be all molecular in origin. The variable transparency of the Martian atmosphere near $\lambda = 0.45\ \mu$ and the spotty appearance of the best violet photographs (Humason, 1961, Plates 3-5) indicate that at the very most half the total UV albedo, or 0.026, can be of molecular origin, reducing the molecular contribution of the visual albedo to $0.026/6 = 0.004$. This reduces the *upper limit of the pressure* of the Martian atmosphere to about *30 millibars* at the very most. UV polarization data discussed below confirm this conclusion. Consistent with this interpretation of the UV albedo is the absence of a marked increase of reflectivity from 0.40 μ to 0.30 μ, noted on low-dispersion spectra taken with the 82-inch telescope. If molecular scattering alone were responsible, the intensity ratio 0.30 μ/0.40 μ relative to the Sun would be 3.2.

The other extreme assumption, that both the entire UV albedo and the visual atmospheric scattering are due to small particles, leads to an estimate of the particle size. If the particles are quartz ($n = 1.5$), a diagram by Van de Hulst (1952, p. 57) and the UV/V scattering ratio of 0.052/0.012 yield $(n\text{-}1)\pi d/\lambda \simeq 1$ for $\lambda = 0.35\ \mu$ and hence, $d = 0.22\ \mu$. If they are ice ($n = 1.31$) the dimension will be about 0.35 μ, in agreement with an earlier estimate made in this manner by Schatzman (1951) and a more complete discussion including Dollfus's visual polarization measures by Kuiper (1952, p. 393). Allowance for the Rayleigh scattering by the molecules and very small particles present, will make d slightly larger than the values stated. The estimate is rough because the differences between the phase functions at 0.35 and 0.55 μ have been neglected.

The Martian haze layer appears on the average to be higher over the tropics than over the polar zones. This follows from the abnormally-large ellipticity of the visual boundary of the planet (compared to the dynamical oblateness, which is well determined), a boundary that visual observation shows to be not the solid surface but *the top of the haze layer.* This observation is consistent with the observed atmospheric optical depth larger than unity for $\lambda \leq 4500$ Å, any possible wavelength dependence of opacity, and the large value of the air mass ($\simeq 40$) on the Martian limb at opposition. The excess height over the equator is about 17 km (Kuiper, 1952, p. 422), a value confirmed by additional measures of the visual oblateness made with the 82-inch telescope in 1956 and 1958. A roughly ellipsoidal haze distribution is to be expected from the thermally-driven convection in analogy with the latitude variation of the terrestrial tropopause level; and the associated vertical distributions of condensation products and dust. [My own observations would indicate that in summer the height of the terrestrial haze layer over continents is about 4-5 km at 30° N (region of McDonald Observatory), 3 km at 35° N (region of Albuquerque, N. M.), 2 km at 43° N (S. Wisconsin), and 0 km at the arctic circle. Above these levels the sky is of "coronographic" quality.]

If the Martian haze particles are ice, they are probably confined to the upper parts of the convective troposphere, where adiabatic cooling of surface air has led to supersaturation of water vapor. Denser clouds, if present, will occur in this same zone. If the particles were dust, they would extend downward with increasing concentration toward the surface. The presence of darker regions in the haze

layer having no correspondence to dark surface markings (Humason, *op. cit.*, Plates 3-5) may then be either thin darker dust clouds rising into the general haze layer or, more likely, veils of different-sized ice particles (see below).

It has sometimes been assumed that the greater strength of the blue veils and clouds toward the Martian limb is due to lower surface temperatures. This assumption is unwarranted. The average limb effect shown on UV photographs corresponds closely to the *secant of the air mass*. This is particularly well seen on Humason's 200-inch photographs which further show that the "lumpy" appearance of the veil is not limited to the limb but extends over the entire disk.

Systematic measurements of the reflectivity and polarization in the UV, coupled with high-resolution photography, can yield information on the *composition of the haze*. Only a few polarization measurements are yet available. They were made by Gehrels with the 82-inch telescope on 10 nights in 1959-61 (Gehrels and Teska, 1962, p. 173). Remarkable changes were detected, not correlated with phase, and therefore presumably due to variable particle size. For instance, at phase angle $\alpha = 43°3$ the polarization at 0.32 μ changed from 1.5% to 9.8% in 7 days (Aug. 22-29, 1960), while at 0.36 μ the polarization was found 0.1% at $\alpha = 43°3$ but 7.6% at $\alpha = 36°1$. *Rayleigh scattering by molecules,* which would cause a monotonic increase of polarization with α and show no time-variations, contributes therefore only *a minor fraction of the observed brightness*. The ever-changing veils and clouds must be largely responsible.

Gehrels' measures may be compared with theoretically-computed values for the above-mentioned alternative models of composition and particle diameter: quartz, $d \cong 0.22\ \mu$; and ice, $d \cong 0.35\ \mu$. I am much indebted to Dr. B. M. Herman of the Institute of Atmospheric Physics for making the computations. They are based on the Mie theory for spherical particles which Dr. Herman programmed for the IBM 7072. The computations yield the scattered intensities I_1 and I_2 in the two principal planes of polarization, from which the total intensities $I_1 + I_2$ and the polarizations, $P = (I_1 - I_2)/(I_1 + I_2)$ have been derived. Table 1 and Figure 1 show the first exploratory results, for quartz and ice (three diameters). The Gehrels measures quoted above were entered in Figure 1 to which was added a value for $\alpha = 35°$ taken from Figure 10 of the Gehrels-Teska paper, derived by a slight extrapolation of a well-defined relationship (to $\lambda^{-1} = 2.9$). It is seen that the Gehrels measures strongly favor *ice composition,* but that a much fuller investigation is warranted.

Figure 2 and Table 2 contain the data for spherical ice particles of 8 different dimensions, also based on Dr. Herman's computations. It is seen that for the smallest particles there is tendency toward alternation between the integral (2.0, 3.0) and half-integral (2.5, 3.5) values of the scattering parameter $2\pi a/\lambda$. If the different Martian veils shown on photographs each have very homogeneous composition in particle size, some very remarkable polarization contrasts may be expected in *high-resolution photography through a birefringent crystal,* provided that the wavelength band of the photography is kept narrow ($\triangle\lambda \simeq 300$ Å). This will be a very promising field of further study.

Presumably there will be some spread in the particle sizes in any one veil and certainly in low-resolution photography or photometry over the Martian disk. Therefore, it is of interest to determine the effect of *mixing* on the resultant polarization. Two types of mixtures are considered here, one of a fairly narrow spread in diameter and one a broader spread that automatically destroys the alternation effect cited above. The results are found in Table 3 and Figure 3. The mixtures are found by assigning the following weights to the 8 parameter values 2.0, 2.5, 3.0 . . . 5.5:

A: 1, 4, 10, 4, 1, 0, 0, 0; B: 0, 0, 1, 4, 10, 4, 1, 0; C: 0, 0, 0, 0, 1, 4, 10, 4 (these emphasize the *integral* values of $2\pi a/\lambda$).

A': 4, 10, 4, 1, 0, 0, 0, 0; B': 0, 1, 4, 10, 4, 1, 0, 0; C': 0, 0, 0, 1, 4, 10, 4, 1 (these emphasize the *half-integral* values).

A'': 2, 7, 10, 7, 2, 0, 0, 0; B'': 0, 0, 2, 7, 10, 7, 2, 0; C'': 0, 0, 0, 0, 2, 7, 10, 7 (these *balance* the integral and half-integral values).

At $\lambda = 0.35\ \mu$ the most frequent diameter is $d = 0.33\ \mu$ for mixtures A and A'', 0.44 μ for B and B'', and 0.56 μ for C and C''. A curve for $2\pi a/\lambda = 8$ is added to Fig. 3*a*. At $\lambda = 0.35\ \mu$ it corresponds to $d = 0.89\ \mu$. Such particles will appear *white* visually and occasional white clouds are seen on the planet.

The polarization curves in Figures 3*a* and 3*b* show that the effect of the alternation is still present, even for these mixtures. If the Martian veils (averaged over the finite areas observed) contain the assumed spread in particle sizes, then only $\alpha < 20°$ will yield interpretable results. For a larger spread, such as is assumed in Figure 3*c*, both $\alpha < 20°$ and $\alpha > 30°$ can be used. For a very small spread the

TABLE 1

Phase Angle	Polarization (%)					Total Intensity				
	A	B	C	D	E	A	B	C	D	E
0°.....	0.0	0.0	0.0	0.0	0.0	0.13722	0.44710	5.0827	0.51121	0.43792
5.....	0.0	— 0.9	— 2.6	— 0.4	— 0.4	0.13522	0.43305	4.8654	0.50547	0.43286
10.....	0.0	— 3.9	—10.6	— 1.6	— 1.6	0.12935	0.39349	4.2863	0.48866	0.41806
15.....	— 0.2	....	—23.8	....	....	0.11995	.....	3.5316	.....	.....
20.....	— 0.7	—16.1	—39.7	— 7.4	— 7.5	0.10762	0.27131	2.8193	0.42723	0.36415
25.....	— 1.9	—23.1	—50.7	—13.0	—13.2	0.09316	0.21303	2.3077	0.38703	0.32907
30.....	— 4.2	—22.5	—47.2	—21.1	—21.7	0.07756	0.17426	2.0377	0.34442	0.29212
35.....	— 8.6	— 4.1	—29.0	—32.7	—33.8	0.06195	0.16627	1.9352	0.30285	0.25643
40.....	—16.0	+27.1	— 4.8	—48.1	—50.0	0.04760	0.19662	1.8703	0.26609	0.22539
45.....	—26.9	+53.8	+19.4	—66.4	—69.0	0.03593	0.26781	1.7413	0.23811	0.20256
50.....	—37.4	+69.9	+42.2	—83.8	—86.5	0.02845	0.37668	1.5380	0.22302	0.19161
55.....	—34.2	+78.4	+62.6	—94.0	—95.6	0.02682	0.51435	1.3494	0.22509	0.19638
60.....	—11.1	+82.6	+72.9	—91.7	—91.6	0.03291	0.66686	1.3071	0.24881	0.22088
180.....	0.0	0.0	0.0	0.0	0.0	8.9902	95.723	830.36	17.589	16.765
					σ_S	.....	1.7109	.....	1.7510	1.6470
					σ_B	.....	9.0694	.....	2.6212	2.2454
					σ_B/σ_S	.....	5.3011	.....	1.4969	1.3633

Polarizations and total intensities ($I_1 + I_2$) for five types of spherical particles all computed for $\lambda = 0.35\mu$: (A) ice ($n = 1.31$), $2\pi a/\lambda = 2.09$, $d = 2a = 0.233\ \mu$; (B) ice, $d = 0.35\ \mu$; (C) ice, $d = 0.525\ \mu$ (D) quartz ($n = 1.50$), $d = 0.22\ \mu$, no absorption; (E) as (D), $K = 0.01$ (weak absorption).

TABLE 2a

Phase Angle	2.0	2.5	3.0	3.5	4.0	4.5	5.0	5.5
0°.....	0.0	0.0	0.0	0.0	0.0	0.0	0.0	0.0
5	+ 0.0	+ 0.2	— 0.1	— 0.8	— 0.7	— 3.2	— 2.4	— 8.9
10	+ 0.1	+ 0.9	— 0.0	— 3.2	— 2.4	—13.2	— 8.7	—36.7
15	+ 0.1	+ 1.9	+ 0.7	— 7.5	— 3.8	—31.2	—14.4	—67.4
20	0.0	+ 3.3	+ 3.4	—14.3	— 2.1	—55.1	—11.9	—40.6
25	— 0.2	+ 5.0	+10.0	—24.4	+ 5.5	—71.2	+ 1.8	+21.2
30	— 0.3	+ 6.7	+22.0	—38.2	+18.7	—54.4	+19.1	+61.0
35	+ 0.6	+ 8.1	+38.2	—54.5	+33.1	— 9.8	+31.9	+81.6
40	+ 5.2	+ 8.8	+54.4	—68.3	+44.4	+33.0	+37.5	+91.0
45	+18.7	+ 8.0	+66.7	—70.0	+50.7	+63.0	+34.4	+89.0
50	+41.1	+ 4.6	+74.3	—52.5	+52.0	+81.7	+17.9	+67.6
55	+61.1	— 2.8	+77.8	—21.0	+47.9	+90.5	—20.0	+18.6
60	+71.9	—15.7	+78.4	+13.2	+36.4	+87.7	—47.6	—35.2
65	+76.4	—34.4	+76.7	+41.8	+13.3	+70.1	— 2.5	—54.8
70	+77.7	—55.9	+72.7	+62.1	—25.2	+36.6	+37.7	—40.8
75	+77.4	—71.5	+66.2	+73.7	—58.6	— 7.0	+53.1	—10.4
80	+75.9	—70.7	+56.0	+76.9	—40.1	—46.2	+54.3	+21.3
85	+73.5	—51.7	+40.6	+72.7	+ 0.9	—61.7	+43.4	+37.3
90	+70.1	—24.7	+16.9	+61.6	+26.6	—44.5	+14.4	+31.0
95	+65.8	— 0.5	—16.7	+43.5	+37.7	—11.0	—42.5	+ 9.2
100	+60.9	+16.5	—48.7	+17.0	+39.9	+15.1	—76.2	—21.2
105	+55.4	+26.2	—50.6	—18.5	+36.0	+26.6	—34.1	—46.7
110	+49.5	+30.4	—27.4	—52.6	+25.7	+26.8	+ 1.5	—38.3
115	+43.6	+31.0	— 6.3	—56.5	+ 5.3	+18.9	+16.0	—10.3
120	+37.6	+29.3	+ 5.4	—32.0	—29.1	+ 3.1	+18.5	+ 5.7
125	+31.9	+26.4	+10.6	— 9.8	—50.3	—22.6	+12.3	+ 9.3
130	+26.5	+22.8	+12.1	+ 1.8	—32.1	—42.4	— 6.4	+ 5.0
135	+21.5	+19.0	+11.6	+ 6.5	—12.8	—28.4	—38.4	— 8.4
140	+17.0	+15.3	+10.2	+ 7.6	— 3.2	—12.0	—37.1	—28.2
145	+13.0	+11.8	+ 8.3	+ 7.0	+ 0.7	— 1.8	—16.3	—23.0
150	+ 9.5	+ 8.7	+ 6.4	+ 5.8	+ 2.0	+ 1.1	— 5.8	— 9.2
155	+ 6.6	+ 6.1	+ 4.6	+ 4.3	+ 2.0	+ 1.8	— 1.7	— 3.0
160	+ 4.2	+ 4.0	+ 3.0	+ 2.9	+ 1.6	+ 1.5	— 0.2	— 0.8
165	+ 2.4	+ 2.2	+ 1.7	+ 1.6	+ 1.0	+ 1.0	+ 0.2	— 0.1
170	+ 1.1	+ 1.0	+ 0.8	+ 0.7	+ 0.5	+ 0.5	+ 0.2	+ 0.1
175	+ 0.3	+ 0.2	+ 0.2	+ 0.2	+ 0.1	+ 0.1	+ 0.5	+ 0.03
180	0.0	0.0	0.0	0.0	0.0	0.0	0.0	0.0

Polarization (%) of spherical ice particles for values of the scattering parameter $2\pi a/\lambda = 2.0$-5.5.

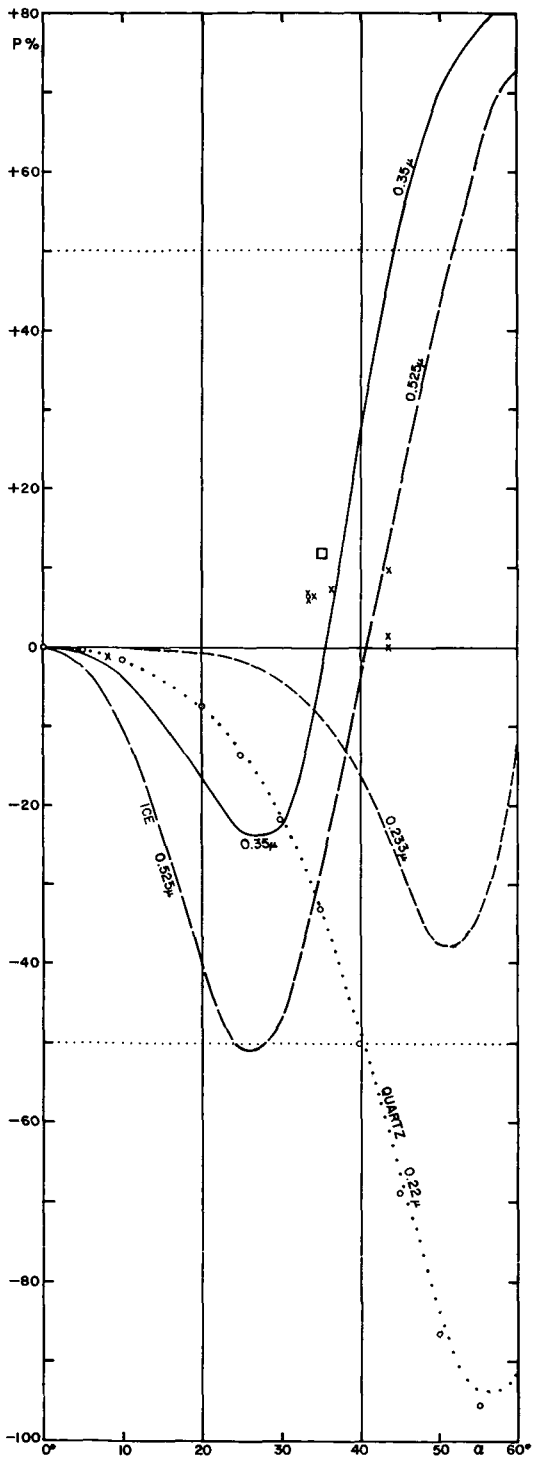

Fig. 1. Computed polarizations for sub-micron ice and quartz spheres if observed at $\lambda = 0.35\ \mu$ (cf. Table 1). Polarization measures of Mars from Gehrels and Teska, 1962.

results will be complex (Figures 2*a-d*).

The extremely-strong forward scattering of the haze particles will give Mars in the far UV some properties resembling Venus in visual light; i.e., the *phase integral in the UV will be larger than in the visual* and the Martian Bond albedo at 0.35 μ will be about 0.07, not 0.05. It is also seen from the backscattering coefficients of Table 2 that variations in particle size alone can produce large variations in surface brightness over the planetary disk.

A further estimate of the total molecular content of the Mars atmosphere can come from the albedo of the planet in the *far* UV, at wavelengths so short that the molecular scattering exceeds the particle scattering. Where this occurs may be estimated as follows: the extinction coefficient for pure air at 0° C and 1 atm pressure is 10^{-7} cm^{-1} at 5740 Å (Van de Hulst 1952, p. 55) or 10^{-9} cm^{-1} at 10 mb. If the Martian scale height is 20 km, the molecular extinction coefficient for the Martian atmosphere becomes 2.10^{-3} per 10 mb of surface pressure. The molecular contribution to the albedo for a uniform disk (2 air masses average) will be $2 \times 3/8$ of the extinction or about 0.0016 per 10 mb at $\lambda = 0.57\ \mu$ or, by the λ^{-4} law, 0.23 per 10 mb at $\lambda = 0.15\ \mu$. Well below 0.18 μ the ice particles will be nearly opaque. Table 3 shows Dr. Herman's computations of the scattering by both transparent and nearly-opaque particles for which $2\pi a/\lambda = 8$; at $\lambda = 0.15\ \mu$ the corresponding particle size is $d = 0.38\ \mu$; at $\lambda = 0.12\ \mu$ it is $d = 0.306\ \mu$. Therefore, the computations apply to ice particles of about 0.35 μ diameter, as found to be present, when observed in the 0.12-0.15 μ region. The computed backscattering per unit solid angle of these particles in terms of total scattering, is 0.044 for transparent particles and 0.186 for particles with the absorption coefficient $k = 1.0$; and 0.138 for $k = 0.765$. These values suggest that observations designed to determine the *total molecular scattering* in the Martian atmosphere may be optimum at the shortest wavelength at which the haze particles are still transparent, i.e., about 0.18 μ.

It is of interest to note that the *Martian blue haze may be simulated* in the laboratory. This may be done by pumping liquid nitrogen into an open vessel placed in very dry air, such as a mountain-observatory site has in winter. The evaporating nitrogen then freezes the atmospheric water vapor into sub-micron ice crystals producing a *blue* cloud, much like light smoke. If the atmospheric water-vapor content is larger, a white cloud is produced

TABLE 2b

PHASE ANGLE	2.0	2.5	3.0	3.5	4.0	4.5	5.0	5.5
0°	0.062944	0.69815	0.35503	1.9472	1.6997	3.1703	4.2673	3.5196
5	0.061821	0.69271	0.34976	1.9023	1.6539	3.0109	4.0904	3.1781
10	0.058541	0.67662	0.32832	1.7739	1.5323	2.5850	3.6596	2.4107
15	0.053368	0.65063	0.30048	1.5796	1.3770	2.0297	3.2154	1.8090
20	0.046734	0.61587	0.27098	1.3453	1.2422	1.5151	2.9947	1.8867
25	0.039222	0.57389	0.24754	1.1005	1.1753	1.1822	3.0850	2.7193
30	0.031552	0.52644	0.23779	0.87387	1.1998	1.0952	3.3635	3.8852
35	0.024561	0.47547	0.24808	0.68856	1.3056	1.2267	3.5596	4.7451
40	0.019192	0.42297	0.28224	0.55966	1.4500	1.4800	3.4108	4.8588
45	0.016484	0.37093	0.34081	0.49341	1.5704	1.7358	2.8274	4.2515
50	0.017581	0.32125	0.42051	0.48826	1.6038	1.9013	1.9736	3.3533
55	0.023751	0.27582	0.51421	0.53740	1.5108	1.9412	1.2087	2.6743
60	0.036439	0.23660	0.61134	0.63169	1.2934	1.8771	0.91878	2.4674
65	0.057333	0.20593	0.69891	0.76183	1.0044	1.7620	1.3055	2.6266
70	0.088463	0.18690	0.76299	0.91876	0.74230	1.6479	2.2538	2.8765
75	0.13232	0.18409	0.79092	1.0920	0.63140	1.5691	3.3485	3.0689
80	0.19196	0.20438	0.77441	1.2661	0.78845	1.5562	4.0547	3.3087
85	0.27112	0.25807	0.71383	1.4181	1.2816	1.6699	4.0018	3.7811
90	0.37429	0.36005	0.62376	1.5177	2.0902	2.0271	3.2526	4.4416
95	0.50664	0.53092	0.53990	1.5365	3.0784	2.7780	2.4179	4.9356
100	0.67390	0.79773	0.52670	1.4679	4.0015	4.0125	2.5028	4.9882
105	0.99206	1.1941	0.68464	1.3626	4.5632	5.6210	4.4514	5.0673
110	1.1369	1.7589	1.1548	1.3735	4.5411	7.1987	8.5026	6.6489
115	1.4432	2.5345	2.1184	1.8050	3.9791	8.1312	13.665	11.412
120	1.8041	3.5603	3.7872	3.1467	3.4177	7.9841	17.776	19.452
125	2.2202	4.8708	6.3842	6.0736	4.0953	7.2059	18.583	27.842
130	2.6885	6.4847	10.112	11.390	8.0210	7.9582	15.922	31.693
135	3.2020	8.3992	15.108	19.908	17.813	14.671	14.359	29.035
140	3.7489	10.584	21.405	32.257	36.232	33.822	24.890	28.190
145	4.3129	12.975	28.884	48.671	65.439	72.569	63.957	52.923
150	4.8736	15.476	37.253	68.782	106.10	136.30	148.74	139.36
155	5.4076	17.962	46.041	91.502	156.66	225.75	289.39	321.69
160	5.8898	20.287	54.631	115.15	212.96	334.75	481.09	610.52
165	6.2958	22.300	62.327	137.09	268.61	449.89	699.88	975.20
170	6.6036	23.859	68.434	155.17	316.03	552.69	905.83	1342.4
175	6.7957	24.845	72.365	167.06	347.97	624.08	1053.6	1617.2
180	6.8611	25.182	73.721	171.20	359.25	649.66	1107.4	1719.3
σ_S	0.61996	1.0763	1.5528	2.0554	2.5616	2.9683	3.3787	3.6289
σ_B	0.03147	0.22341	0.07889	0.31792	0.21247	0.31312	0.34138	0.23270
σ_B/σ_S	0.051	0.207	0.051	0.155	0.083	0.106	0.101	0.064

Total scattering intensity of spherical ice particles for values $2\pi a/\lambda = 2.0$-5.5; σ_S = total scattering, σ_B = back scattering, both in terms of πa^2.

TABLE 3a

PHASE ANGLE	POLARIZATION (%)				TOTAL INTENSITY					
	A	B	C	D	A	B	C	D	E	F
0°	0.0	0.0	0.0	0.0	0.37904	1.0523	1.8877	4.9230	8.8937	5.9679
5	− 0.4	− 1.0	− 3.7	−51.0	0.77878	2.0315	3.5428	3.9300	8.8155	5.9101
10	− 1.6	− 6.2	−14.0	−73.7	0.73381	1.8373	3.0585	5.0046	8.5959	5.7654
15	− 3.4	−12.9	−24.7	+ 6.2	0.67780	1.5861	2.5730	12.381	8.2920	5.5658
20	− 5.3	−15.5	−22.3	+42.2	0.59216	1.3565	2.3577	20.293	8.0258	5.4282
25	− 6.2	−13.3	+ 9.7	+59.3	0.51937	1.2108	2.5069	19.047	7.9589	5.4273
30	− 4.8	− 3.3	+25.1	+72.2	0.46053	1.1738	2.8819	9.6889	8.1707	5.5725
35	+ 0.4	+14.6	+44.1	+68.6	0.42233	1.2262	3.1994	4.1785	8.5191	5.7515
40	+ 9.7	+31.5	+54.3	+48.1	0.41111	1.3176	3.2059	9.0643	8.6833	5.7934
45	+21.5	+43.8	+55.8	+44.4	0.42262	1.3894	2.8312	16.383	8.4664	5.6408
50	+33.1	+50.7	+46.6	−30.8	0.45323	1.3995	2.2294	15.411	8.0864	5.4624
55	+42.9	+52.2	+22.8	+21.2	0.49647	1.3373	1.6874	7.8383	8.0372	5.5154
60	+50.2	+47.6	+ 2.8	−87.4	0.54582	1.2249	1.4663	4.2914	8.5087	5.8276
180	0.0	0.0	0.0	0.0	94.443	402.86	1045.48	6444.8	3371.6	3171.25
				σ_S	1.5618	2.4921	3.3020	3.5124	1.4899	1.3548
				σ_B	5.2910	2.8896	3.0577	1.5384	0.27793	0.18650
				σ_B/σ_S	3.3877	1.1595	0.92601	0.43799	0.18789	0.13766

Polarizations and intensities for three mixtures of spherical ice particles defined in the text and $2\pi a/\lambda = 8$ (D, no absorption; E, $K = 1.0$; F, $K = 0.765$).

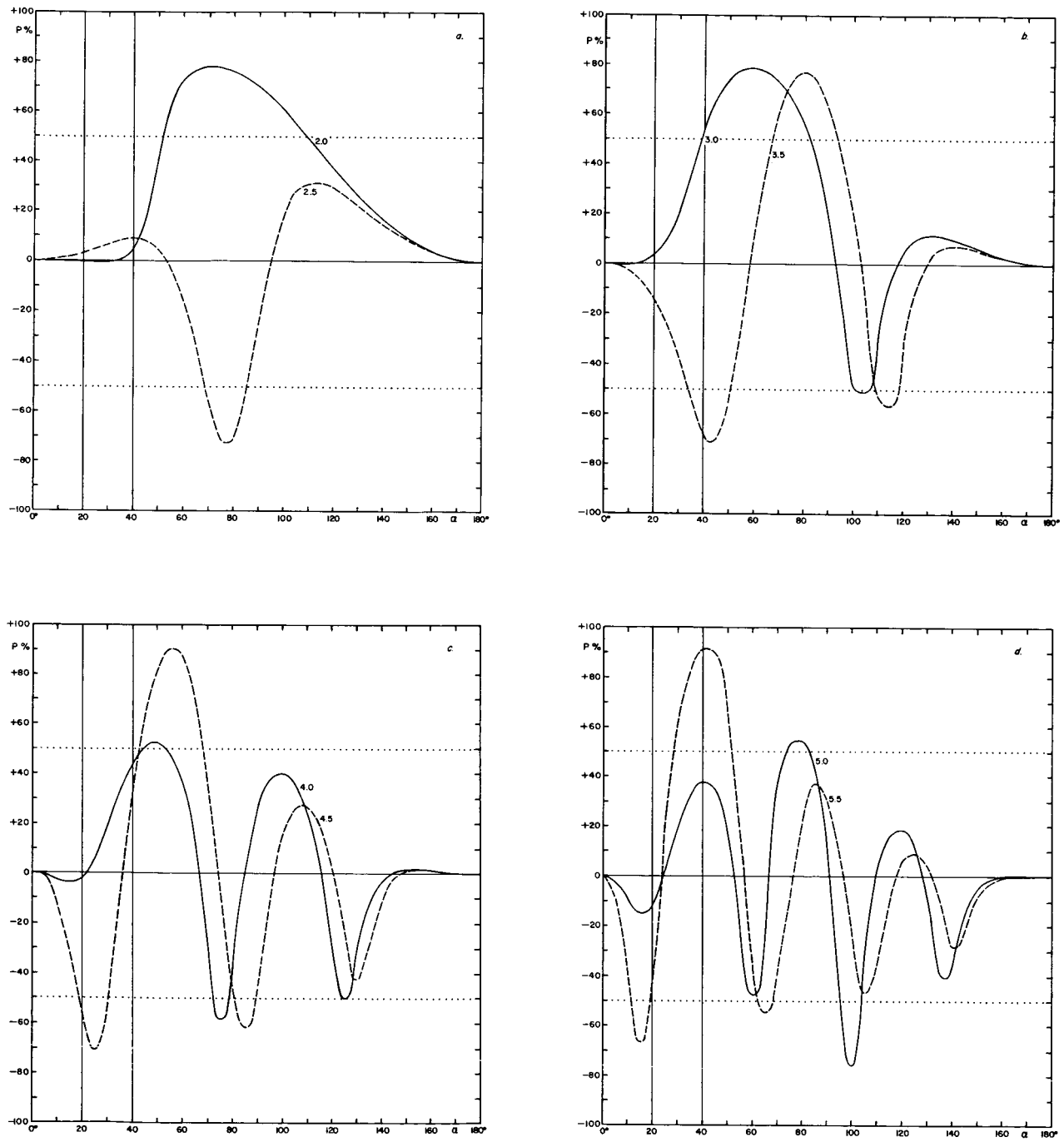

Fig. 2. Computed polarization curves for sub-micron ice spheres with eight values of the scattering parameter $2\pi a/\lambda$, entered in the figures (cf. Table 2).

TABLE 3b

POLARIZATION AND INTENSITIES FOR THREE MIXTURES OF SPHERICAL ICE PARTICLES DEFINED IN THE TEXT

PHASE ANGLE	POLARIZATION (%)			TOTAL INTENSITY		
	A′	B′	C′	A′	B′	C′
0°	0.0	0.0	0.0	0.55797	1.5869	3.0519
5	0.0	— 0.9	— 3.1	0.55098	1.5367	2.9083
10	0.0	— 3.7	—11.3	0.53093	1.4222	2.5401
15	— 0.1	— 8.9	—23.2	0.50007	1.2623	2.1028
20	+ 0.5	—13.0	—30.7	0.46183	1.0818	1.7665
25	+ 1.4	—17.0	—17.2	0.42034	0.92262	1.6342
30	+ 3.1	—17.3	— 1.3	0.37977	0.80553	1.6982
35	+ 6.0	—11.7	+23.1	0.34388	0.74012	1.8581
40	+10.2	— 0.8	+41.9	0.31553	0.72144	1.9831
45	+15.6	+12.0	+54.0	0.29641	0.73427	1.9847
50	+21.5	+23.6	+60.0	0.28701	0.76013	1.8582
55	+27.0	+32.6	+59.3	0.28671	0.78455	1.6751
60	+31.0	+38.9	+51.5	0.29415	0.80247	1.5359
180	0.0	0.0	0.0	39.145	205.94	7126.94
			σ_S	2.3067	2.0528	2.9565
			σ_B	3.6666	3.8607	2.4486
			σ_B/σ_S	1.5895	1.8807	0.82822

TABLE 3c

POLARIZATIONS AND INTENSITIES FOR THREE MIXTURES OF SPHERICAL ICE PARTICLES DEFINED IN THE TEXT

PHASE ANGLE	POLARIZATION (%)			TOTAL INTENSITY		
	A″	B″	C″	A″	B″	C″
0°	0.0	0.0	0.0	0.91405	2.2166	3.5731
5	— 0.5	— 1.8	— 4.3	0.89559	2.1360	3.2522
10	— 1.8	— 7.0	—15.8	0.84352	1.9218	2.8704
15	— 3.8	—14.5	—28.7	0.76704	1.6452	2.3761
20	— 6.1	—20.9	—26.4	0.67913	1.3920	2.1632
25	— 7.8	—20.6	+ 6.4	0.59375	1.2285	2.3273
30	— 7.6	— 8.7	+27.2	0.52296	1.1780	2.7268
35	— 4.1	+ 9.7	+47.6	0.47461	1.2171	3.0773
40	+ 3.2	+27.8	+59.5	0.45140	1.2916	3.1299
45	+13.2	+41.5	+62.0	0.45115	1.3444	2.8202
50	+23.8	+50.0	+53.5	0.46838	1.3412	2.2971
55	+33.4	+53.1	+31.2	0.49656	1.2823	1.8237
60	+44.1	+50.3	+ 4.8	0.53040	1.1984	1.6225
180	0.0	0.0	0.0	101.58	416.78	1091.38
			σ_S	1.9635	2.5230	3.2727
			σ_B	4.5475	3.1438	2.9460
			σ_B/σ_S	2.3161	1.2460	.90015

(larger crystals). Filter observations of objects seen through such a blue cloud duplicate very well the wavelength dependence of extinction by the Martian haze. Shadows cast by these blue clouds are brownish. An effort will be made in collaboration with Professor Alvar Wilska to make electron micrograms of these blue particles.

In summary, we find (1) the molecular content of the Mars atmosphere cannot be determined from visual polarization measurements; (2) *the surface atmospheric pressure is well below 30 millibars.* A sharper limit can be derived from further UV measures.

3. *Atmospheric Particles: General*

In addition to the blue-violet haze layer and the whitish clouds embedded in it, one occasionally observes *yellowish dust clouds.* Excellent photographs of such clouds are found in a chapter by Finsen (1961). These clouds set broad density limits on the Martian atmosphere because they are both generated and upheld by aerodynamic forces. The absence of rain on Mars will result in a much longer residence time of fine particulate matter in the atmosphere, and part of the UV haze layer could be remnants of dust storms. I am much indebted to Dr. James E. McDonald of the Institute of Atmos-

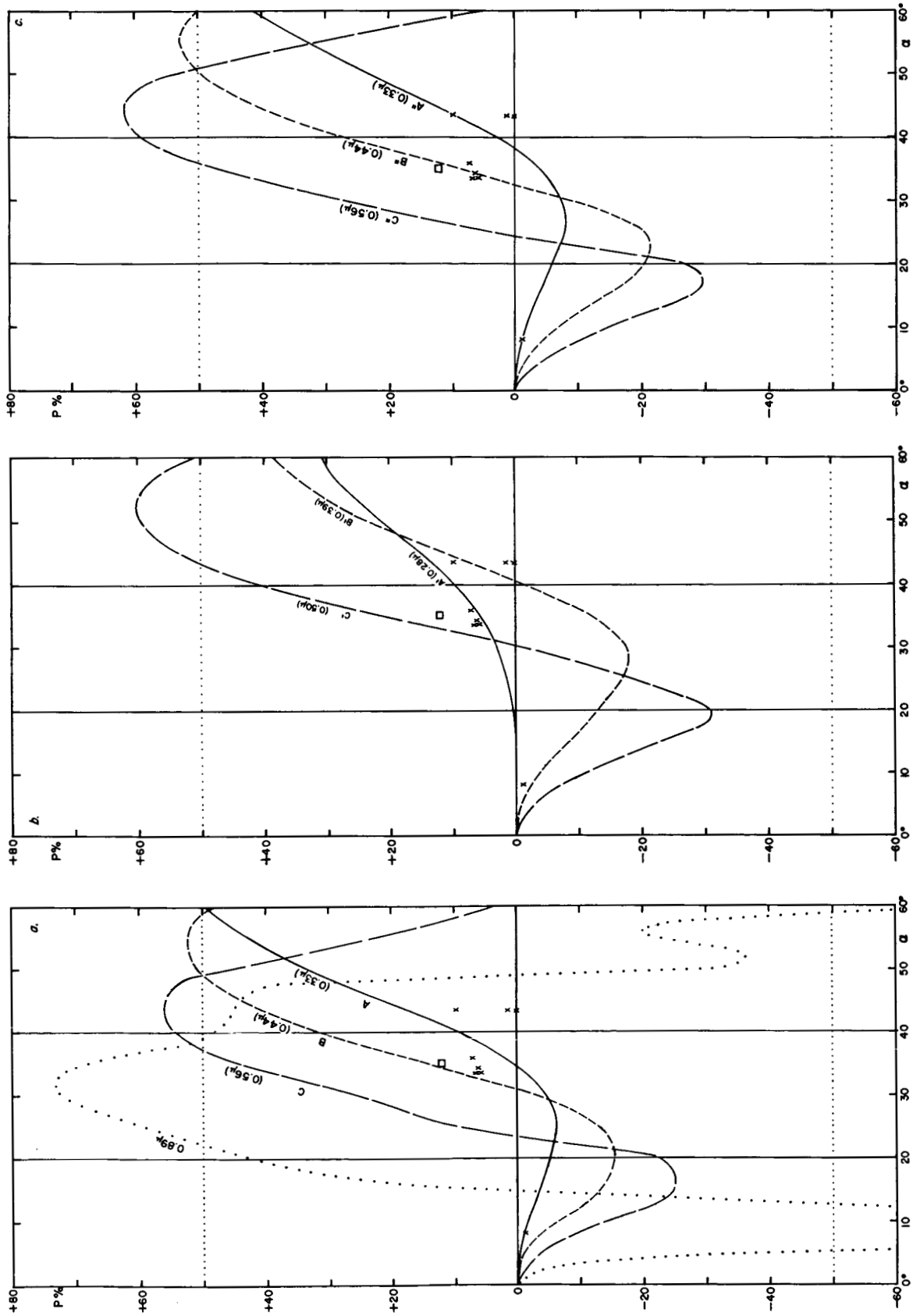

Fig. 3. Computed polarizations for three sets of mixtures of sub-micron ice spheres if observed at λ 0.35 μ, with available polarization measures entered (Gehrels, Teska, 1962) (cf. Table 3); (*a*) mixtures centered on integral values of scattering parameter, (*b*) mixtures centered on half-integral values, (*c*) "balanced" mixtures (see text).

pheric Physics, University of Arizona, for discussions on this general topic; this section depends largely on data and references he has supplied.

The atmospheric dust content will be a balance between (a) injection into the atmosphere and (b) elimination by free fall or scavenging by condensation products, which in the case of Mars must be limited to ice crystals. Evidence for such crystals, in addition to the haze and cloud phenomena already reviewed, is found in the presence of cloud caps over the poles in winter (cf. de Vaucouleurs, 1954, Sec. 47; Dollfus, 1961, p. 376). The crystals in these clouds may contain silicate condensation nuclei as do most terrestrial snow flakes. Ice deposited onto atmospheric dust could be responsible for the *variable transparency* of the general haze near $\lambda = 0.45\ \mu$, the "blue clearings" (Slipher, 1962), which appear to involve a temporary reduction in average particle size by perhaps 10 percent. This reduction could occur through a general temperature rise, or subsidence of an upper tropospheric air mass to the lower unsaturated zone; or else through a comparatively dust-free polar air mass moving into lower latitudes.

The elimination of atmospheric dust by free fall is governed by Stokes's law

$$V = \frac{\rho g d^2}{18\,\eta} \qquad (1)$$

(ρ = particle density; g = gravity; d = diameter; η = coeff. of viscosity) for the particles considerably larger than the mean free path in the Martian atmosphere ($d > 10\ \mu$); and for smaller particles by the Stokes-Cunningham law

$$V = \frac{\rho g d^2\,(1 + k\lambda/d)}{18\,\eta} \qquad (2)$$

(λ is the mean free path; k a numerical factor of the order of unity). This law allows for the increased terminal velocity resulting from the discontinuities in the gaseous medium.

Dr. McDonald has kindly allowed the writer to quote from his computations of the terminal velocity as a function of d made for $\rho = 1$ and $g = g$ (Earth). They extend over the range $0.02\ \mu \leq d \leq 20\ \mu$ and a large range of atmospheric densities. For silicate particles on Mars the product $g\rho$ will be the same as used in McDonald's computations; they are reproduced in Table 4 for the range of atmospheric densities likely to be of interest. The three values of the pressure correspond to the levels 20 km, 30 km, and 40 km in the terrestrial atmosphere. (The temperature differences between the terrestrial stratosphere, ~220°K at 30 km, and the Martian troposphere are unimportant.)

TABLE 4

TERMINAL VELOCITIES OF SILICATE PARTICLES IN MARTIAN ATMOSPHERE
(Courtesy Dr. J. McDonald)
(V in cm/sec)

d (μ)	V for 55 mb	V for 11 mb	V for 2.7 mb
0.02	0.0002	0.001	0.004
0.10	0.0011	0.005	0.02
0.20	0.0024	0.011	0.04
1	0.014	0.06	0.2
2	0.033	0.12	0.4
10	0.5	0.8	2
20	1.7	2.5	5

It is seen that for large particles (20 μ) the terminal velocities indeed approach Stokes's law, which makes V independent of the gas density. For particles with $d \simeq 0.2\ \mu$, which could be partly responsible for the violet haze, there is a first-power dependence on gas density or pressure; but the rate of fall is so slow that a precise knowledge of atmospheric circulation would be needed to derive any conclusions: for 11 mb pressure, these particles fall 1 km in 10^7 seconds or 4 months; and 10 km (probably a representative height for this layer) in 3 years. Thermal convection and the annual circulation of the atmosphere could retain these particles in the atmosphere almost indefinitely.

The elimination of dust by rain in the *terrestrial* atmosphere has been investigated by Greenfield (1956). He finds that particles between about 0.1 and 10 μ have the lowest probability of being swept up. McDonald (1964) has emphasized the reasons: particles with $d >> 10\ \mu$ have so much inertia that rain drops collide with them and sweep them up. The very small particles ($d << 0.1\ \mu$) collide with droplets also, in this case because of their Brownian motion. This leaves the intermediate group for which the Brownian motion is small and the inertia also small, so that the particles are carried with the aerodynamic flow past the droplets.

Because of the very low frost point (around −78°C, see section 4) it cannot rain on Mars. Furthermore, at the very low Martian temperatures, the ice crystals settling over the polar caps are presumably platelets or prisms 1-10 μ in size rather than large, complex snowflakes (Fletcher, 1962, p. 259 ff). Therefore, the principal scavenging process will not be particle collison but rather *deposition of ice on silicate particles* that subsequently

fall, e.g., on the polar caps. The optical properties of the Martian polar regions through their annual cycle may give some indication of the degree of particle depletion there during the Martian winter.

The second aspect, the production and *atmospheric injection* of dust, is a process widely studied for the Earth. Reference is made to four monographs: *Micromeritics* (Dallavalle, 1948), *Particulate Clouds* (Green and Lane, 1957), *Air Chemistry and Radioactivity* (Junge, 1963), and *The Mechanics of Aerosols* (Fuks, 1955). It appears that the size-frequency curves of aerosols are usually normal gaussian error curves in log d; but the data are not always sufficient to show whether this law holds for all particles in the atmosphere or merely the part collected by special devices. Fletcher (1962, pp. 68-69) considers that the observed low frequency of dust particles with $d \leq 0.1\ \mu$ is real, because such particles are difficult to produce. Dr. McDonald further points out that even after dust particles are produced by grinding action (wind erosion) they will tend to stick to larger particles because natural aerodynamic gradients are far less than the surface-contact forces. Therefore, it is probable that also on Mars the injection of particles with $d < 0.1\ \mu$ is inappreciable.

With dust present in the Martian atmosphere its particles will act as active nuclei for the deposition of ice as soon as the temperature falls below the local frost point. The largest silicate particles will statistically be the most suitable hosts because they have the largest probability of presenting an area of sufficient size and with the proper lattice constant for attachment of an ice embryo (Fletcher, 1962, p. 210 ff.). Physically, this process can occur for temperatures below about –20°C, depending on the composition of the dust (*op. cit.* pp. 245-250). As is true for the Earth, meteoritic dust will make a contribution to the total dust content (*op. cit.* pp. 250-258).

The growth rate of the ice crystals is given by

$$\frac{dM}{dt} = \text{const.}\ r\,(n_o - n_c), \tag{3}$$

in which M is the mass of the particle, r its radius, n_o the concentration of vapor molecules at a distance and n_c the concentration at the crystal surface (Fletcher, *op. cit.*, p. 266). If relative effects of ventilation are neglected ($n_o - n_c = \text{const.}$) it follows that

$$r = \text{const.}\ \sqrt{(t - t_o)}, \tag{4}$$

in which the constant may be positive, zero, or negative depending on the sign of $(n_o - n_c)$; n_c depends on T and the nature of the surface. Partly because of the latter factor, a forecast on the steady-state distribution of diameters of the very small ice crystals in an atmosphere with exceedingly low values of n_o and n_c is not readily made. The effect of surface curvature will tend to favor the larger ice crystals, but those well above 1 μ will fall out from the haze layer (cf. Table 1) and evaporate in the lower, unsaturated parts of the atmosphere. A cloud with rather uniform particle diameters may therefore result, and may account for the blue-violet haze layer actually observed. Because of atmospheric circulation and subsidence of air masses, inhomogeneities in the haze layer will be expected. Conversely, the *circulation of the Martian atmosphere will in principle be accessible to systematic study from the Earth through a continuous patrol by UV photography and polarimetry with the highest possible resolution.* A constant component might be detected that would be molecular, leading to an independent determination of the atmospheric gas content.

The repeated falling out of the largest ice crystals from the haze layer means that in the steady state the water-vapor mixing ratio of the lower troposphere will be larger, and clouds with increased crystal size within the haze layer can be formed by convective updraft from below. The frost deposits on the polar areas and their periodic evaporation at ground level will have a similar enriching effect. In this manner a "lumpy" pattern as observed on the UV photographs can be accounted for.

An interesting question concerns the *electrical* state of a Martian dust cloud. Experience with conditions of extremely low humidity on the Earth, such as are found in the Sahara Desert, indicates the possibility of large electrical gradients in dust clouds and frequent small lightning discharges.

The atmospheric density cannot be found with precision from the mere occurrence of dust storms. At the McDonald Observatory I have observed particle sizes in terrestrial dust storms by collecting the dust on exposed sticky surfaces (glass, coated with oil), 10-15 meters above the ground. It was found, among others, that for 20 miles-per-hour (9 meters-per-second) winds, the dust ranged in size up to 25 μ diameter. The "gustiness" of the wind, expressed as the vertical rms velocity, is about 0.1 of the horizontal wind speed, or $\pm$ 0.9 mps, whereas on the Earth the rate of fall of a 25 μ particle of $\rho = 2.5$, according to Dr. McDonald's table, is 0.05

mps. The ratio of 1/18 must represent the net ascent of dust-laden air near the surface in an otherwise near-random process. For Mars winds of similar magnitude (4-10 mps, Antoniadi 1930, pp. 45-46) have been derived from moving cloud masses; Martian dust storms may require double this speed or more.

If an 18 meter-per-second (40 mph) wind is assumed as typical for a Martian dust storm and the surface pressure were 10 mb, the aerodynamic force per unit area on the dust would be ρV^2 or 1/20 of the force acting on the terrestrial dust referred to. Particles of 25 $\mu/20 = 1.25$ μ would then be carried away on Mars, which is not inconsistent with the observed yellowish color of the dust; though, for the assumed wind velocity, *the pressure could not be much less or the particles raised would not be yellow.* The rate of fall of such particles would be about 0.07 cm per second (see Table 4) so that the dust could stay in a quiet atmosphere for 1-10 days, not inconsistent with the observations.

As Mr. T. Owen has pointed out to the writer, there is an alternative mechanism for the injection of dust into the Martian atmosphere: *dust devils.* In terrestrial deserts these are frequent and their dust columns are often visible to heights of 1-2 km, particularly when viewed in polarized light normal to the sun. The heating of the Martian soil in a sky almost always perfectly clear must be conducive to the formation of dust devils. They cannot, of course, be responsible for the massive dust clouds referred to above.

The discussion of Section 2 sets an upper limit to the molecular content of the Martian atmosphere; that of Section 3 a very rough lower limit. Taken together an atmospheric pressure around 10-20 mb appears plausible. The limits can be sharpened by further work, and UV polarization measures and photometry should yield an actual value of, not merely a limit to, the molecular scattering power.

4. The Spectral Records

The infrared spectrum of the planet yields data on both the atmospheric composition and the pressure more specific than do the data on atmospheric scattering.

The spectrum from 1-2 μ was observed in 1947 with resolutions $\lambda/\triangle\lambda$ of about 80, which led to the discovery of CO_2 in the atmosphere. "The bands near 1.6 microns were three times as strong in the Mars spectrum as in the Moon spectrum taken at the same altitude. Spectra of the Sun at different altitudes confirm this conclusion. Because of pressure effects on the band intensity, the CO_2 content of the Mars atmosphere will actually be somewhat larger than that of the Earth if the total pressure on Mars is less than on the Earth, as is likely. No other gases having strong infrared absorptions, like CH_4, NH_3, or N_2O were found. They could not be present except in exceedingly small quantities" (Kuiper 1947). The CO_2 bands recorded were the (strong) central pair of the tetrad (301, 221, 141, 061) near 1.6 μ. In 1948 the somewhat stronger triad (201, 121, 041) was observed also (Kuiper 1949, p. 335), with intensities roughly consistent with the 1.6 μ group.

Further, the Martian polar caps were observed and found to exhibit the reflection spectrum of H_2O snow, not CO_2 snow (*op. cit.*, pp. 336-337). From the gradient of the reflection curve near 2 μ it was found that the ice crystals of the polar caps were much smaller than in terrestrial snow, but were nearly matched by frost deposited on dry ice.

In the first part of the 19th century it was generally held that the maria on the planet were genuine seas. This concept was challenged by Kaiser (1872), who however offered no substitute explanation. Liais and Cruls (1878) and Trouvelot (1884) were the first to hypothesize that the dark areas were vegetation. The assumption that the snows of the polar caps "melted" at 0°C continued to be made, however (except by authors who supposed the caps to be frozen CO_2). It is true that the measured temperatures of the caps were much below 0°C, but Coblentz (1926) attributed this to Martian atmospheric absorption. The writer (1931), comparing the measured Martian temperatures with data on water vapor then available (the Mt. Wilson measures of 1925), concluded that the frost point on Mars was about −56°C and that no free liquid water can exist on the planet; only ice and water vapor. Since the water-vapor data were marginal, the actual frost point could be lower. A better determination was made from the extent of the polar cap, on the assumption that the theoretically-computed temperature at its boundary represents the frost point (Kuiper 1952, p. 389); and from the presence of ice particles in the Martian atmosphere at temperatures that may be estimated. In this manner $T_f =$ −78°C was derived, with an upper limit of −73°C; and the total amount of precipitable water in the Martian atmosphere of the order of 8 μ (for the upper limit of −73°C the corresponding amount is 18 μ).

Grandjean and Goody (1955) computed the atmospheric CO_2 abundance from Kuiper's observations of the 1.575 and 1.605 μ bands on the assumption that $p = 100$ mb. Sinton (1961) published low-resolution spectra of Mars and the moon taken in 1954, indicating the presence of the 10-12 μ bands of CO_2; Weaver *et al.* (1963) announced the observation from a balloon of the 2 μ bands of CO_2 merged as one feature and computed the upper limit of Martian water vapor to be 40 μ; while Dollfus (1963, 1964) attempted to observe Martian water vapor near 1.4 μ by using narrow-band filter photometry at the Jungfraujoch and found 150 μ of H_2O. An excellent high-dispersion spectrum taken in the 0.8-0.9 μ region with the Mt. Wilson 100-inch coudé spectograph by Spinrad, Münch, and Kaplan (1963, 1964) recorded Doppler-separated Martian H_2O at 0.82 μ and CO_2 at 0.87 μ. They found 14 ± 7 μ of H_2O, confirming the estimate from the size of the polar cap but contradicting the high value derived by Dollfus.

5. *McDonald Spectra, 1962-63 Opposition*

Spectral records for the 1-2.5 μ region were obtained with the 82-inch telescope during the past several oppositions, but those taken in December 1962 - January 1963 are the most complete and have been extensively calibrated in the laboratory. These Mars spectra are reproduced here, together with lunar and some preliminary laboratory comparisons. The more definitive laboratory calibrations of CO_2 are found in *Communications* No. 32 by Owen and Kuiper; and those of trace constituents in *Comm.* No. 34 by Kuiper and Cruikshank. A preliminary account of the spectra was presented at the Liège Conference, June 1963 (Kuiper 1963).

The smallest slit width used in the Mars records is 0.3 mm (2 seconds of arc at the Cassegrain focus) which results in resolution $\lambda/\triangle\lambda$ of about 1000 and $\triangle\lambda = 0.001$-0.002 μ. In the photographic infrared (0.75-1.1 μ) photographic spectra with much higher resolution have been obtained at Mt. Wilson and elsewhere but a few rapid-scan records (0.01 μ or 100Å per minute) with the same medium resolution as used beyond 1 μ are included here for comparison purposes. These records are shown in Figures 4 and 6, with Figures 5 and 7 showing lunar comparisons taken on the same night. The lunar image on the slit was thrown far out of focus to reduce spurious intensity changes in the spectra resulting from the drift of the lunar image over the slit; even so, the lunar comparisons had to be run faster and have somewhat reduced resolution. The atmospheric humidity was only about 1 mm precipitable water in the overlying atmosphere but still too high to show the Martian water vapor directly.

In Figure 8 the record is extended to 1.4 μ; the scanning rate was again 0.01 μ per minute. The lunar comparison in Figure 9, taken at 0.05 μ per minute, has somewhat less resolution and less electronic noise. Figure 8 shows the (103) and (023) bands of CO_2 at 1.20 and 1.22 μ, and marginally, the (241) band at 1.32 μ. These may be compared with the laboratory bands shown in Figure 14. The Martian 1.2 μ bands, (103) and (023), have on the basis of Figure 8 and 9, equivalent widths of 2.0Å and 1.3Å, respectively. In the laboratory comparison shown in Figure 14 the widths are 3.1Å and 1.9Å, respectively.

Figure 10 is the first record obtained during the past opposition of the 1.4-1.8 μ region, with Figure 11 serving as a lunar comparison for it as well as for Figure 12.

On the dry night, December 8, 1962, three records of the 1.4-1.8 μ region were obtained which are shown in Figure 12; the top graph is not a direct trace, but the average of the two lowest traces, which had a shorter time constant (5.5 seconds) than the third (11 sec) and show, therefore, more electronic noise. The top graph will therefore have an intrinsic noise comparable to the $\tau = 11$ sec trace placed just below, but have somewhat increased resolving power. The upper two graphs are independent of one another and together contain the substance of Figure 12. It is seen that they define the Martian 1.6 μ tetrad of CO_2 moderately well. Figure 13 shows two additional scans, obtained mid-January 1963, with a laboratory trace added for purposes of identification. Figure 14 serves the same purpose for the Martian records of Figure 12.

Planimeter measurements of the two strong bands at 1.6 μ on Figure 12 show the equivalent width of the Martian plus telluric CO_2 absorptions to be 1.20 times as large as that of the laboratory comparison, which is 80 meters of CO_2 at $p = 17$ cm or 18 m atm. The telluric components may be subtracted with the aid of Figure 11. The equivalent widths of the 1.575 and 1.605 μ bands average 12.8Å on Figure 11 and 27.6Å on Figure 12. On December 8, 1962, Mars was receding from the sun at a rate of 1.65 km/sec and approaching the Earth at a rate of 13.65 km/sec. Hence the Martian CO_2 bands were displaced corresponding to -13.6 km/sec or by -0.72Å. The Michigan Atlas of the

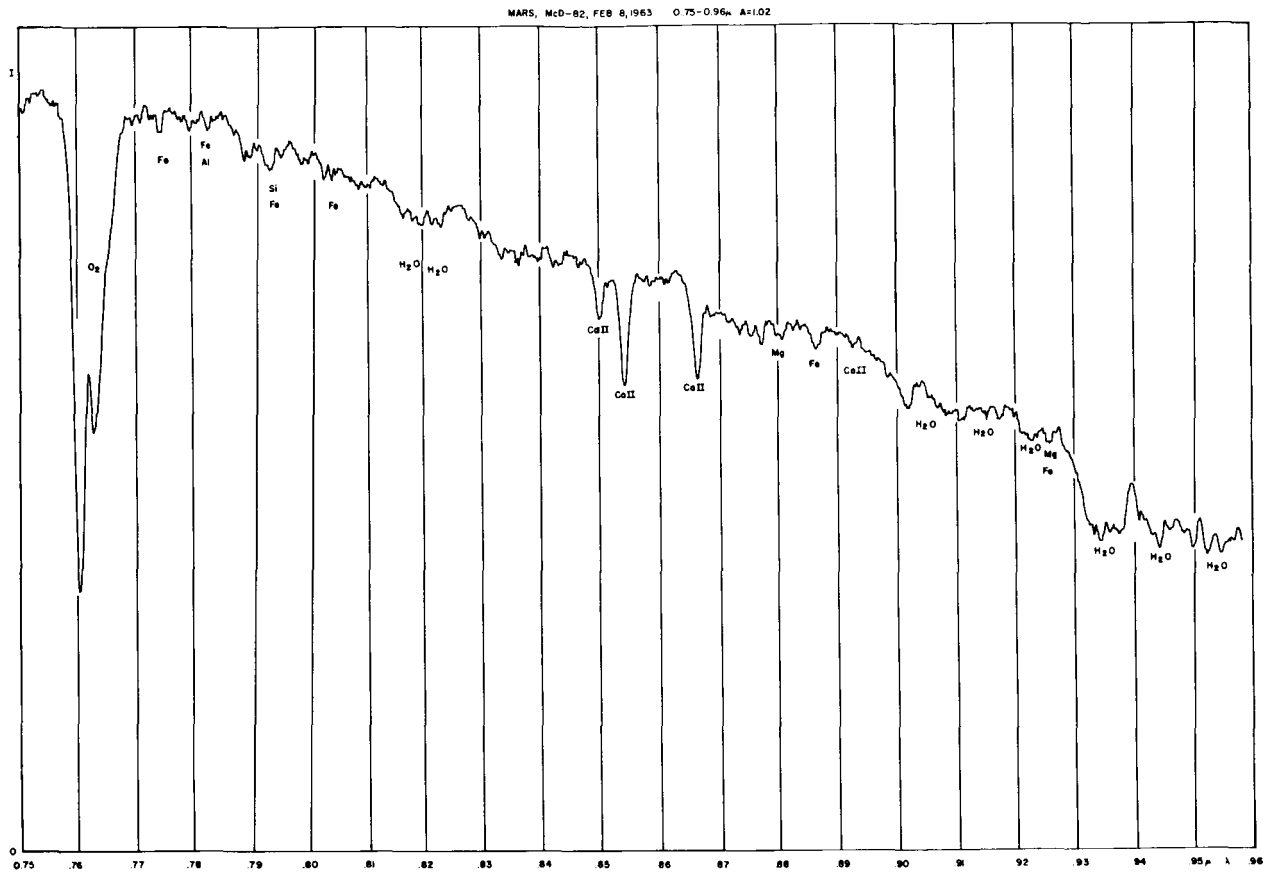

Fig. 4. Mars, equatorial strip, 0.75-0.96 μ, McDonald Observatory, February 8, 1963; T = 52° F, relative humidity (H) = 0.34, declination (Dec.) + 21°1, hour angle (H.A.), 0^h21^m-0^h31^m W, air mass 1.02; Dumont S-1 photomultiplier, grating 1.0 μ, RG 8 filter, entrance and exit slits both 0.25 mm, scanning rates 12.5/0.5, time constant (τ) = 1 sec.

solar spectrum (Mohler, *et al.*, 1950), small sections of which are reproduced in Figure 16, shows that for the two bands in question the Martian and telluric CO_2 lines will have been completely separated. (The separation is somewhat larger than shown because instrumental broadening in Fig. 16 is about 0.5Å.) Since the two bands are each about 0.02 μ = 200Å wide, the average telluric absorption is 6.4 percent and the reference continuum of the Mars absorption may therefore be regarded to be depressed by this amount. The average equivalent width of the Mars bands on December 8 was therefore (27.6–12.8)/0.936 = 15.8Å.

The observed Martian spectra are a blend of solar, telluric, and Martian absorptions. The calibration of these spectra would therefore best be made by channeling natural sunlight, received through the Earth atmosphere, through an absorption tube that simulates the Martian atmosphere; though one cannot reproduce this way the apparent radial velocity of the planet.

Mr. T. Owen has succeeded in obtaining such composite spectra. Only the 2-meter tube (allowing an 80-meter total path length) was available at the time the bulk of this paper was prepared and the numerical comparisons must still allow for the pressure difference, Mars-laboratory, at the point of intensity match. It was found from records such as shown in Figure 15 that p = 11 cm (11.5 meter atm of CO_2) well represents the Martian spectrum. Improved comparisons made with the long absorption tube are found in *Comm.* No. 32.

The Martian spectral record is continued to 2.5 μ in Figures 17, 19 and 20, with Figure 18 giving three lunar comparisons and Figure 21 laboratory comparisons. The matching of the curves of Figure 21 with the 2 μ CO_2 absorptions of Mars leads to a similar result as discussed on the basis of Figure 15.

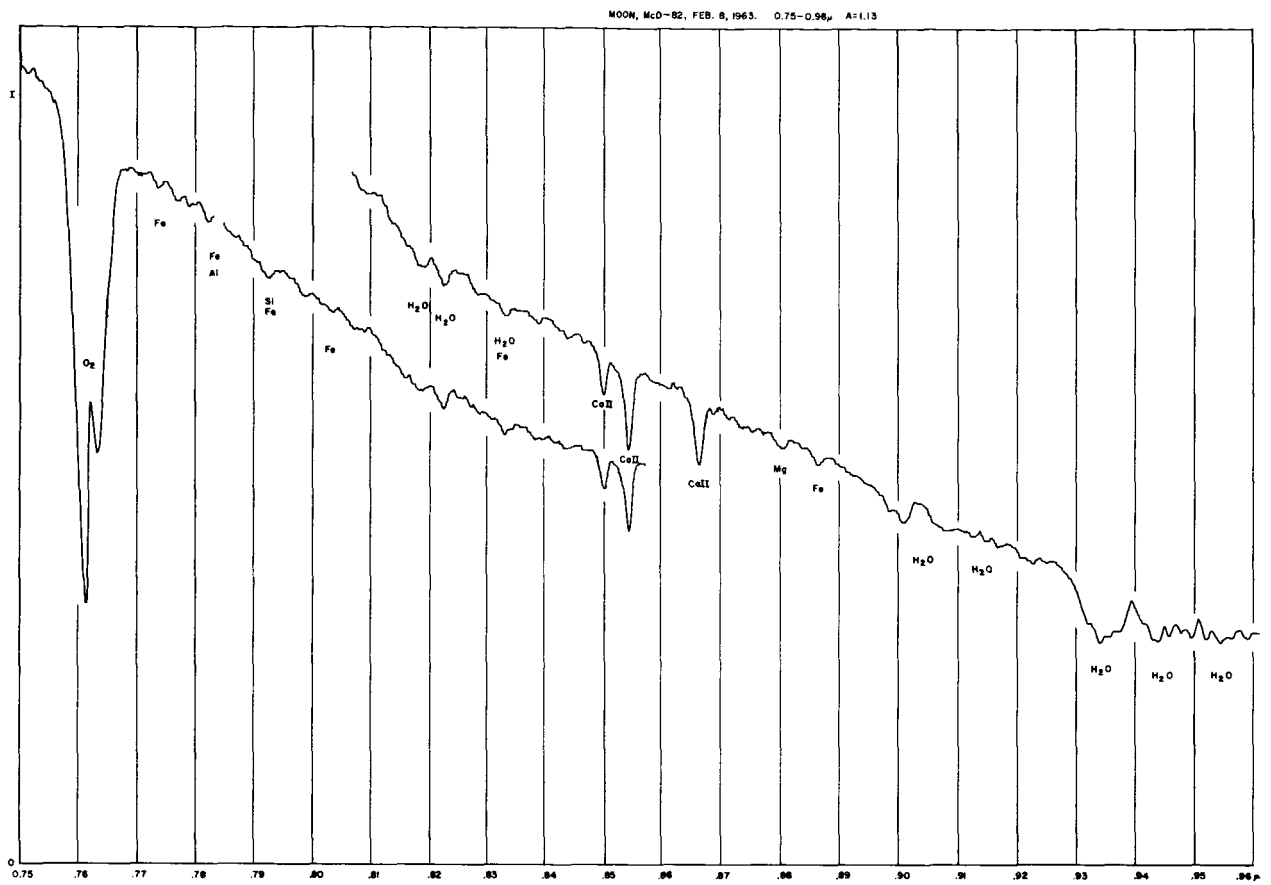

Fig. 5. Moon comparison for Figure 4, 0.75-0.96 μ, February 8, 1963; T = 52° F, H = 0.34, Dec. + 17°1, H.A. 1^h42^m-1^h52^m W, air mass 1.13, Cell S-1, grating 1.0 μ, RG 8 filter, slits 0.25 mm, scan 12.5/0.5, τ = 1.0 sec.

6. *Gases Other Than* $C^{12}O_2^{16}$

The λ 0.87 μ band observed at Mt. Wilson allows a determination of the Martian CO_2 abundance; this subject is treated by Mr. Owen in *Comm.* No. 33 on the basis of two new calibrations. The spectra here reproduced allow, upon calibration, a determination of the atmospheric pressure and an estimate of the total quantity of constituents other than CO_2 (*Comm.* No. 32 by Owen and Kuiper). There remains to examine direct spectral evidence for both constituents other than CO_2 and isotopic bands.

Only one CO_2 *isotopic band* is distinctly visible, λ 2.15 μ of $C^{12}O^{16}O^{18}$ (Figures 17 and 19). The boundaries at 2.14 and 2.18 μ shown in Figure 17 were taken from the much stronger Venus absorption (*Comm.* No. 15). The profile is disturbed by the solar hydrogen line B7 whose equivalent width was found to be 1.8Å from the records of the Michigan Atlas and 3Å from Figure 18. With allowance for B7 the equivalent width of the 2.15 μ CO_2 band in Mars was from Figure 17 found to be 6.9 ± 1Å.

Laboratory calibrations were made at p = 6 cm and 12 cm, with path lengths 180, 360, 720, and 1440 meters. Two of the spectra are reproduced in Figure 22. The measured equivalent widths are listed in Table 5; each entry is based on two or three spectra.

TABLE 5

EQUIVALENT WIDTHS IN Å OF λ 2.15 μ ($C^{12}O^{16}O^{18}$)

PATHLENGTH	p = 6 cm	p = 12 cm
180 m.....	—	4.8
360 m.....	3.7	9.4
720 m.....	6.2	14.4
1440 m.....	8.65	22.5

The measures of Table 5 are plotted logarithmically in Figure 23a. The abscissae are the products of the abundance w (in meter-atm) and pressure p (in cm Hg); the ordinates are the equivalent widths (EW) in Å. The measures are well represented by

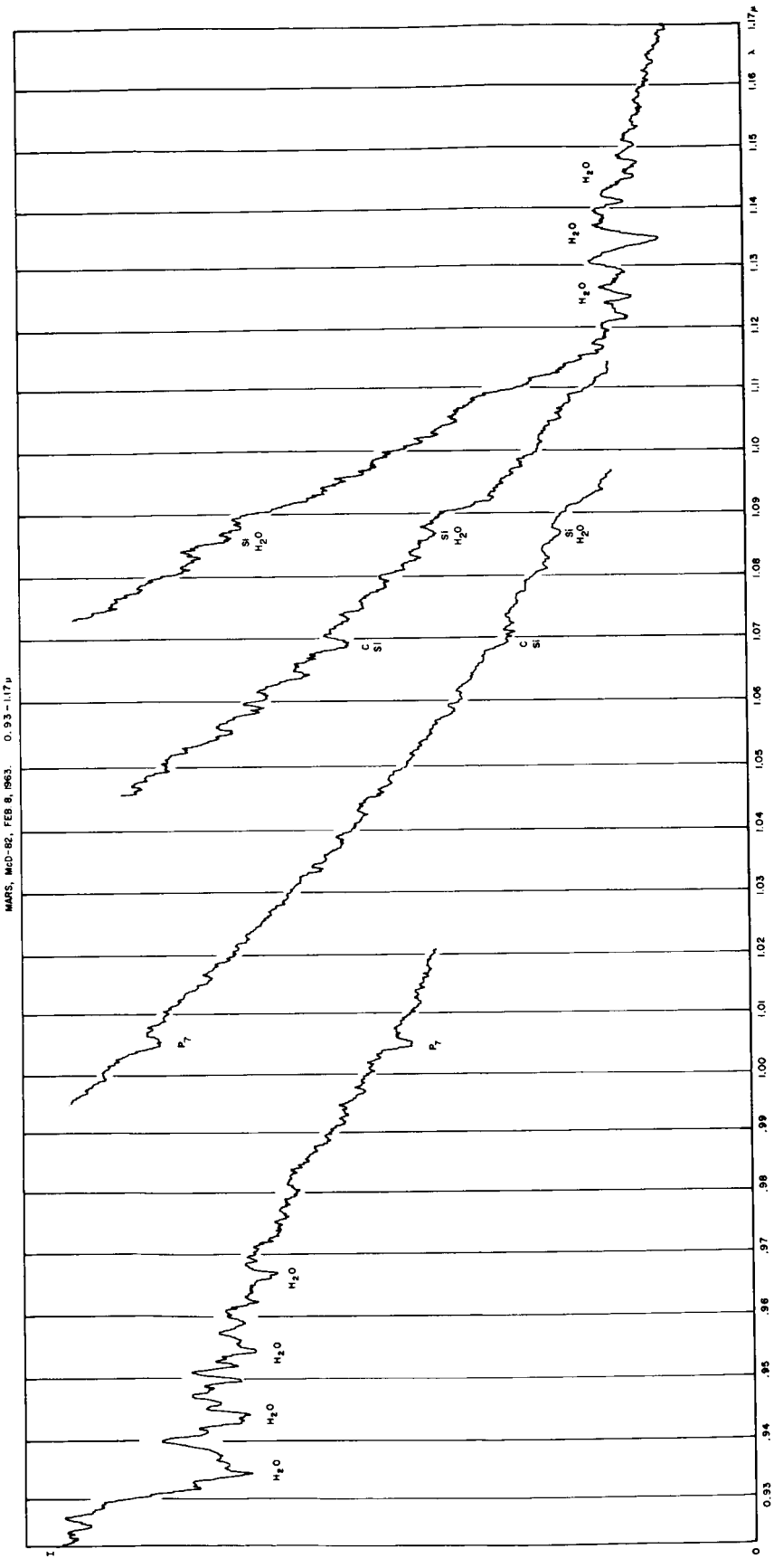

Fig. 6. Mars, 0.93-1.17 μ, February 8, 1963, overlapping scans with different gains. T = 51° F, H = 0.35, Dec. + 21°1, H.A. 0^h14^m-0^h21^m W, Cell S-1, 1.0 μ grating, RG 8 filter, 0.25 mm slits, scan 25/1 or approximately 0.01 μ/min (two right-hand traces), 12.5/0.5 or 0.02 μ/min (two left-hand traces); τ = 2 sec and 1 sec, respectively.

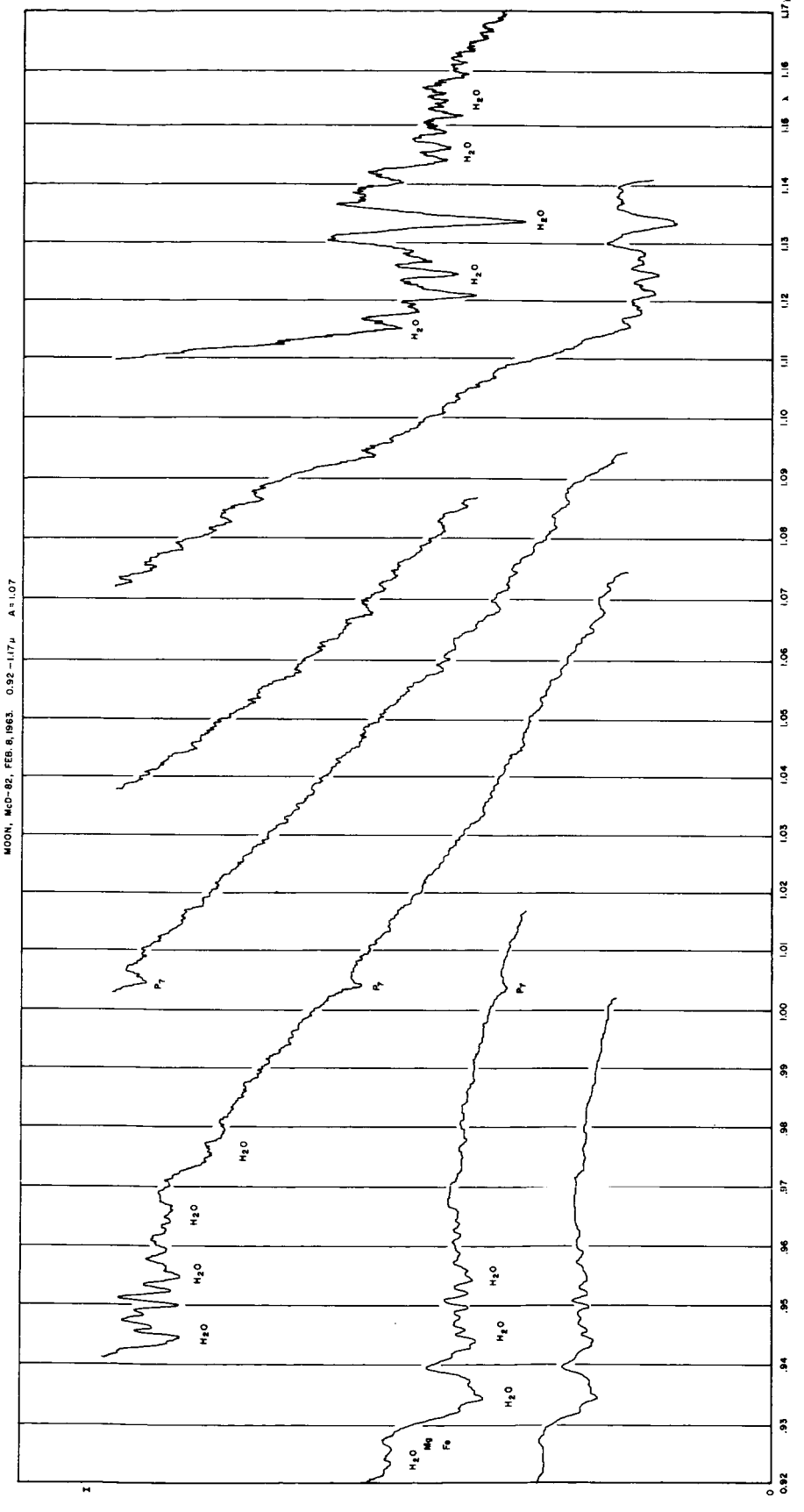

Fig. 7. Moon comparison for Figure 6, 0.92-1.17 μ, February 8, 1963, T = 51° F, H = 0.35, Dec. + 17°.3, air mass 1.07, Cell S-1, grating 1.0 μ, filter RG 8, slits 0.25 mm, scan 12.5/0.5, τ = 1 sec.

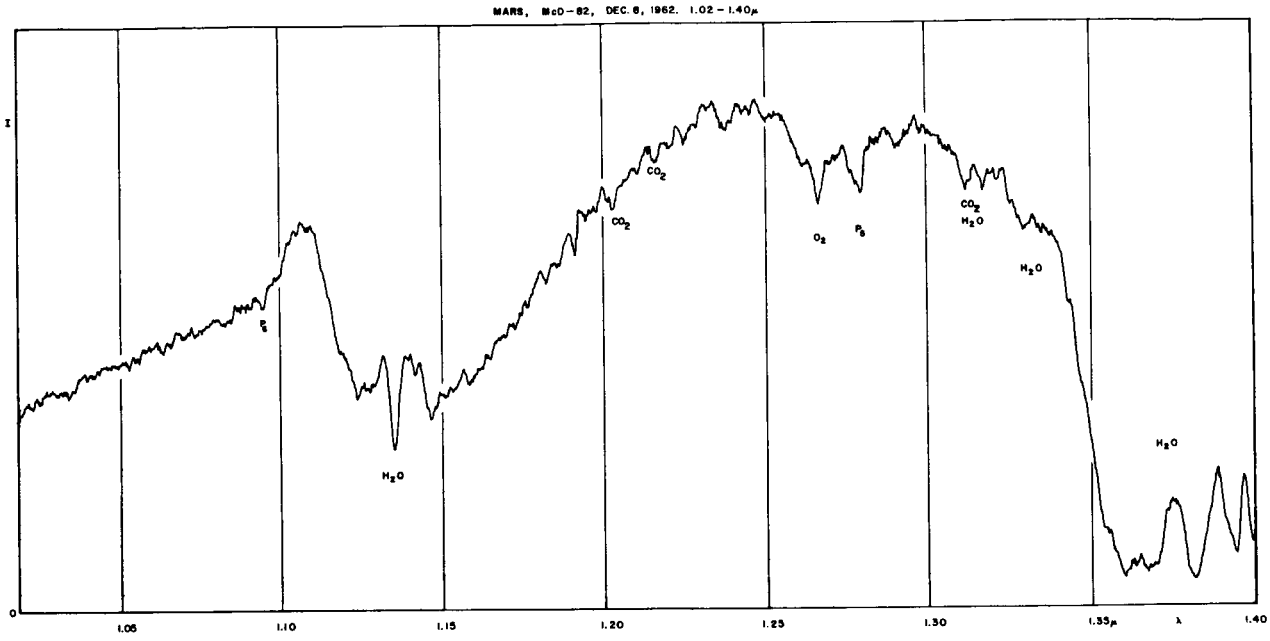

Fig. 8. Mars, 1.02-1.40 μ, December 8, 1962, T = 42° F, H = 0.55, Dec. + 16°4, H.A. 0^h12^m E - 0^h24^m W, 0.25 by 0.25 mm cell + Fabry lens, grating 1.6 μ, filter 2540 Corning, slits 0.7 and 1.0 mm, scan 25/2, τ = 5.5 sec.

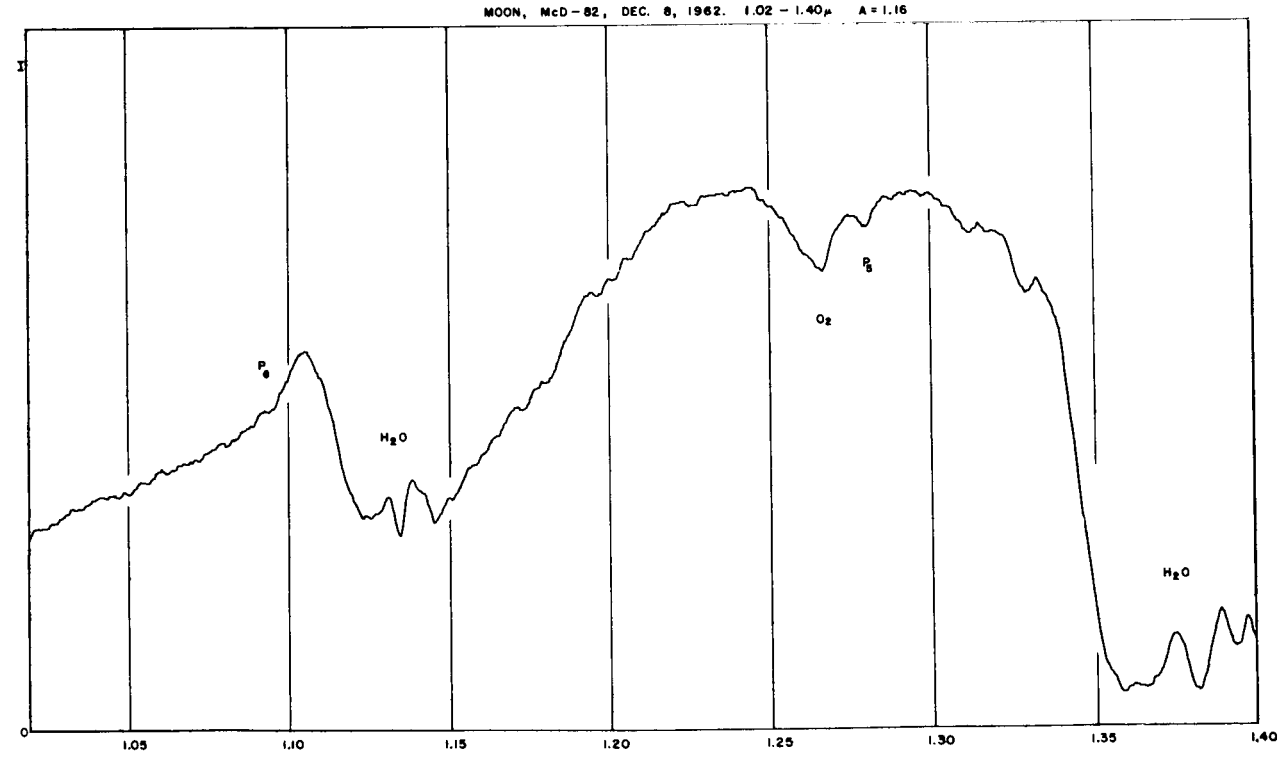

Fig. 9. Moon comparison for Figure 8, 1.02-1.40 μ, December 8, 1962, T = 42° F, H = 0.55, Dec. + 7°0, H.A. 1^h23^m-1^h30^m W, air mass 1.16, cell 0.25 by 0.25 mm + Fabry lens, grating 1.6 μ, filter 2540, slits 0.7 and 1.0 mm, scan 5/0.5, τ = 1 sec.

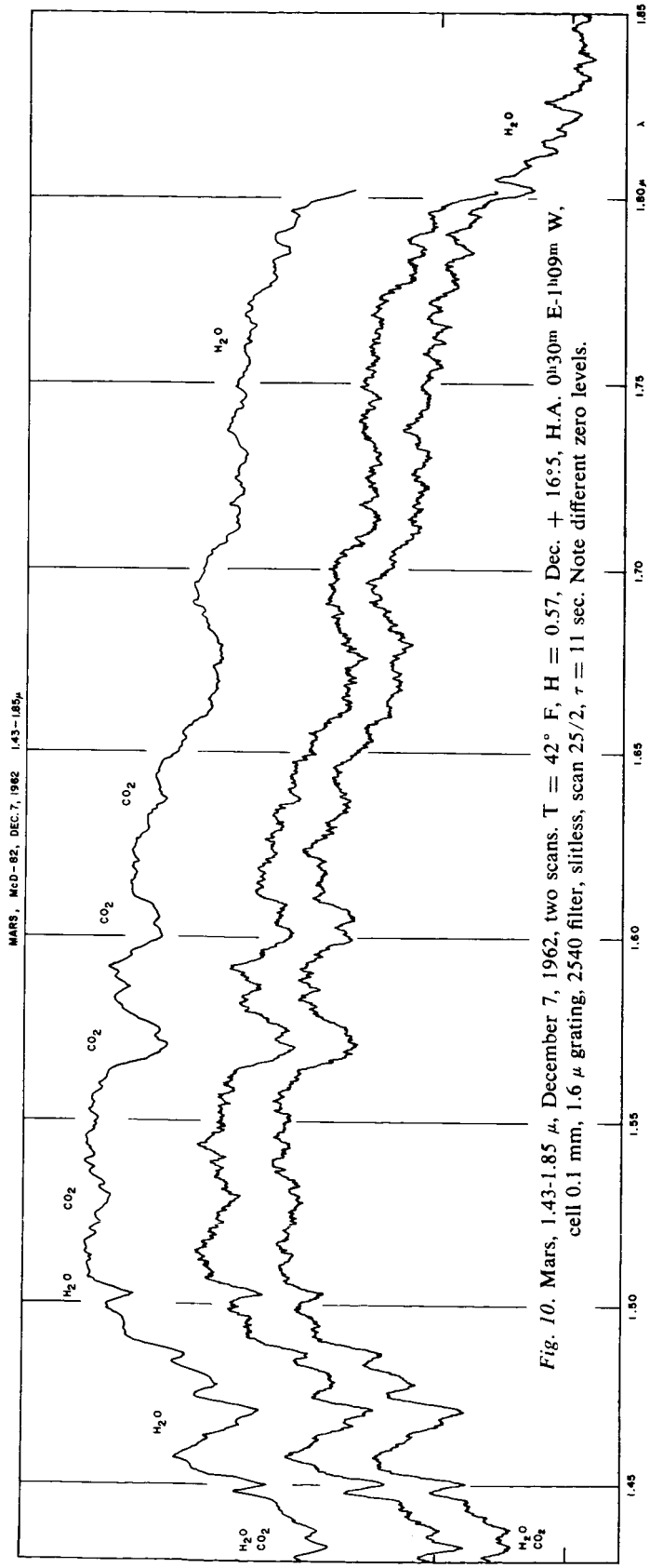

Fig. 10. Mars, 1.43-1.85 μ, December 7, 1962, two scans. T = 42° F, H = 0.57, Dec. + 16°.5, H.A. 0^h30^m E-1^h09^m W, cell 0.1 mm, 1.6 μ grating, 2540 filter, slitless, scan 25/2, τ = 11 sec. Note different zero levels.

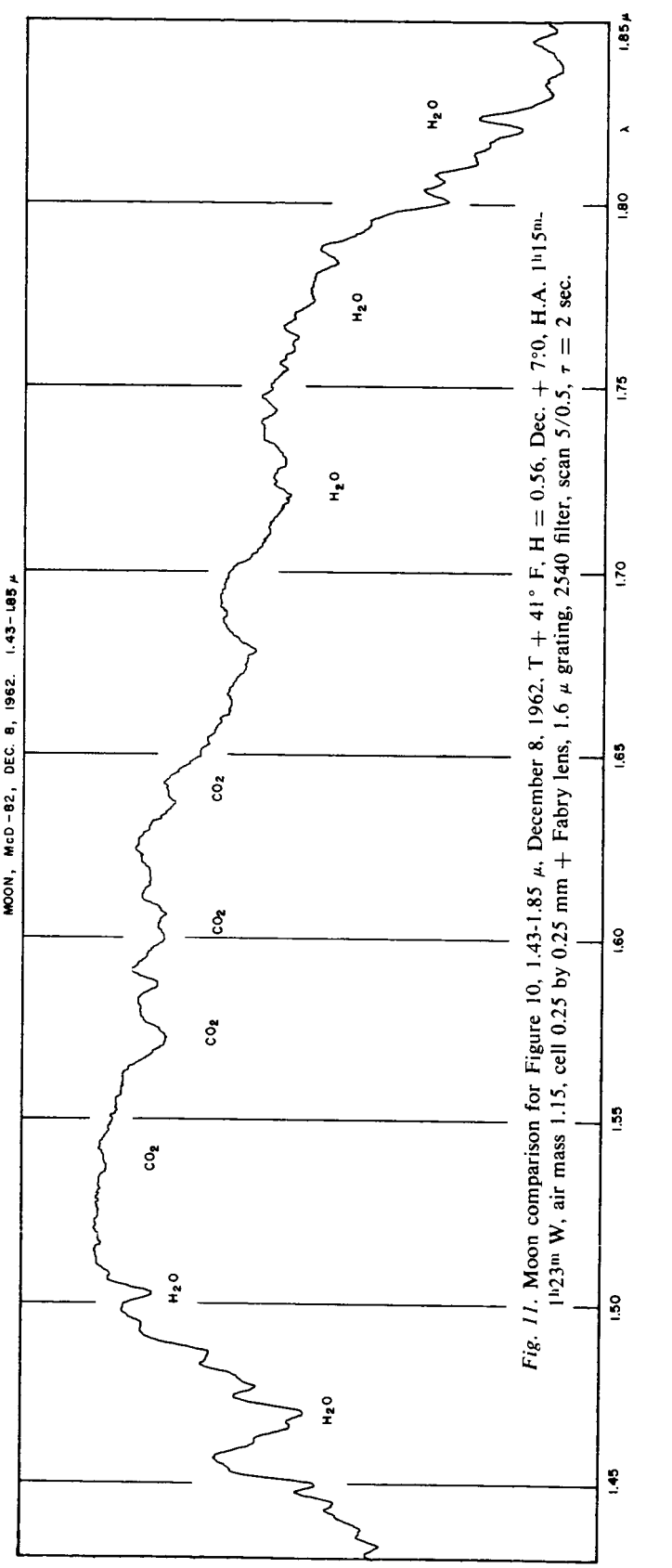

Fig. 11. Moon comparison for Figure 10, 1.43-1.85 μ, December 8, 1962, T + 41° F, H = 0.56, Dec. + 7°.0, H.A. 1^h15^m-1^h23^m W, air mass 1.15, cell 0.25 by 0.25 mm + Fabry lens, 1.6 μ grating, 2540 filter, scan 5/0.5, τ = 2 sec.

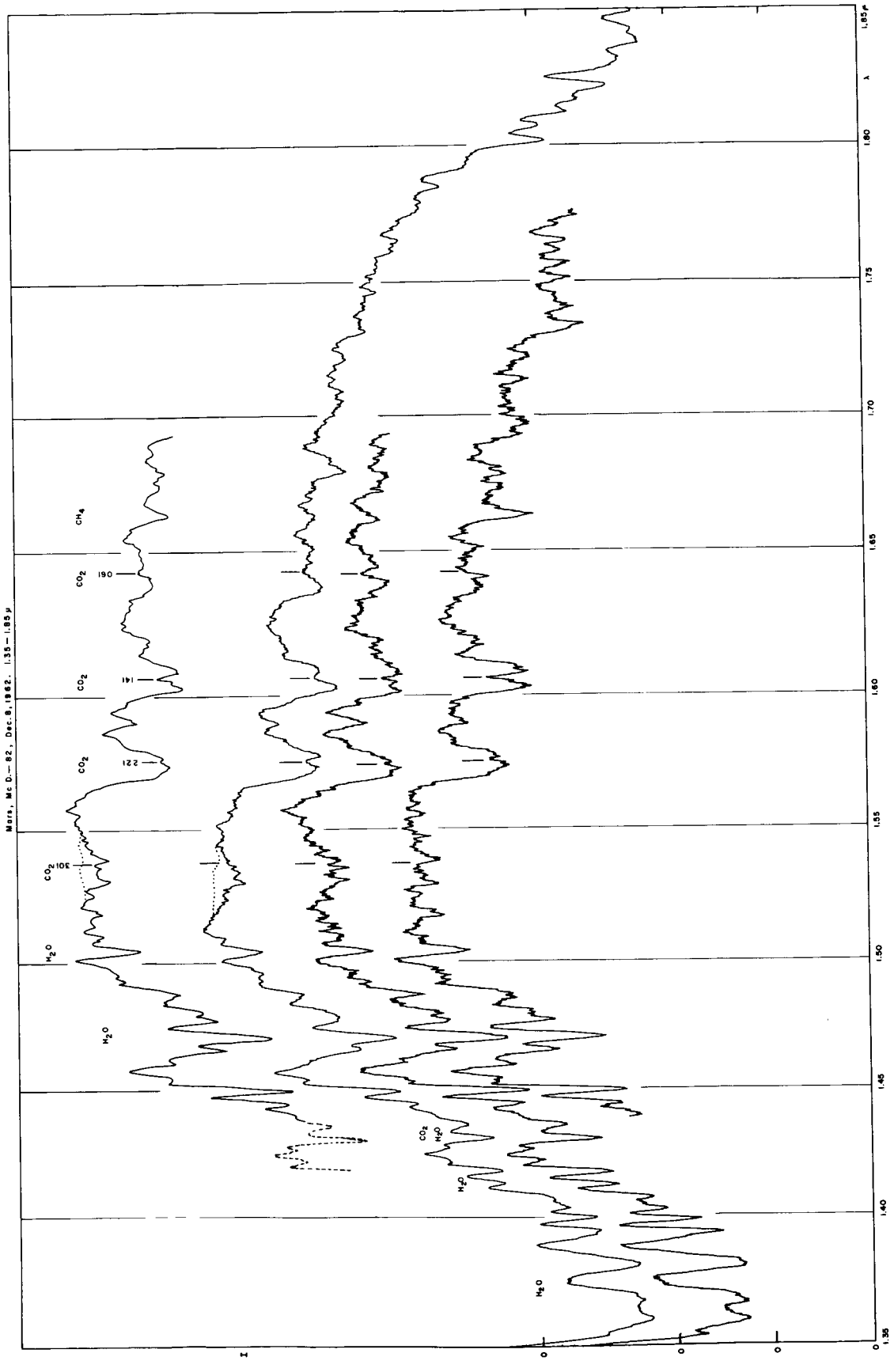

Fig. 12. Mars, 1.35-1.85 μ, December 8, 1962, three scans. T = 42° F, H = 0.55, Dec. + 16°.4, 0.25 by 0.25 mm cell + Fabry lens, 1.6 μ grating, 2540 filter, slits 0.7 and 1.0 mm, scan 25/2. *Upper* spectrum: H.A. 1^h09^m-0^h19^m E (after this, Figure 8 was recorded), τ = 11 sec; *middle* spectrum: H.A. 0^h28^m-1^h02^m W, τ = 5.5 sec; *lower* spectrum: H.A. 1^h05^m-1^h38^m W, τ = 5.5 sec. Graph on top is *average* of two lowest (τ = 5.5 sec) scans.

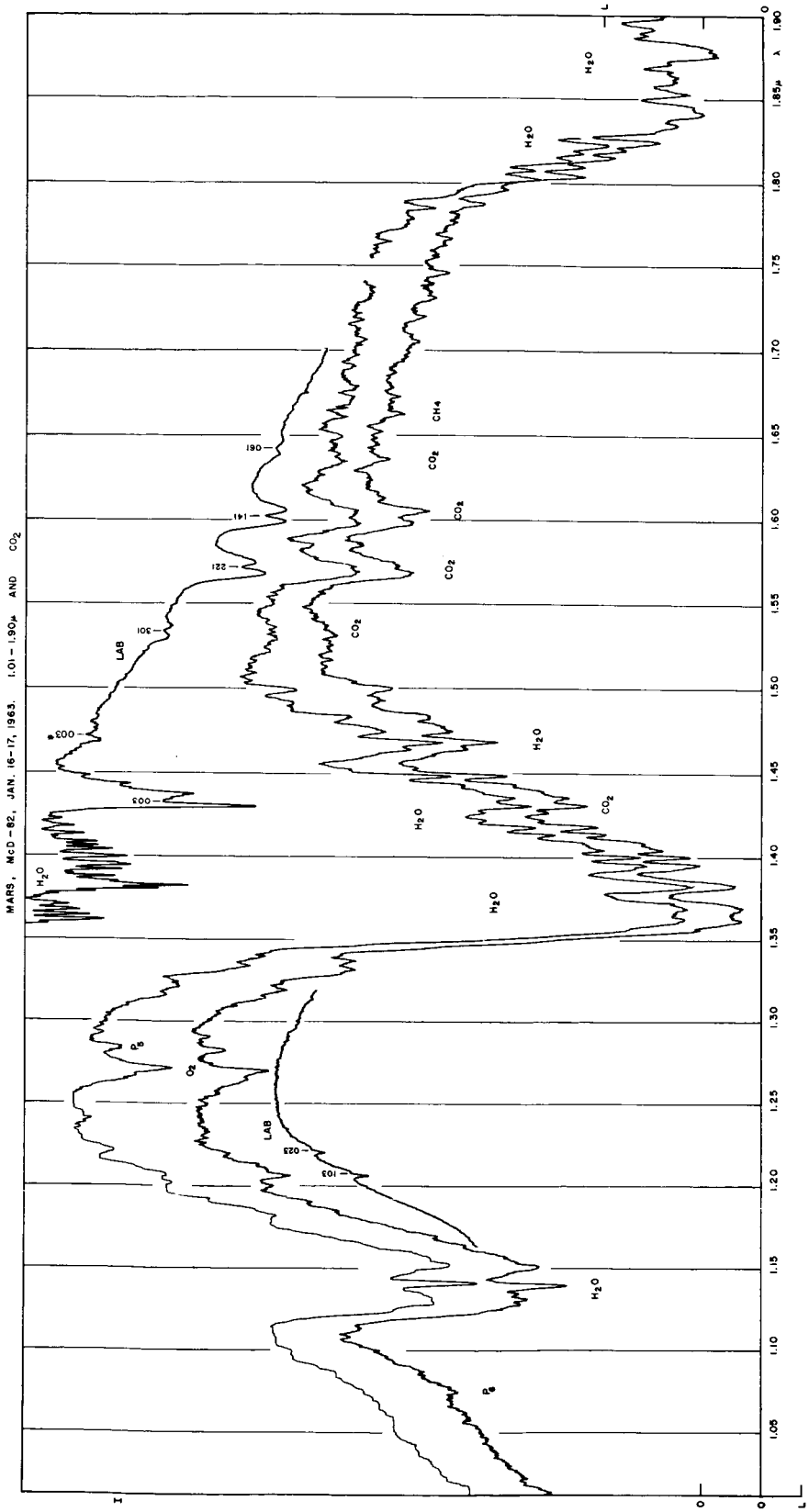

Fig. 13. Mars, 1.01-1.90 μ, Dec. + 18°.3, two scans, cell 0.1 mm, 1.6 μ grating, 2540 filter, first slit 1.0 mm, scan 12.5/2, $\tau = 5$ sec. *Lower* spectrum: January 16, 1963, T = 33° F, H = 0.50, H.A. 2^h57^m-3^h40^m W. *Upper* spectrum: January 17, 1963, T = 39° F, H = 0.51, H.A. 1^h00^m-1^h40^m W. CO_2 for comparison, 80-meter path at $p = 17$ cm.

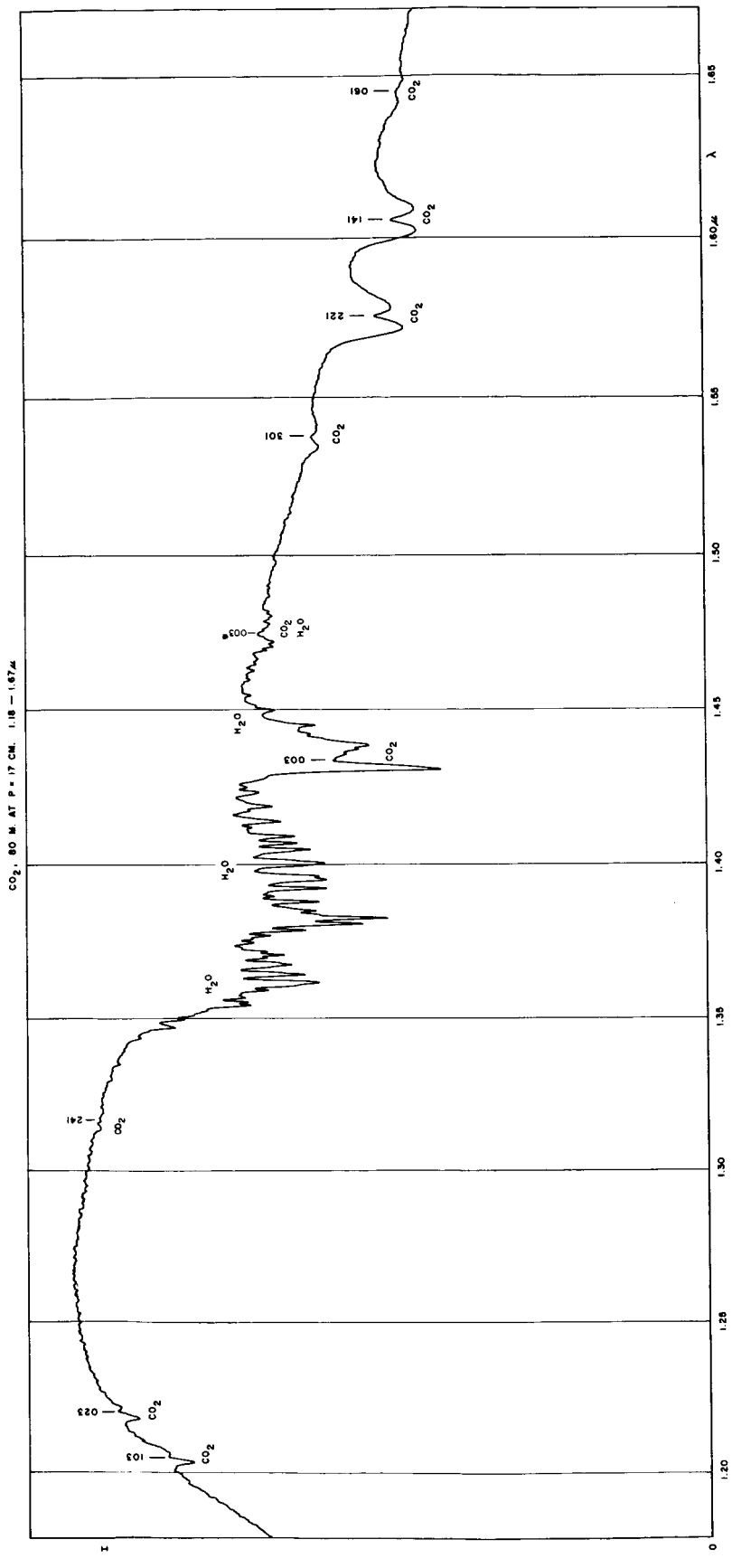

Fig. 14. Laboratory spectrum, 80 meters of CO_2 at $p = 17$ cm. Residual H_2O in laboratory and spectrometer, amount roughly 0.1 mm precipitable water; cell 0.25 mm, 1.6 μ grating, 2540 filter, slit 0.3 mm, scan 12.5/1, $\tau = 1$ sec.

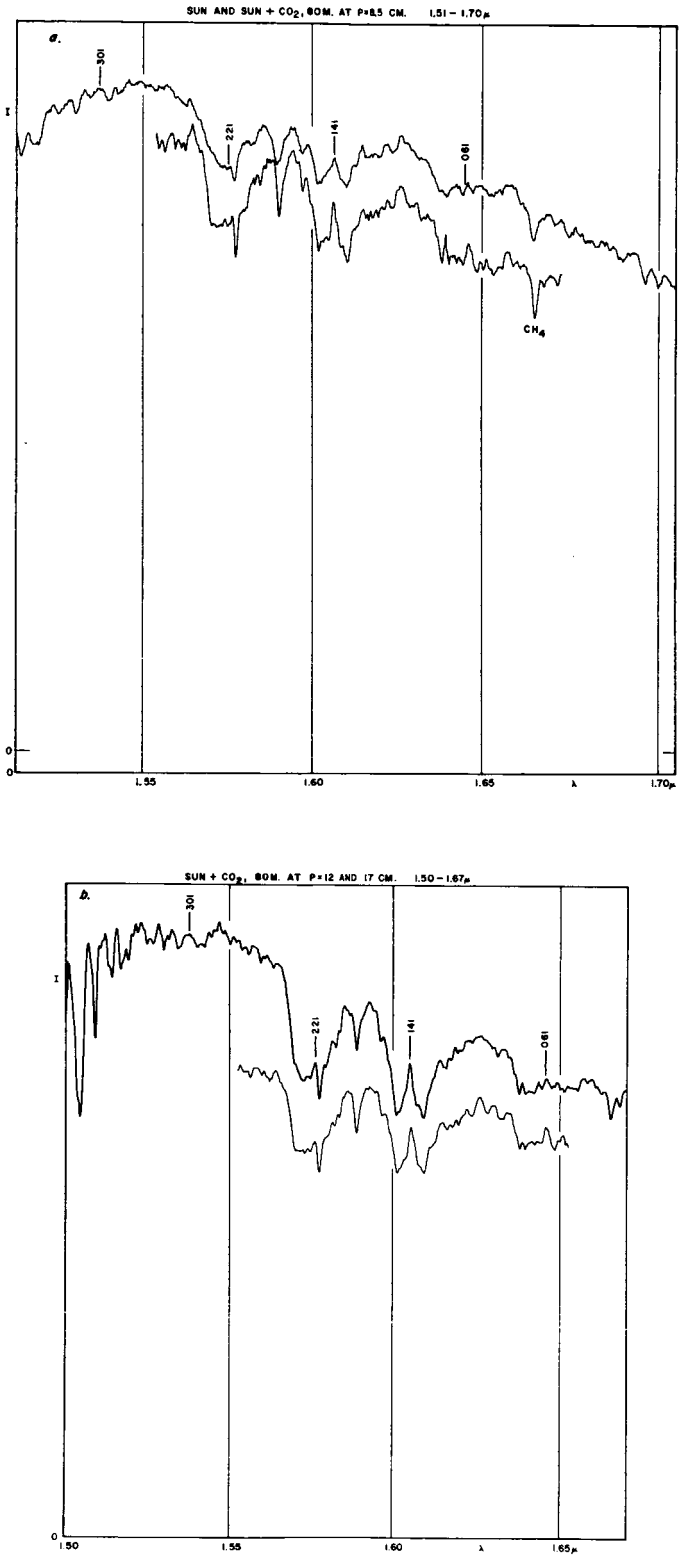

Fig. 15. Solar spectra, 1.50-1.70 μ, June 13 and 14, 1963, observed through 80 meters of CO_2 at $p = 0$, 8.5, 12, and 17 cm, for comparison with 1.6 μ Mars bands; 0.25 mm cell, 1.6 μ grating, 2540 filter, 0.3 mm slit, scan 12.5/1, $\tau = 1$ sec.

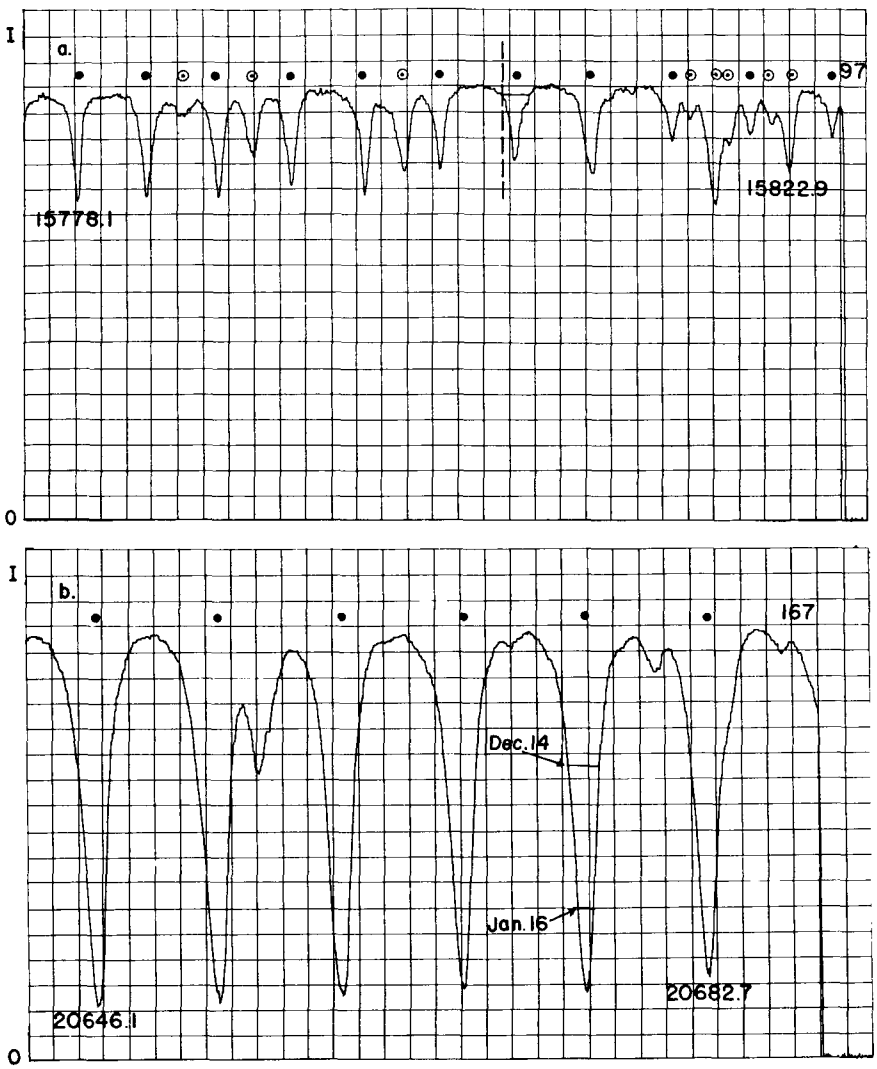

Fig. 16. Two small sections of Michigan Atlas of solar spectrum; dots signify telluric components. Displaced positions of Martian CO_2 lines indicated; (a) λλ 15775-15826 Å, Mars Dec. 8, 1962, V = −13.6 km/sec, Δλ = 0.72 Å; (b) λλ 20642-20689 Å, Mars Dec. 14, 1962, V = −13.2 km/sec, Δλ = −0.91 Å; and Jan. 16, 1963, V = −6.5 km/sec, Δλ = −0.45 Å.

Fig. 17. Mars, 1.90-2.50 μ, December 14, 1962, two scans. T = 40° F, H = 0.81, Dec. + 16°3, 0.25 by 0.25 mm cell + Fabry lens, 2 μ grating, 2 μ filter, slitless, (Mars image ≃ 1.5 mm) and 1.0 mm, scan 25/2, τ = 5.5 sec. *Lower* spectrum: H.A. 0^h11^m-0^h39^m W, *upper* spectrum: H.A. 0^h48^m-1^h16^m W. Dotted line represents lunar comparison profile, Figure 18. Vertical lines at λ = 2.14 and 2.18 μ are boundaries of 2 ν_3 isotopic band of CO_2 as observed on Venus. Martian absorption is confined between these boundaries, confirming identification.

Fig. 18. Moon, 1.92-2.50 μ, December 14, 1962, three scans, for comparison with Mars in Figure 17. T = 41° F, H = 0.81, Dec. + 19°8, 0.25 by 0.25 mm cell + Fabry lens, 2 μ grating, 2 μ filter, slits 1.5 and 1.0 mm, scan 5/0.5, τ = 1 sec. *Upper* spectrum: H.A. 1^h11^m-1^h17^m W, *middle* spectrum: H.A. 1^h19^m-1^h25^m W, *lower* spectrum: H.A. 1^h33^m-1^h39^m W.

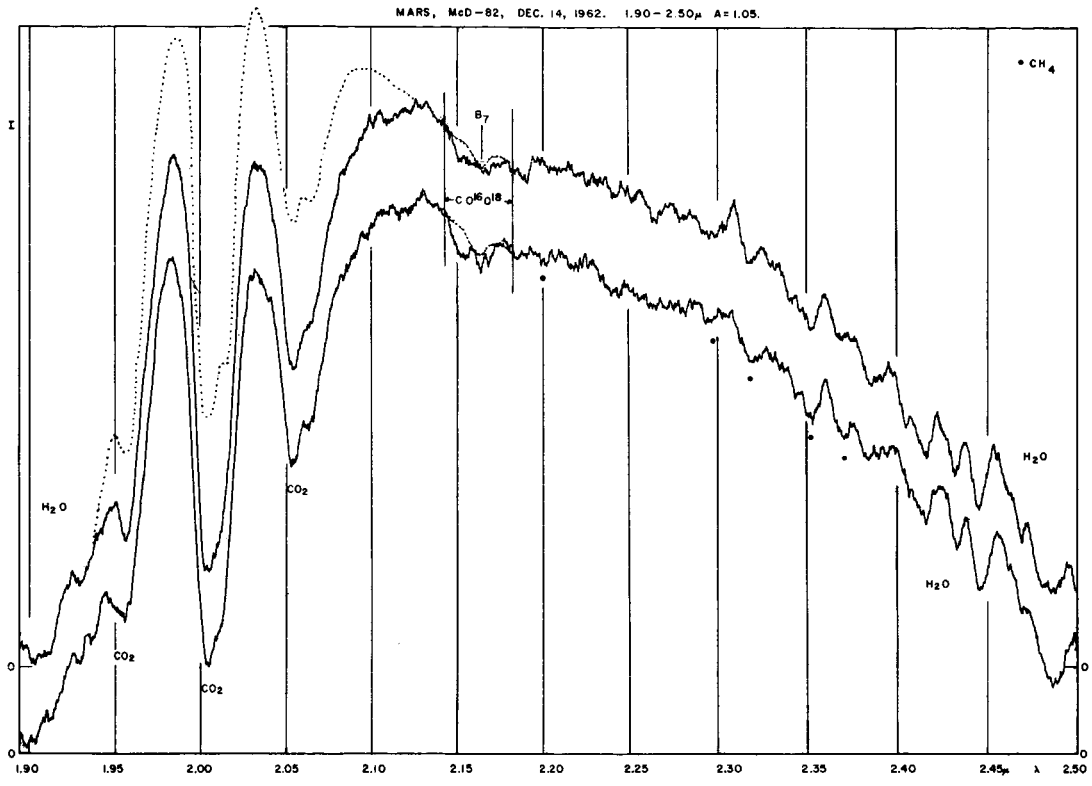
MARS, McD-82, DEC. 14, 1962. 1.90-2.50μ A=1.05.
• CH4
I
B7
C O16O18
H2O
CO2
CO2
CO2
H2O
H2O
0
0
0
1.90
1.95
2.00
2.05
2.10
2.15
2.20
2.25
2.30
2.35
2.40
2.45μ
λ
2.50

17.

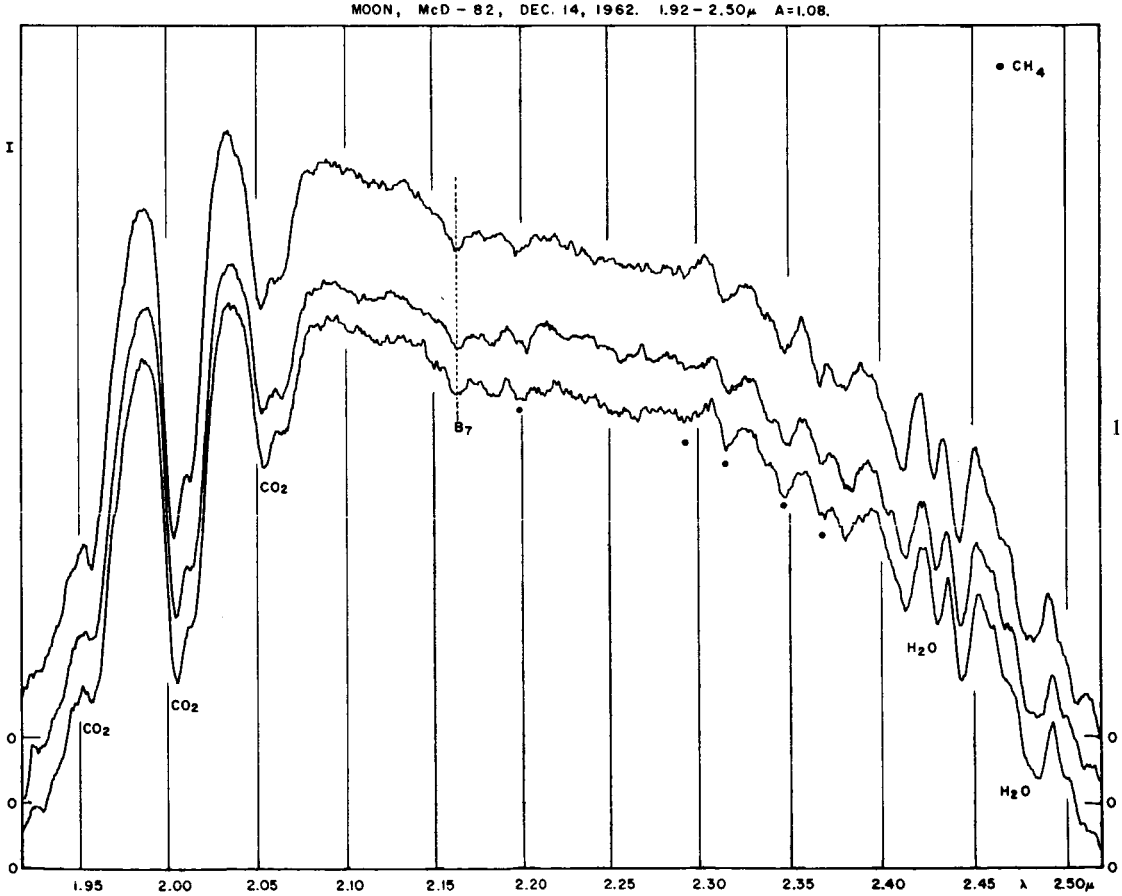
MOON, McD - 82, DEC. 14, 1962. 1.92 - 2.50μ A=1.08.
• CH4
I
B7
CO2
CO2
CO2
H2O
H2O
0
0
0
0
0
0
1.95
2.00
2.05
2.10
2.15
2.20
2.25
2.30
2.35
2.40
2.45
λ
2.50μ

18.

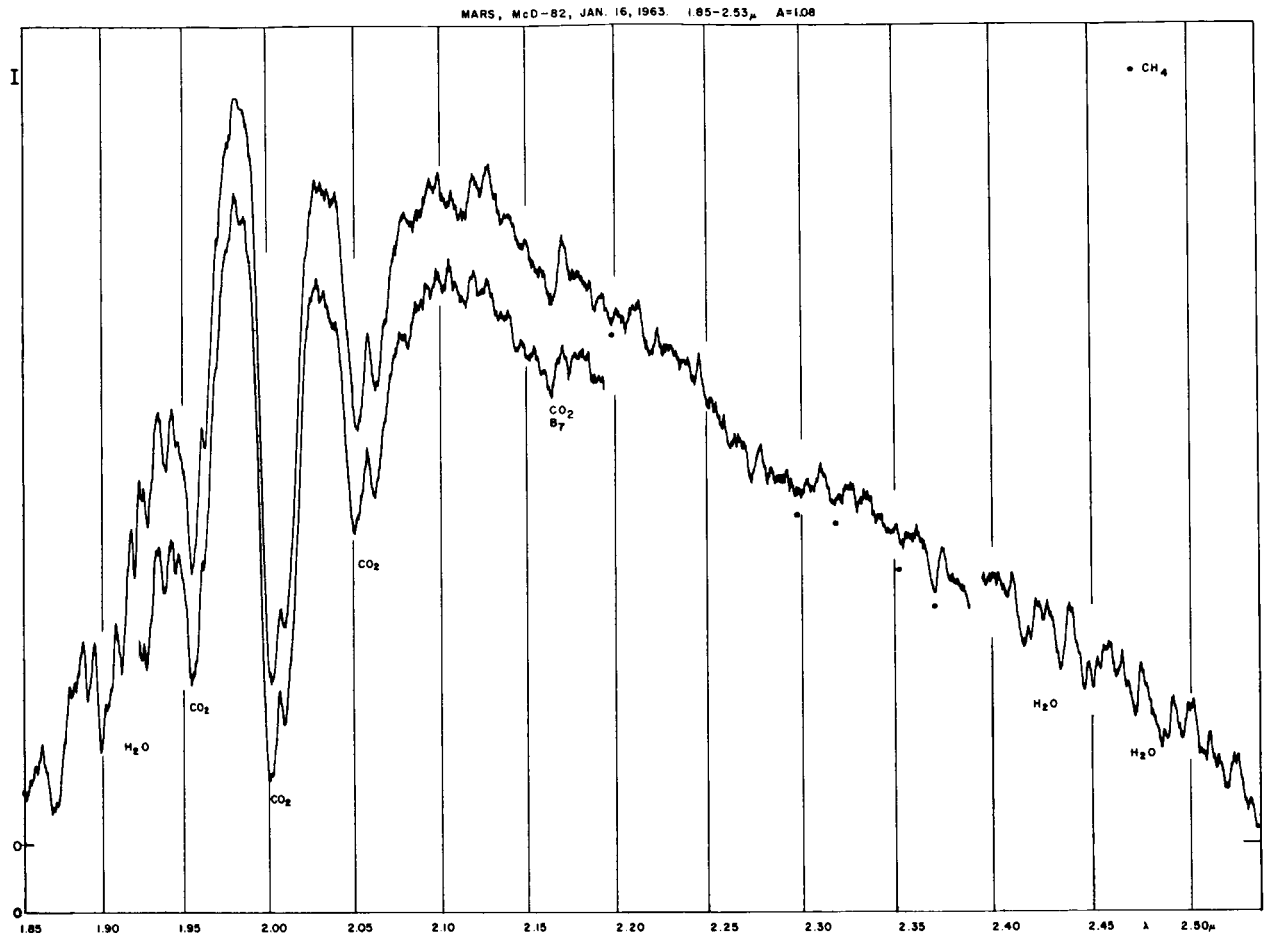

Fig. 19. Mars, 1.85-2.53 μ, January 16, 1963, two scans. T = 33° F, H = 0.52, Dec. + 18°2, cell 0.1 mm, 1.6 μ grating (increased resolution), 2 μ filter, slitless and 1.0 mm slit, scan 25/5, τ = 20 sec. *Lower* spectrum: H.A. 2^h12^m-2^h49^m, *upper* spectrum: H.A. 0^h38^m-2^h08^m W.

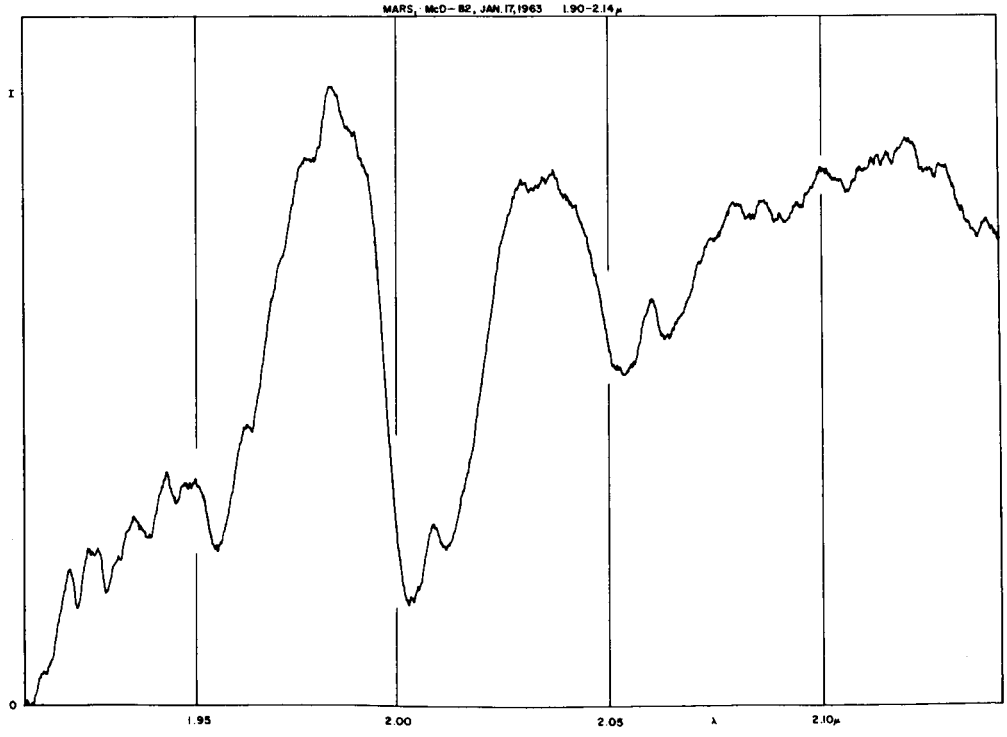

Fig. 20. Mars, 1.90-2.14 μ, January 17, 1963, Dec. + 18°3, H.A. 2^h36^m-3^h02^m W, cell 0.1 mm, 1.6 μ grating (increased resolution), 2 μ filter, slitless and 1.0 mm, scan 25/2, τ = 20 sec.

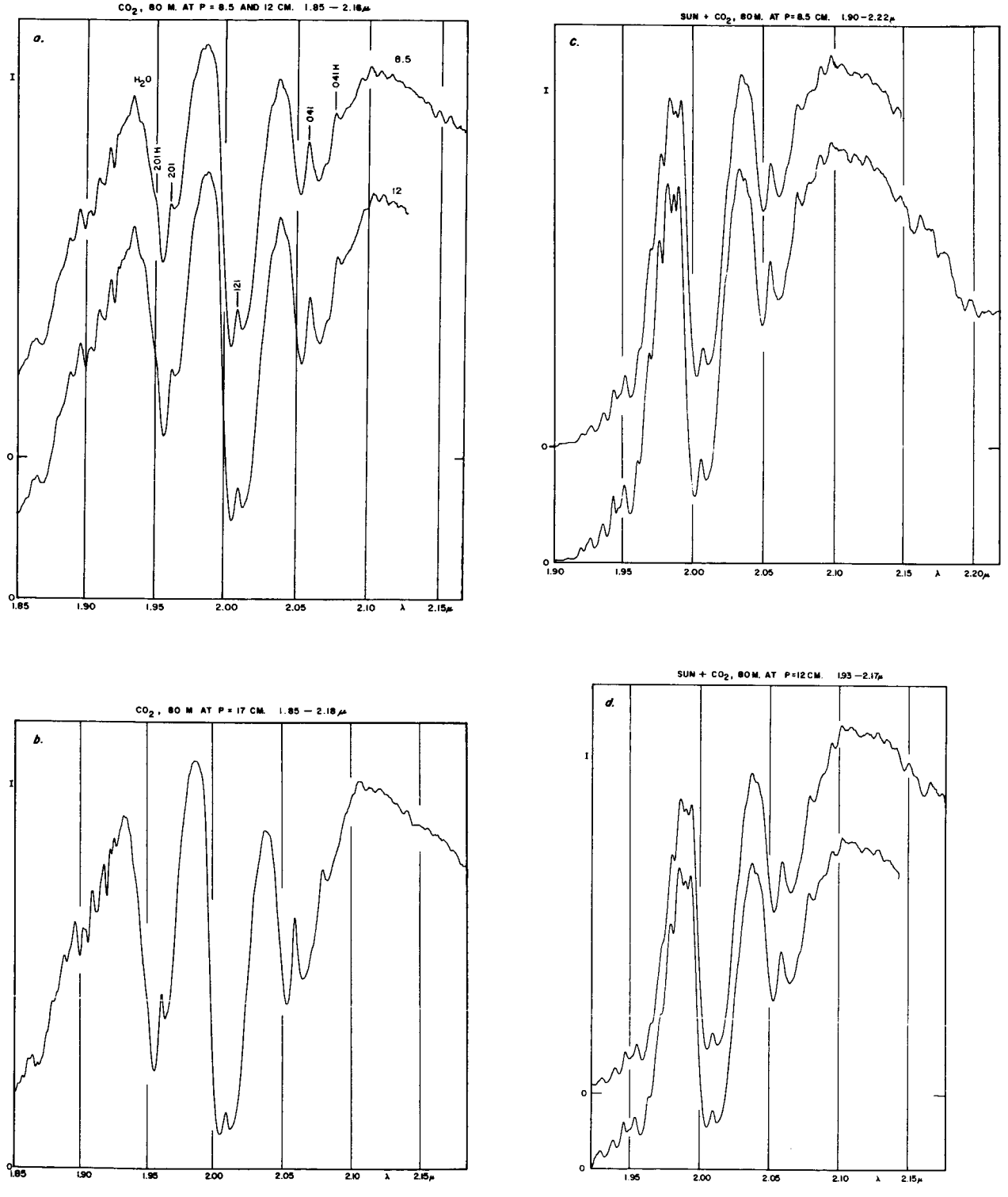

Fig. 21. a, b: Laboratory spectra of CO_2, 1.85-2.17 μ, 80 meters at $p = 8.5$, 12, and 17 cm: *c, d*: solar spectra, 1.90-2.20 μ, observed through 80 meters of CO_2 at $p = 8.5$ and 12 cm; June 13 and 14, 1963; all with 0.25 mm cell, 2 μ grating, 2 μ filter, 0.3 mm slit, scan 12.5/1.

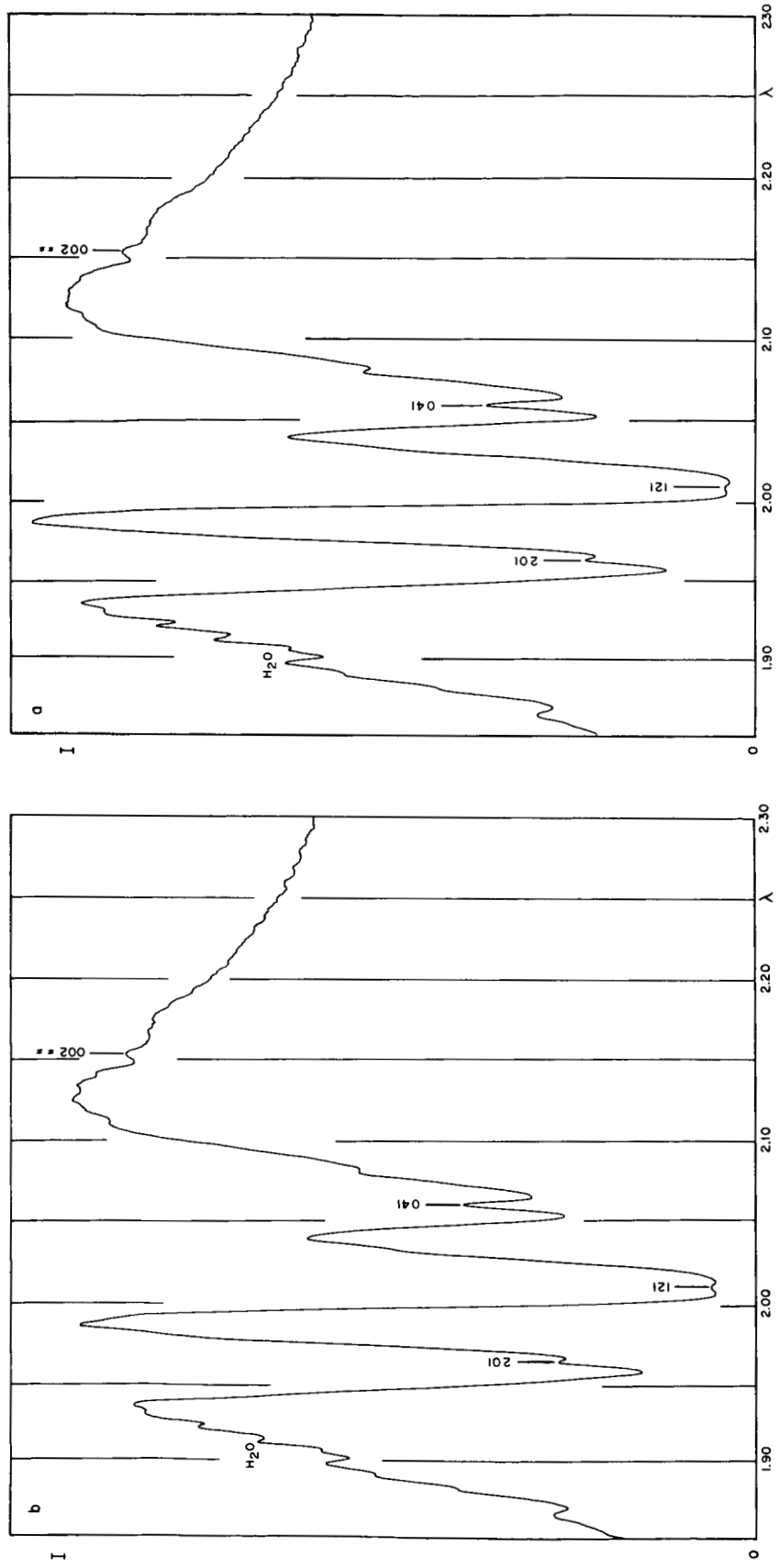

Fig. 22. Laboratory spectra of CO_2, 1.85-2.30μ. (a) 360 meters at $p = 12$ cm. (b) 1440 meters at $p = 6$ cm. Cf. measures in Table 5.

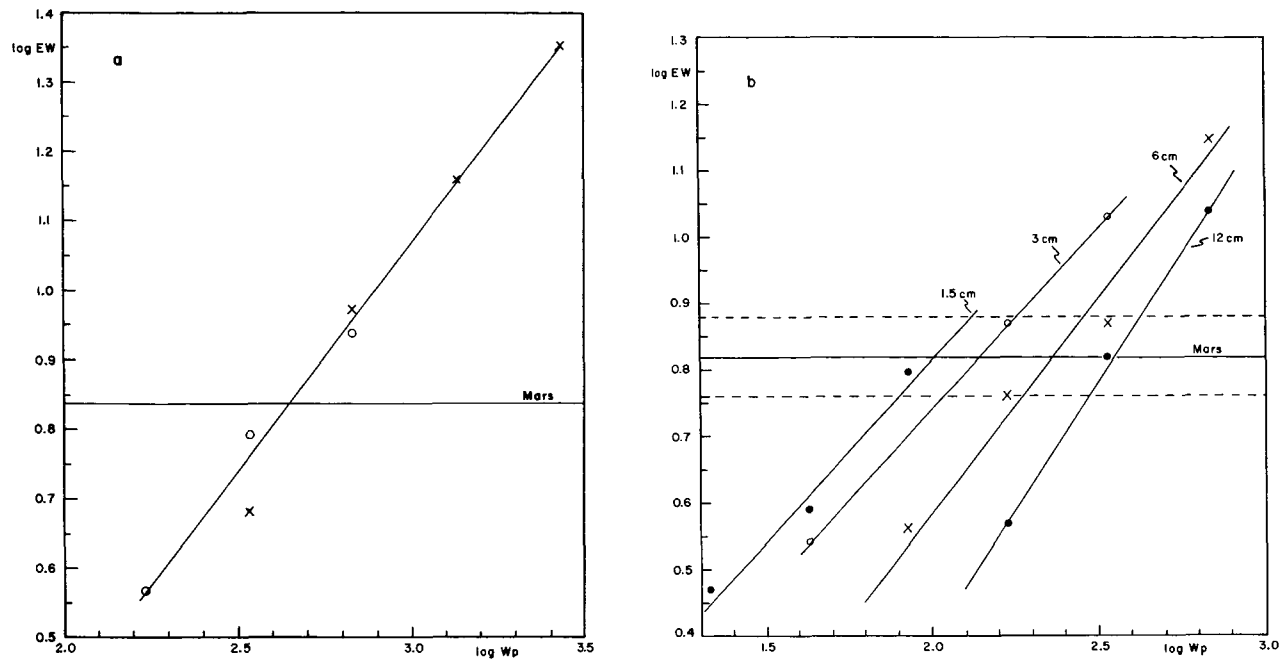

Fig. 23. (a) Equivalent widths (EW) in Å vs. *wp* for λ 2.15 μ of $C^{12}O^{16}O^{18}$ based on laboratory measures (Cf. Table 5) with intensity of band in Mars spectra indicated. (b) Measurements of λ = 1.5377 μ band of $C^{12}O_2^{16}$ for comparison with isotopic band shown in (a), with intensity of Mars band and its margin of uncertainty indicated.

the linear relation

$$\log EW = 0.654 \log wp - 0.894. \qquad (5)$$

The coefficient of *wp* indicates that EW increases with a power of *wp* intermediate between 1 and ½ (in accordance with the fact that the band is rather weak). If this relationship holds down to the low mean pressure of the Martian atmosphere (with the rotational lines getting narrower but deeper, keeping EW constant) then one finds from EW = 7Å the value of log *wp* = 2.65. In part because the pressure broadening of the Martian CO_2 bands is caused mostly by gases other than CO_2 (cf. *Comm.* No. 32), the appropriate value of *p* in the derivation of *w* is not readily estimated.[1] Therefore, a differential method is used, comparing the λ 2.15 μ band of $C^{12}O^{16}O^{18}$ with a band of similar strength due to $C^{12}O_2^{16}$, the 301 band at λ = 1.5377. This latter band has on the Mars spectra of Figure 12 a mean EW = 6.6 ± 1Å; the dotted lines shown are based on the lunar spectrum of Figure 11.

Laboratory calibrations of the 301 band were taken from the spectral runs made for *Comm.* No. 32. The results are listed in Table 6, and are plotted in Figure 23b. Clearly, the representation of EW by *wp* is not very suitable for this band. The cause for this is seen from Figure 14 of *Comm.* No. 32, which shows that the pressure dependence of EW is not $p^{1/2}$ but $p^{1/4}$, though the dependence on *w* is not far from $w^{1/2}$. As a result the values obtained at lower pressures are displaced to the left in the diagram. The intersect of the relation for the equivalent Martian pressure is therefore uncertain[1] but definitely occurs well below log *wp* = 2.65, defined in Figure 23a. This indicates that the O^{18}/O^{16} ratio in the Martian atmosphere is *larger* than in the terrestrial atmosphere. A more complete laboratory study of this problem is being undertaken and distinctly improved observations of Mars will be possible early 1965 with a 5-inch beam IR spectrometer now completed. The precise O^{18}/O^{16} ratio for Mars is, of course, of great interest for the photochemical history of the Martian atmosphere and the Martian escape rate of oxygen.

Another isotopic band, λ 1.47 μ of $C^{13}O_2^{16}$, is in Figures 12 and 13 too heavily contaminated with telluric H_2O to give the C^{13}/C^{12} isotopic ratio, which for Venus was indeed determinable. It should be possible to detect this band from a high-altitude station, where a Martian spectrum somewhat resembling Figure 14 should be obtainable.

Other gases whose presence was tested are

[1]The discussion in *Comm.* No. 32 would indicate that for $C^{12}O_2^{16}$, $w \simeq 150$, $p \simeq 0.3$, $\log pw \simeq 1.7$.

TABLE 6

EQUIVALENT WIDTHS IN Å OF λ 1.538 OF $C^{12}O_2^{16}$
(second entries are logarithms)

PATHLENGTH (METERS)	$p = 1.5$ cm		$p = 3$ cm		$p = 6$ cm		$p = 12$ cm	
90	....	....	....	....	....	....	3.7	0.57
180	....	....	....	....	3.66	0.563	6.6	0.82
360	....	....	3.45	0.54	5.76	0.76	11.0	1.04
720	2.97	0.47	5.05	0.70	7.4	0.87	....	....
1440	3.9	0.59	7.45	0.87	14.05	1.148	....	....
2880	6.27	0.797	10.8	1.033	....	....	....	....

CO, CH_4 NH_3, H_2S, NO, N_2O, $COCl_2$, HCHO, and COS. The discussion follows an earlier effort (Kuiper 1952, Table 9) but with increased resolution. The results are all negative, with the limits attained stated below. The precision can probably be improved by a further order of magnitude during the next Mars opposition with improved equipment now completed.

The CO test is best made from the (2,0) band at λ 2.35 μ. The laboratory calibration may be taken from Figure 25 of the Venus study (*Comm.* Vol. 1, p. 115). No evidence for the presence of CO was found, with 4 cm atm placed as the upper limit. This corresponds to *1 cm atm in a vertical column on the planet.*

For the other gases it was necessary to obtain new laboratory comparisons. This work was done jointly with Mr. Dale Cruikshank, graduate-student assistant in this Laboratory. Because of the interest these laboratory runs have for future work as well, a set of them is being published in *Comm.* No. 34.

Several CH_4 bands are suitable for the tests: at λ 1.6657 μ, 2.199 μ, the overlapping system between 2.25-2.30 μ, the bands at 2.3165 μ and 2.373 μ. These features have been marked with dots in Figures 12, 13, 17, and 18. A close comparison between the lunar records and those of Mars show that within the precision of the data the CH_4 features in the Mars spectra are entirely telluric, which puts an upper limit of about 0.4 cm atm for the Martian contribution or 1 mm in a vertical column on the planet. This limit is 100 times less than the earlier limit (Kuiper, 1952).

The ammonia tests yield the following results. The λ 1.515 μ band gives for Mars $\leq$ 11 cm at 10 cm pressure or 1.5 cm atm. The λ 1.98 μ band gives $<$ 0.5 cm atm, 1/3 of the above amount, also observed at $p = 10$ cm. The NH_3 bands between 2.2-2.3 μ give $<$ 0.4 cm atm at $p = 10$ cm. The amount in a vertical column is therefore $<$ 1 mm atm measured at $p = 10$ cm, an amount 20 times less than the limit derived previously (Kuiper, 1952).

For N_2O no strong bands exist for $1\mu < \lambda < 2\mu$. The band at λ 2.10 μ makes the Martian equivalent absorption $<$ (2/3) 11 cm path at $p = 3$ cm; whereas the λ 2.25 μ yields $\leq$ 11 cm at $p = 3$ cm. The former test is therefore somewhat sharper and yields 0.3 cm atm at $p = 3$ cm or 0.8 mm atm for the vertical column (measured at $p = 3$ cm), an improvement by the factor of 2500 over the earlier limit (Kuiper, 1952).

The tests for NO are not sensitive. The λ 1.79 μ band gives $<$ 60 cm at 1.26 atm. The upper limit for the vertical column is therefore approximately 20 cm atm, measured at $p = 1.26$.

The test for H_2S in the spectral region covered is not sensitive either. The λ 1.58 μ band gives $<$ 30 cm at $p = 1$ atm or $<$ 7.5 cm atm for the vertical column.

A test was made for $COCl_2$ but no prominent bands exist between 1-2.5μ for a 10 cm path at 1 atm; the test must be repeated in another spectral region.

HCHO (formaldehyde) shows a prominent band at 2.27 μ with 11 cm path at 1 atm. The Martian content of this gas is well below one-tenth of this amount or $<$ 0.3 cm atm in the vertical column.

COS (carbonyl sulphide) was examined on a 5 cm path at $p = 1$ atm. A very strong band occurs at 2.44 μ. The Martian atmospheric content must be $<<$ 0.2 cm atm in a vertical column.

The problem of NO_2 (nitrogen dioxide), a widely debated topic, is examined by Mr. Marshall in *Comm.* No. 35. Because many electronic bands can be observed in the accessible photographic region the best test for the presence of this gas on Mars is not in the infrared but in the photographic spectrum.

7. *Ratio Spectra, Mars : Moon*

The Martian and lunar records here reproduced allow the derivation of approximate *ratio spectra* in which the spectral distribution of Mars is expressed

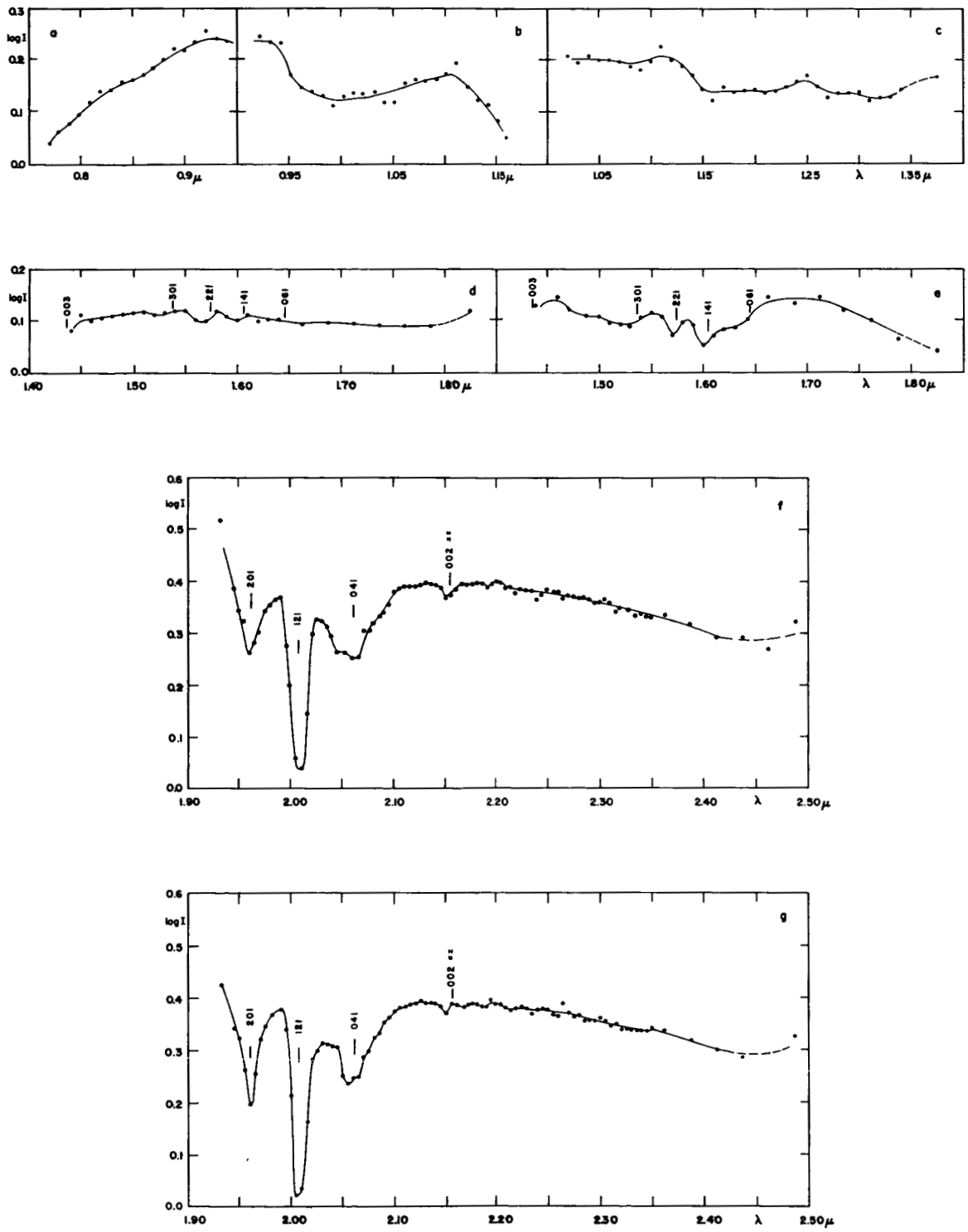

Fig. 24. Spectral intensity ratios Mars/Moon, on logarithmic scale (a) 0.75-0.96 μ, from Figs. 4 and 5; (b) 0.92-1.17 μ, Figs. 6 and 7; (c) 1.02-1.4 μ, Figs. 8 and 9; (d) 1.43-1.85 μ, Figs. 10 and 11; (e) 1.43-1.85 μ, Figs. 12 and 11; (f) 1.92-2.5 μ, Figs. 17 and 18 (measured by GPK); (g) 1.92-2.5 μ, Figs. 17 and 18 (measured by SML).

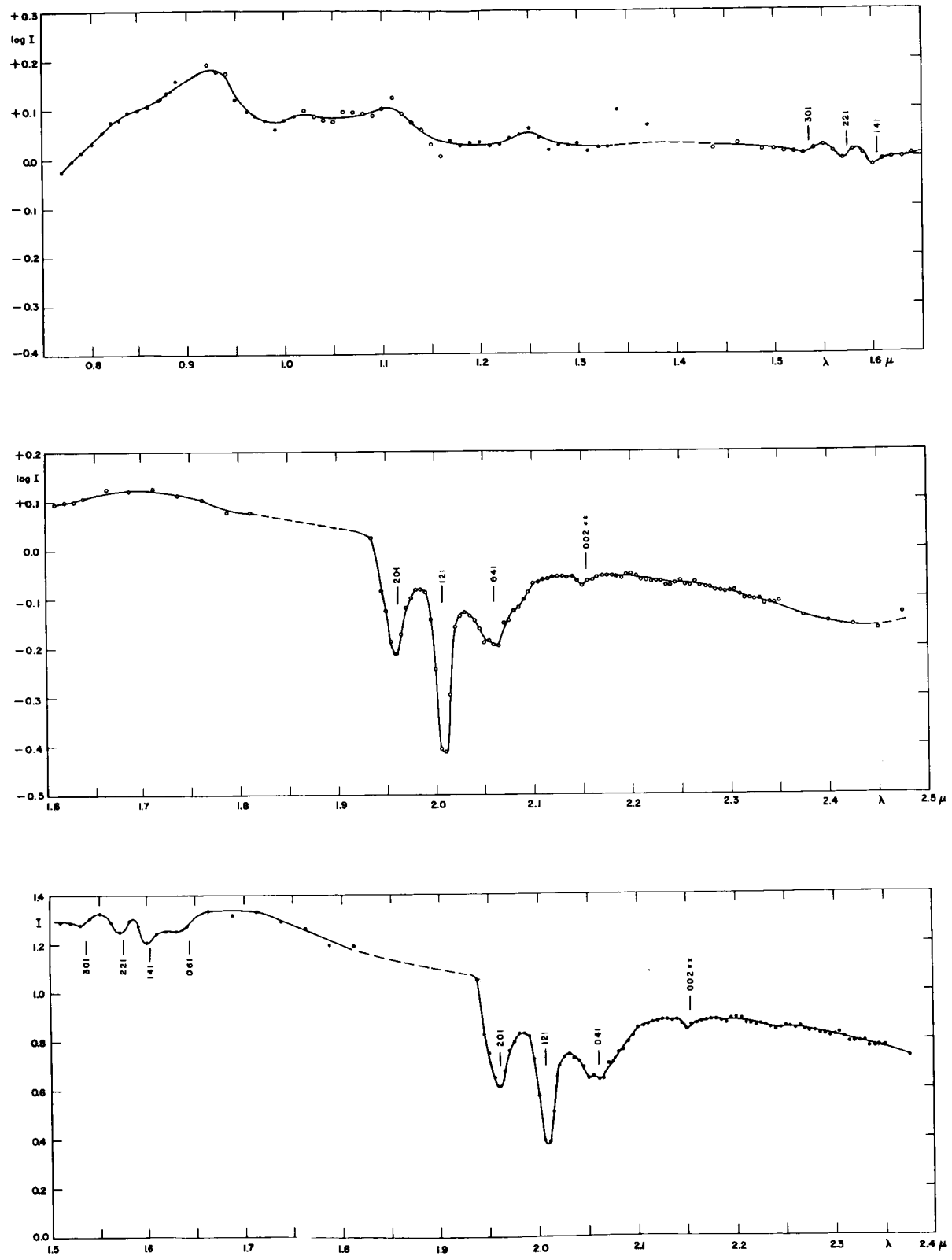

Fig. 25. Spectral intensity ratios Mars/Moon, consolidated. *Upper* and *middle:* average of ratios plotted in Fig. 24 logarithmically combined by vertical adjustments of overlapping sections; *lower:* 1.5-2.5 μ as above but replotted on intensity scale. Martian CO_2 bands identified. Filled circles are single measures, open circles averages in overlapping areas.

in terms of the lunar continuum. Both the telluric and the solar absorptions are thus in principle eliminated though the data will be poor within the heavy H_2O telluric absorptions owing to low residual intensities. The ratios here derived suffer further from one weakness that in principle can be remedied; namely, that the lunar image slowly drifted over the spectrometer slit since no declination drive was used on the telescope. As has been stated, the effects of this drift were minimized by using a grossly-extrafocal lunar image and by making the lunar scans at a rapid rate. Further, several lunar scans were used when practicable.

The ratio measures were made at preselected closely-packed wavelength intervals, using the original spectral traces after a somewhat smoothed interpolation curve had been drawn on them to minimize the random effects of electronic noise. The measures were made by a student-assistant, Mr. S. M. Larson, except for the second set of measures of the 1.9-2.5 μ region which was made by the writer. In this second set, separately reproduced in Figure 24, special attention was paid to the maxima and the minima of the Mars and Moon records, for possibly-improved wavelength consistency.

The heavy telluric H_2O absorptions near 1.4 μ and 1.9 μ cause two breaks in the ratio spectra, indicated by dashes in Figure 25. The relative ordinates of the three segments were placed in approximate accordance with low-disperson runs covering the entire region 0.5-2.5 μ. The positioning of the segments between 0.75-1.4 μ was made from the short overlapping portions.

The ratio spectra so found are shown in Figures 24 and 25. They are considered provisional, particularly with respect to the secondary features between 0.8-1.2 μ, some of which may be due to inadequate lunar calibration. The 1.6 μ region should be fairly precise but the CO_2 bands near 2.0 μ require interpretation, as follows from the discussion accompanying Figure 16b. The measurement of the Martian CO_2 bands can be made unambiguously only during such periods as have either a complete separation of the telluric and Martian rotational lines (as occurred for the 1.6 μ bands; see Figure 16a), or else a central superposition (when Mars is at opposition and has zero radial velocity). During the next opposition the techniques employed here will be further developed.

Acknowledgments. I am indebted to Dr. W. W. Morgan and his staff for making the 82-inch telescope available for the Mars observations; to Dr. H. Johnson for his frequent advice on technical problems; to Mr. A. Binder and Mr. D. Cruikshank for assistance in the observations; to Dr. B. M. Herman of the Institute of Atmospheric Physics for making the computations reproduced in Tables 1-3 and Figures 1-3; to Dr. J. E. McDonald for his advice in the preparation of Section 3; to Mr. T. Owen for his indispensable assistance in the laboratory CO_2 calibrations; to Mr. D. Cruikshank for his assistance with the calibrations described in Sec. 6; to Mrs. Linda Scheer and Miss T. R. McKinney for assistance with the diagrams; and to Mr. S. M. Larson for his assistance in the computations of Tables 1-3 from the machine data, his assistance in Sec. 7, and in the production of Figures 24 and 25.

The program of infrared planetary spectroscopy is supported by the National Aeronautics and Space Administration through Grant No. NsG 161-61.

Note added in proof. The comment on p. 81 regarding the distribution of Martian haze is independent of the occasional presence, repeatedly reported, of what appears to be a surface frost deposit near the sunrise terminator. Such a surface deposit would clearly depend on the daily temperature of the planetary surface.

It has been pointed out to me by Dr. Frank A. Gifford that the Martian dust storms discussed on pp. 89 and 90 could involve saltation of dust particles. I am assuming, however, that the widespread haze condition of the Martian atmosphere usually following local dust storms indicates the presence of airborne dust, as discussed above.

REFERENCES

Antoniadi, E. M. 1930, *La Planète Mars* (Paris: Hermann), pp. 45-46.

Coblentz, W. W. 1926, *Pop. Astron., 33,* 370.

Dallavalle, J. M. 1948, *Micromeritics* (2nd ed.; New York, Toronto, and London: Pitman Pub. Corp.).

de Vaucouleurs, G. 1954, *Physics of the Planet Mars* (London: Faber and Faber).

Dollfus, A. 1961, *Planets and Satellites,* ed. G. P. Kuiper and B. M. Middlehurst (Chicago: University of Chicago Press), Chap. 9.

——— 1963, presentation at NASA Meeting, Washington, D.C., October 1, 1963.

——— 1964, *l'Astronomie, 78,* 41-56.

Finsen, W. S. 1961, *Planets and Satellites,* ed. G. P. Kuiper and B. M. Middlehurst (Chicago: University of Chicago Press), Chap. 17.

Fletcher, N. H. 1962, *The Physics of Rainclouds* (Cambridge: Cambridge University Press).
Fuks, N. A. 1955, *The Mechanics of Aerosols,* trans. E. Lachowicz (Washington: U.S. Department of Commerce).
Gehrels, T. and Teska, T. M. 1962, *Comm. LPL, 1,* 173.
Grandjean, J. and Goody, R. M. 1955, *Ap. J., 121,* 548.
Green, H. L. and Lane, W. R. 1957, *Particulate Clouds: Dusts, Smokes, and Mists* (Toronto, London, and New York: D. Van Nostrand).
Greenfield, S. M. 1956, *J. Meteor., 14,* 115-125.
Harris, D. L. 1961, *Planets and Satellites,* ed. G. P. Kuiper and B. M. Middlehurst (Chicago: University of Chicago Press), Chap. 8.
Humason, M. L. 1961, *Ibid.,* Chap. 16.
Junge, C. E. 1963, *Air Chemistry and Radioactivity* (New York and London: Academic Press).
Kaiser, F. 1872, *Ann. Leiden Obs., 3.*
Kuiper, G. P. 1931, *Hemel en Dampkring, 29,* 224, 228-229.
——— 1947, Harvard College Observatory Announcement Card 851.
——— 1949, *The Atmospheres of the Earth and Planets,* ed. G. P. Kuiper (1st ed.; Chicago: University of Chicago Press), Chap. 12.
——— 1952, *Ibid.,* (2nd ed.), Chap. 12.
——— 1963, *Mémoires Soc. R. Sc. Liège,* Series 5, Vol. 9.
Liais, E. and Cruls, L. 1878, *Mémoire de Mars* (Rio de Janeiro).
McDonald, J. E. 1964, *J. Atmos. Sci., 21,* 13 ff. and in press.
Mohler, O. C., Pierce, A. K., McMath, R. R., and Goldberg, L. 1950, *Photometric Atlas of the Near Infra-red Solar Spectrum, λ 8465 to λ 25,242* (Ann Arbor: University of Michigan Press.)
Schatzman, E. 1951, *Comptes Rendus* (Paris), *232,* 692.
Sinton, W. M. 1961, *Planets and Satellites,* ed. G. P. Kuiper and B. M. Middlehurst (Chicago: University of Chicago Press), Chap. 11.
Slipher, E. C. 1962, *Mars 1905-1961,* Chap. 5.
Spinrad, H., Münch, G., and Kaplan, L. D. 1963, *Ap. J., 137,* 1319-1321.
——— 1964, *Ibid., 139,* 1.
Trouvelot, E. L. 1884, *Comptes Rendus* (Paris), *98,* 789.
Van de Hulst, H. C. 1952, *The Atmospheres of the Earth and Planets,* ed. G. P. Kuiper (2nd ed.; Chicago: University of Chicago Press), Chap. 3.
Weaver, H. F. *et al.* 1963, presentation at AAS Meeting, Tucson, Arizona, April 1963.

NO. 32 A DETERMINATION OF THE COMPOSITION AND SURFACE PRESSURE OF THE MARTIAN ATMOSPHERE

by T. C. OWEN AND G. P. KUIPER

August 24, 1964

ABSTRACT

The spectra of Mars obtained in the 1–2.5 μ region (*Communications* No. 31) are calibrated with the aid of laboratory spectra of pure CO_2 as well as mixtures of CO_2 with N_2 and Ar. Pathlengths up to 3.6 km are used and pressures down to 4 mm. With the aid of the total CO_2 content reviewed in *Comm.* No. 33, based on the Mt. Wilson spectrum, preliminary values are derived for the pressure in the Martian atmosphere and the total amount of gases other than CO_2. The values obtained are 17 ± 3 mb (13 mm Hg) and $(N_2 + Ar)/CO_2 = 6$. Arguments are given indicating that the Ar/N_2 ratio is probably similar to that for the Earth atmosphere ($\simeq 10^{-2}$) and that the O_2 content is probably <7 cm atm.

1. Introduction

This paper contains the laboratory calibrations that have been made for the Mars spectra published in *Communications* No. 31, using the maximum range of available pathlengths and an appropriate range of pressures. The program assumed its present form during the NASA conference on the Mars atmosphere, October 1-2, 1963, when the authors noted that with the total CO_2 content found from weak bands, both the atmospheric pressure and the abundance of any other major constituent, such as N_2, could be determined empirically from measurements on the 1.6 μ CO_2 bands. As one of us (GPK) stated at this Conference, this is so because the band strength is a function of (1) CO_2 abundance, (2) admixture of N_2 or Ar or both, and (3) pressure; and, further, because there are three equations relating these three unknowns: (1) the CO_2 abundance found from weak bands, (2) the observed strength of the 1.6 μ bands, and (3) the computed weight or pressure of the atmospheric column, the surface gravity on Mars being known.

A completely empirical determination of the pressure effects in the gas mixtures is still not quite possible, however, because it would require a pathlength twice the scale height of the Martian atmosphere, or some 40 km. The pathlengths reached here are only about 0.1 of this. While they suffice to give a reasonably precise answer, improvements are desirable and being executed by increasing the available laboratory pathlength to at least 8 km.

2. The Laboratory Program

The spectra were obtained with the same spectrometer (described in *Comm.* No. 16) used for obtaining the telescopic observations of Mars. The absorption tube used has a 72-foot multiple-reflection path and was designed by Mr. Owen to fit the available laboratory space. Part of the records were obtained by the two authors jointly, but the bulk were obtained by Mr. Owen aided by a graduate-student assistant. Four traversals of the tube measure very nearly 90 meters and the program was designed to increase the pathlengths in steps of a factor of two:

90, 180, 360, 720, 1440, 2880 meters, though some intermediate steps were covered and a maximum effort was made: 540, 1080, 2160 and 3600 meters. Matching the steps of two in pathlength are steps of two in pressure: 24, 12, 6, 3, 1.5, 0.75, and 0.4 cm Hg, which correspond very nearly to the following values in millibars: 320, 160, 80, 40, 20, 10 and 5.3. In this manner products of pathlength and pressure (i.e., abundance) resulted, falling into discrete groups progressing in the ratios 1, 2, 4, 8, etc., in abundance. Within each group of constant abundance the band intensity then shows the effects of pressure.

After it was found that the strength of the Martian CO_2 bands cannot be interpreted on the basis of a pure CO_2 atmosphere (the empirically-deduced pressure being inconsistent with the pressure computed from the weight of the column), it was decided to add N_2 to the gas, the most likely constituent of the Mars atmosphere other than small amounts of A^{40}. The pressure effect of N_2 on CO_2 is less than the effect of CO_2 on CO_2, so that these additional runs were needed. Since it was further found that A^{40} affects CO_2 very similarly to an equal amount of N_2, the work on $CO_2 + N_2$ seemed particularly appropriate. A 10%/90% mixing ratio for

TABLE 1
PURE CO_2

PATHLENGTH	$p = 0.4$	0.75	1.5	3	6	12	24 cm
90 m	....	....	....	1*	2*	3*	2*
180	....	....	....	1*	3*	6*	2*
360	....	....	4*	4*	8*	4*	2*
720	....	....	5*	5	3*	....	....
1440	9	8	2	4	4	....	....
2880	2	7	4	4	....	....	....

* 1.2 μ observed also.

TABLE 2
90% N_2, 10% CO_2

PATHLENGTH	$p = 1.5$	3	6	12	24 cm
90 m	....	....	....	2	2
180	....	....	3	2	2
270	....	....	....	....	2
360	3*	4*	3	2	3
540	....	....	....	2	2
720	....	4	2	2	3
1080	....	....	....	3	2
1440	....	3	4	4	....
2160	....	2	3	2	....
2880	....	....	....	3	....
2950	....	....	3	....	....
3600	....	....	4	2	....

*1.2 μ observed also.

TABLE 3
25% CO_2, 75% N_2

PATHLENGTH	$p = 0.75$	1.5	3	6	12	24 cm
90 m	....	....	2	3	4	3*
180	....	4	3	3	3*	3*
360	....	4	3	3	3	2*
450	....	....	....	....	....	2*
720	....	3	3	3*	3*	2*
900	....	....	....	....	4*	....
990	....	....	3	3*	....	....
1440	....	4	4*	3*	3*	....
1800	....	....	....	3*	....	....
1980	....	3	4*	....	....	....
2880	3	3	3	3	4	....

*1.2 μ observed also.

CO_2/N_2 was adopted. When measurements on it showed that the pressure discrepancy was now reversed, a third set of spectra was obtained on an intermediate mixture, $CO_2/N_2 = 0.25/0.75$. Tables 1 to 3 list the combinations of pathlength and pressure actually run.

The CO_2 bands chosen for analysis are those at 1.575 and 1.606 μ, although the spectrometer tracings normally included the weaker bands at 1.538 μ and 1.646 μ. Occasional records were taken of the 1.206 μ and 1.221 μ bands as well. The inventory in Tables 1-3 lists available data.

A representative set of laboratory records is reproduced in Figures 1-10. At the resolution of the Mars observations and the corresponding laboratory runs, the rotational structure of the CO_2 bands is not resolved. The P and R branches are distinct, however, and cause W-shaped absorptions which are well adapted to intensity measurements with a planimeter.

The Mars spectra obtained on December 8, 1962 are the most suitable for study of the 1.6 μ bands. As was reviewed in conjunction with Fig. 16*a* of *Comm.* No. 31, the telluric components of the 1.6 μ bands can be separated from the Martian components. The average equivalent width of the two strong Martian bands is 15.8Å.

The averaged equivalent widths of the two 1.6 μ bands measured on the laboratory spectra are plotted logarithmically against pressure in Figs. 11-13. In most cases two or three spectra were measured, as available (Tables 1-3). The measures were made in duplicate by one of the authors (GPK) and by a graduate-assistant, Miss Thelma McKinney. The curves connect points representing equal abundance with the amounts indicated in the figures. The pressure effects are quite marked and the determination of the Martian atmospheric pressure requires careful consideration.

3. Derivation of the Pressure and Composition of the Martian Atmosphere

As stated in Section 1, the first requirement is information on the total CO_2 content from weak bands, unaffected by pressure broadening. This is provided by a calibration of the intensity of the $5\nu_3$ band of CO_2 observed by Kaplan, Münch, and Spinrad (1964). These authors derived a value of 50 $\pm$ 20 m atm, corresponding to an atmospheric temperature of 200° K. An independent calibration of this spectrogram is made in *Comm.* No. 33 which results in a value of 46 $\pm$ 20 m atm for the same temperature. The difference between these two values is not regarded as significant; for the sake of consistency we will use the second figure. The specification of temperature is necessary for the $5\nu_3$ abundance determination because the relative intensites of the rotational lines are strongly temperature-dependent and in this case the individual lines are resolved. The number of molecules defined by the m atm is referred to NTP. In the PbS region the lines are not resolved and thus the amount of the gas in m atm which will be required in the laboratory optical path to match the Martian equivalent width will simply be $46 \times \frac{T_L}{273} \times \eta$ where T_L *is* the laboratory temperature and η is the effective Martian air mass through which the observations were made. In the present case the slit of the spectrometer ran equatorially across the planet and thus $\eta = \pi$ for weak bands on the linear part of the curve of growth. For bands on the square-root part, $\eta = 2.87$; in the transition region η will be somewhat less (see Appendix). Since the spectrometer slit accepted roughly one-third of the planet's disc, these figures must all be slightly increased. Taken together, such considerations suggest a value for η of about 3 (a discussion of the curve of growth effects displayed by the CO_2 bands is given below). With an average laboratory temperature of 297°K, we find that 150 m atm of CO_2 are required in the laboratory optical path.

One may examine whether a verification of the total Martian CO_2 content could be obtained from the weaker bands of the 1.6 μ tetrad, at λ 1.538 and 1.646 μ. Equivalent widths for the λ 1.538 band were derived for a set of pathlengths and pressures in *Comm.* No. 31 (Table 6 and Fig. 23b). These are replotted against log p (rather than log wp) in Figure 14, which is therefore directly comparable with Figure 11. The Martian band strength was obtained from the two upper curves of Figure 12, *Comm.* No. 31, and found to be 6.6 $\pm$ 1Å (log EW = 0.82 $\pm$ 0.06). This value, with its present margin of uncertainty, is entered in Fig. 14. It is seen that for $w <$ 14 m atm the bandstrength is little dependent on pressure but that already at the strength of the Martian band it is roughly proportional to $p^{1/4}$; whereas at a given pressure EW increases approximately as $w^{1/2}$. Comparison of Figs. 14 and 11 indicates a CO_2 content consistent with that derived from the λ 0.87 μ band though the accuracy of this determination is not good. The reasons are that the pressure effects ($p^{1/4}$ and $p^{1/2}$) are not grossly different and that the EW values for weak bands measured as *blends* are

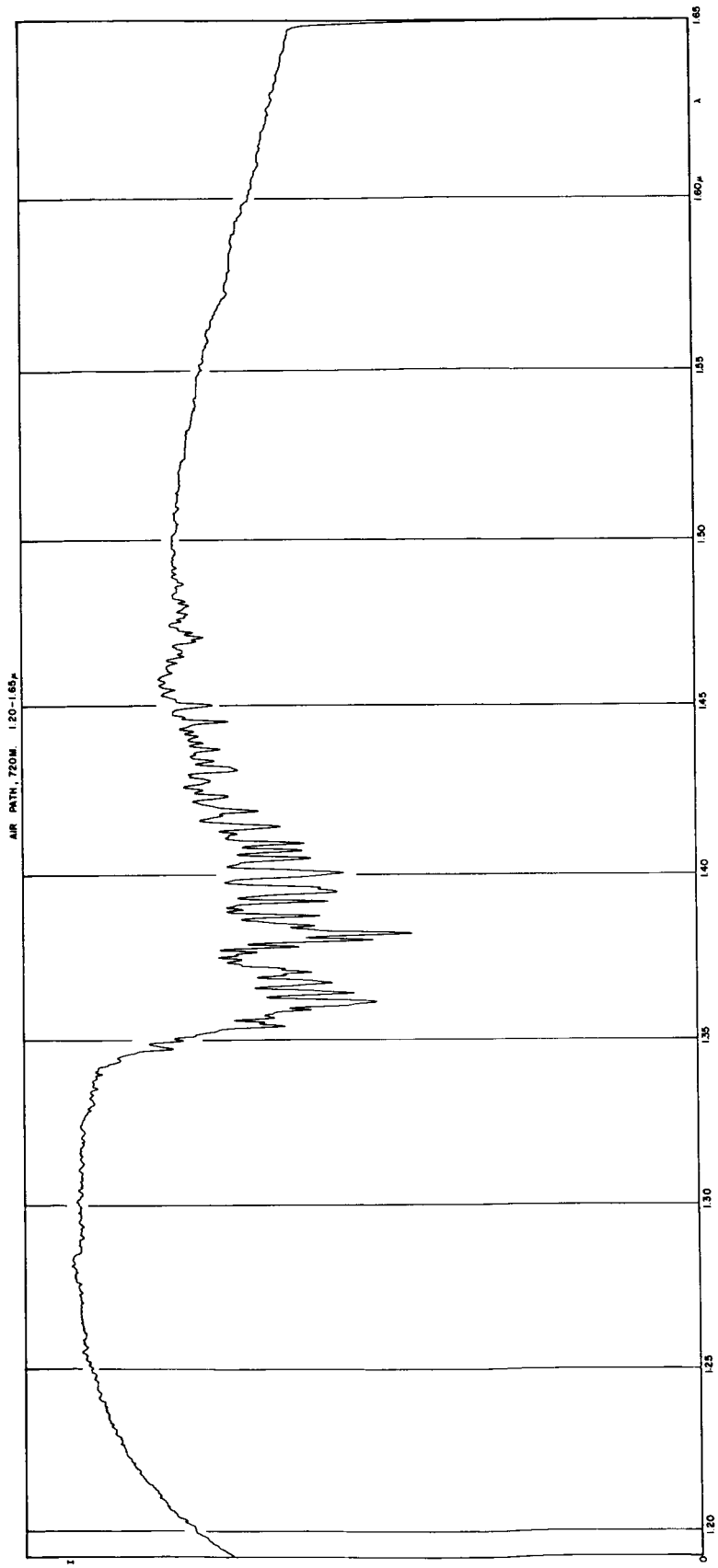

Fig. 1. Air path 1.20–1.65 μ, being a blank run for subsequent figures. Principal features shown are water-vapor absorptions at 1.35–1.50 μ, common to all subsequent runs (path in laboratory and spectrometer); run made at 720-meter path in absorption tube, evacuated.

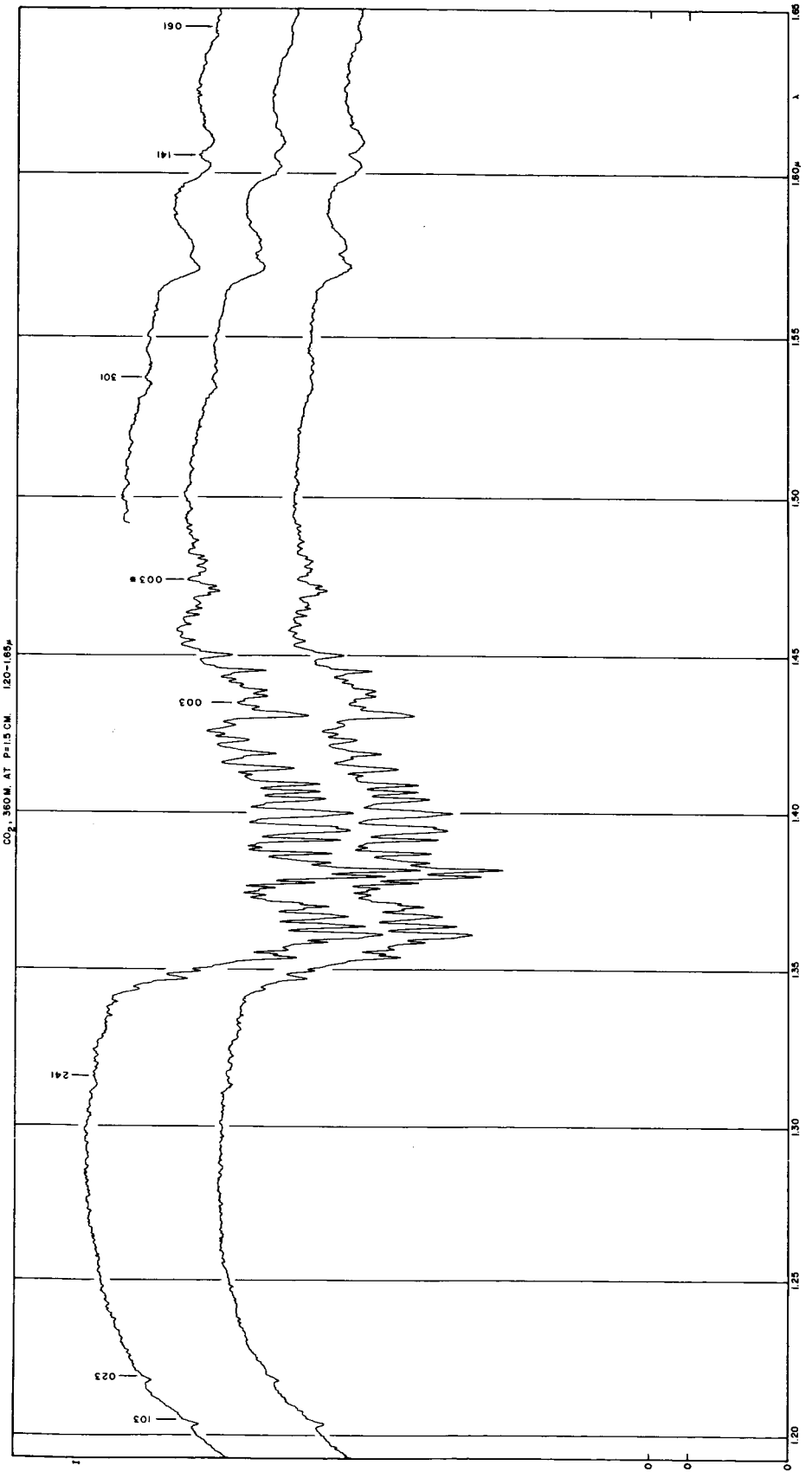

Fig. 2. Spectrometer traces of pure CO_2, 360 meters at $p = 1.5$ cm, 1.20–1.65 μ. For absorptions 1.35–1.50 μ, see Figure 1. Zero levels in order of graphs here and in following figures.

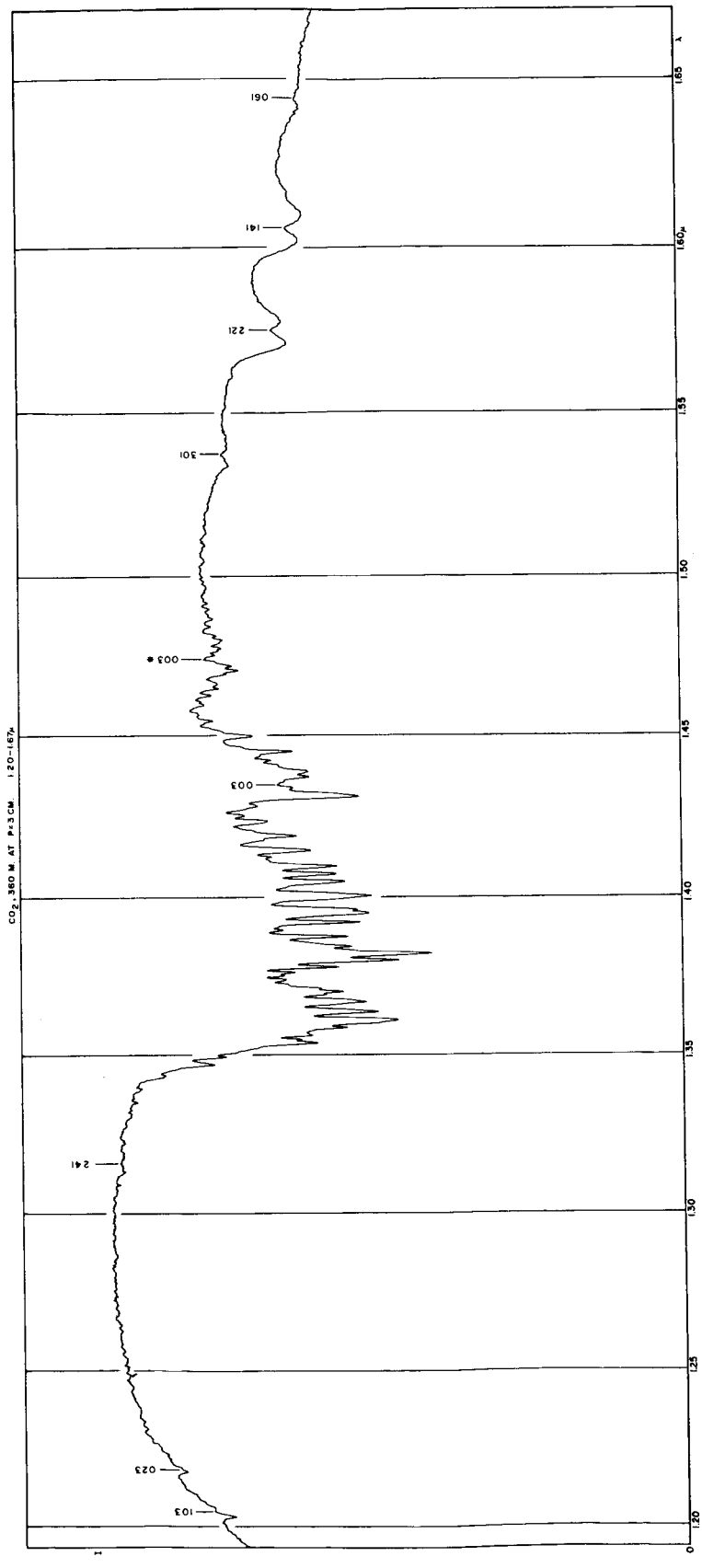

Fig. 3. CO_2, 360 meters at $p = 3$ cm, 1.20–1.67 μ.

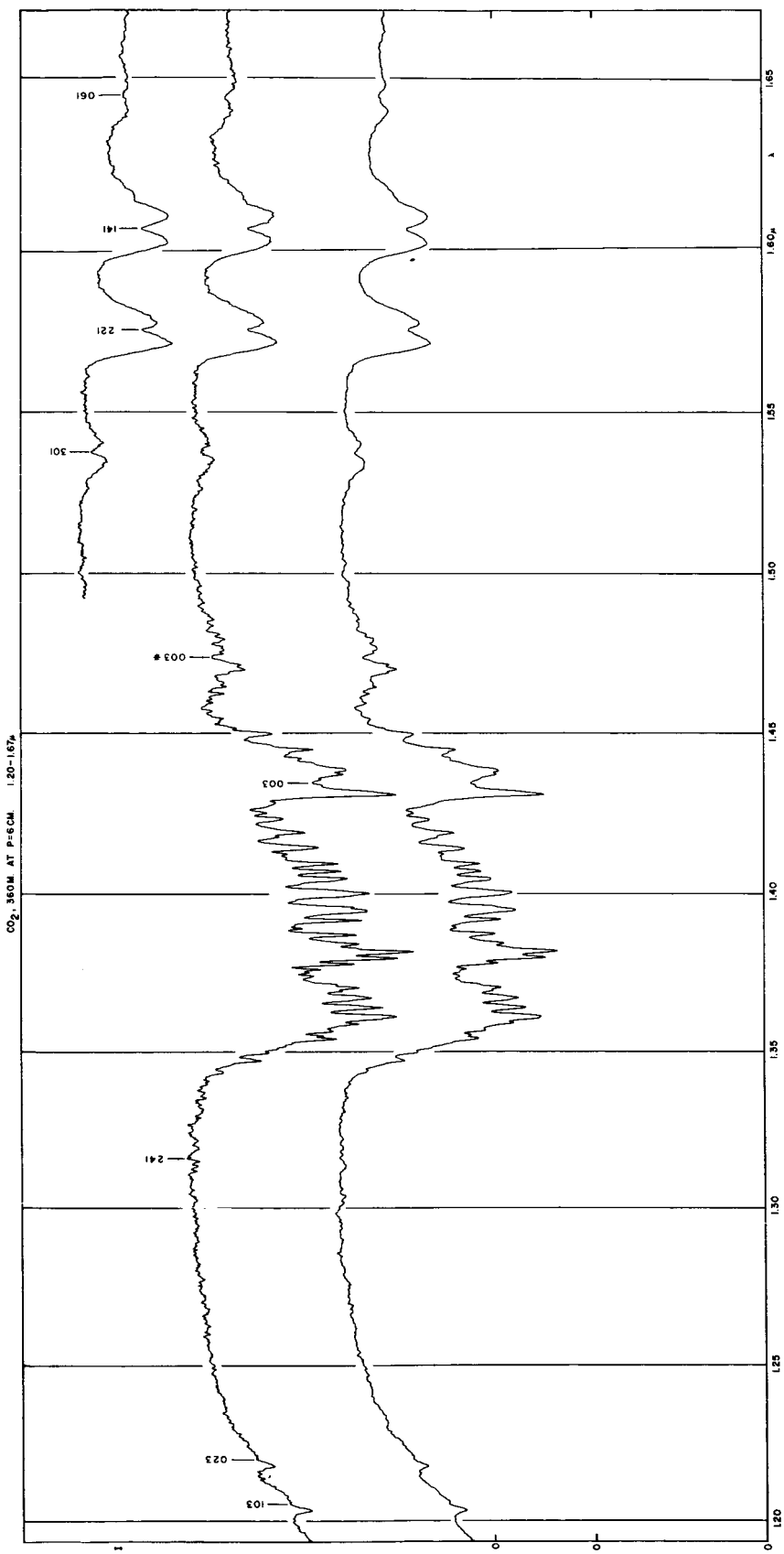

Fig. 4. CO_2, 360 meters at $p = 6$ cm, 1.20–1.67 μ.

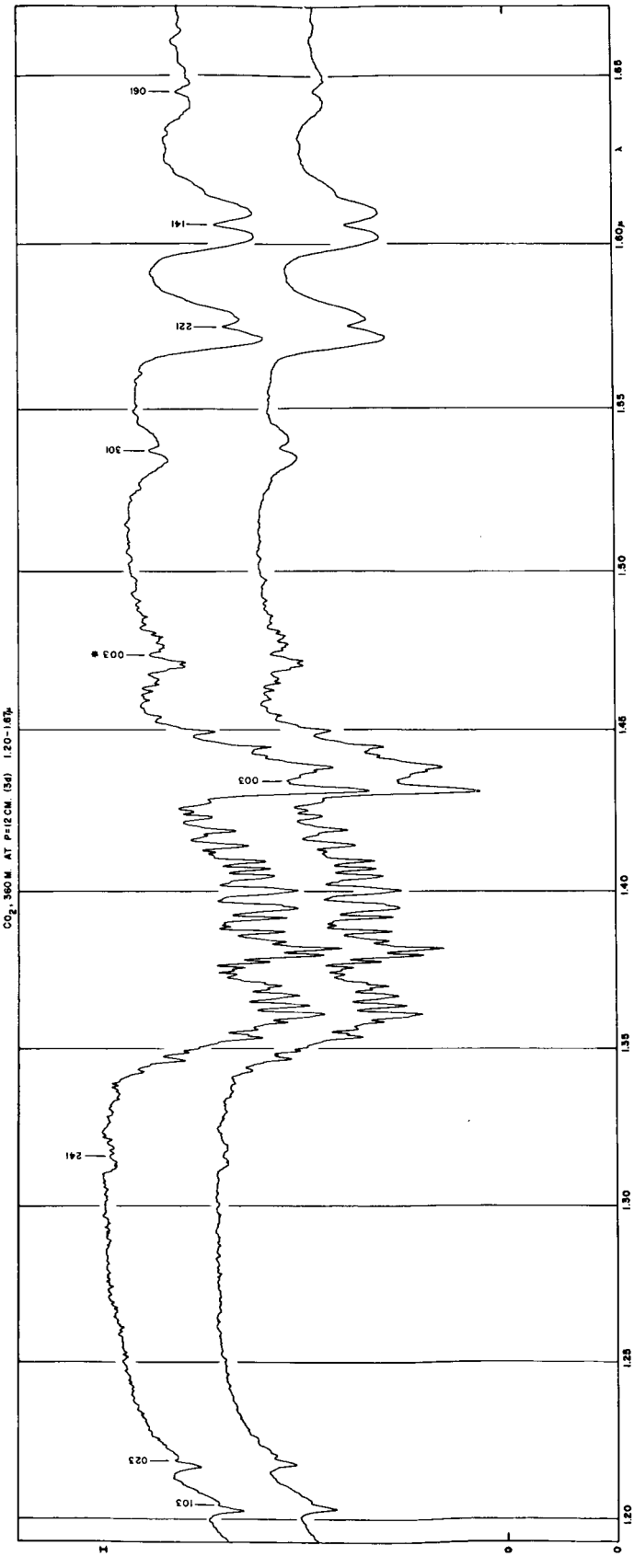

Fig. 5. CO_2, 360 meters at $p = 12$ cm, 1.20–1.67 μ.

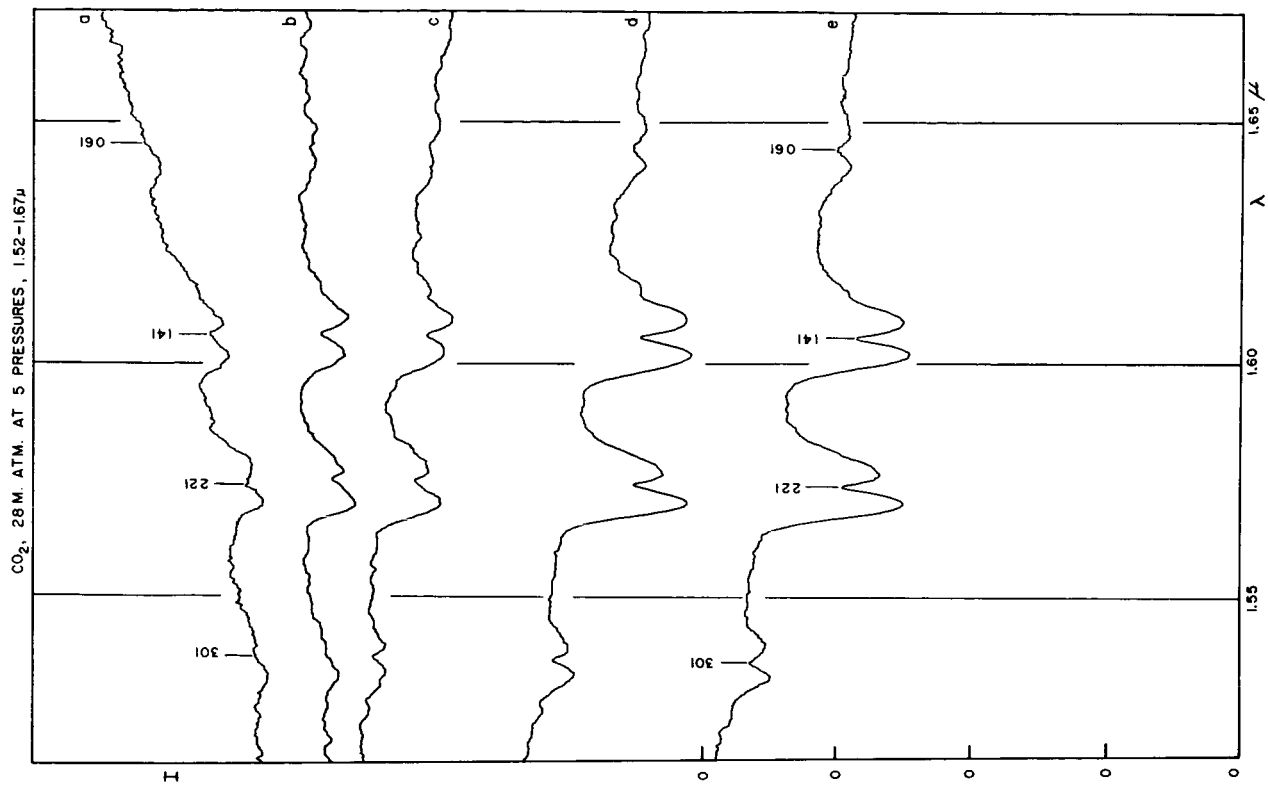

Fig. 6. Pure CO_2, 1.6 μ bands for five combinations of pathlength and pressure having same total abundance; (*a*) 2880 m at 0.75 cm; (*b*) 1440 m at 1.5 cm; (*c*) 720 m at 3 cm; (*d*) 180 m at 12 cm; (*e*) 90 m at 24 cm. The 360 m at $p = 6$ cm trace is found in Fig. 4.

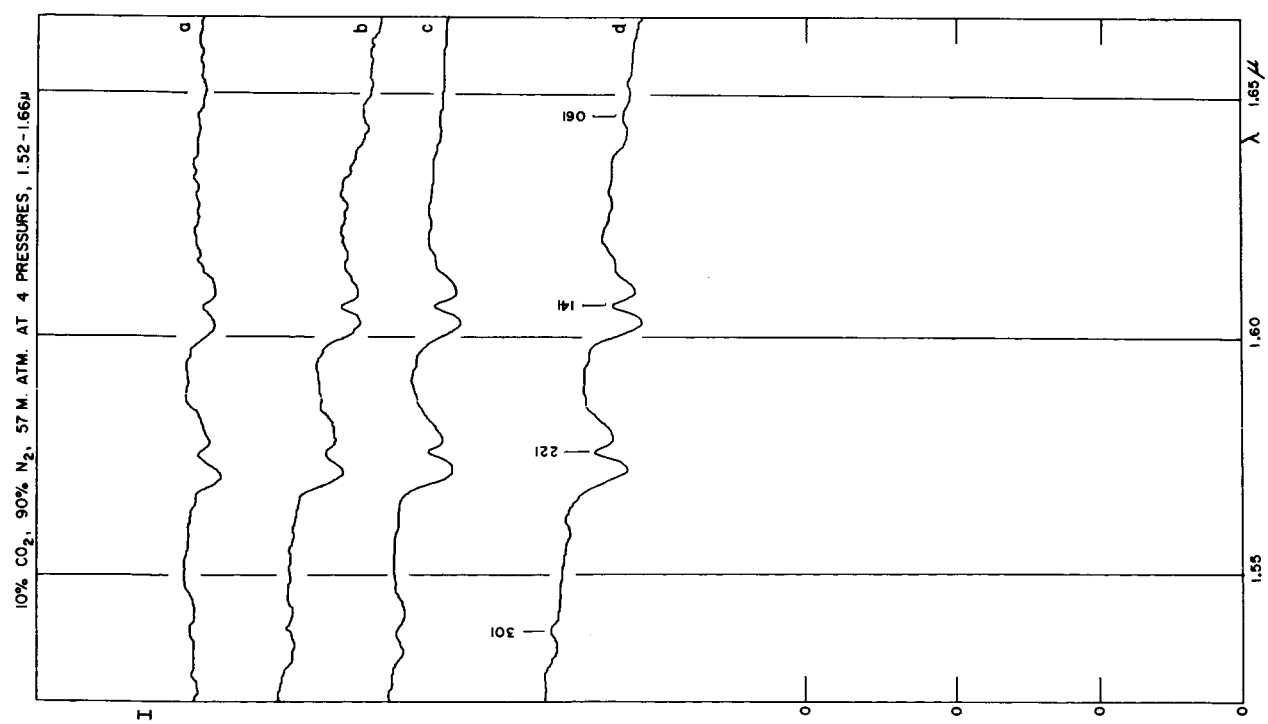

Fig. 7. Mixture of 10% CO_2, 90% N_2; (*a*) 1440 m at 3 cm; (*b*) 720 m at 6 cm; (*c*) 360 m at 12 cm; (*d*) 180 m at 24 cm.

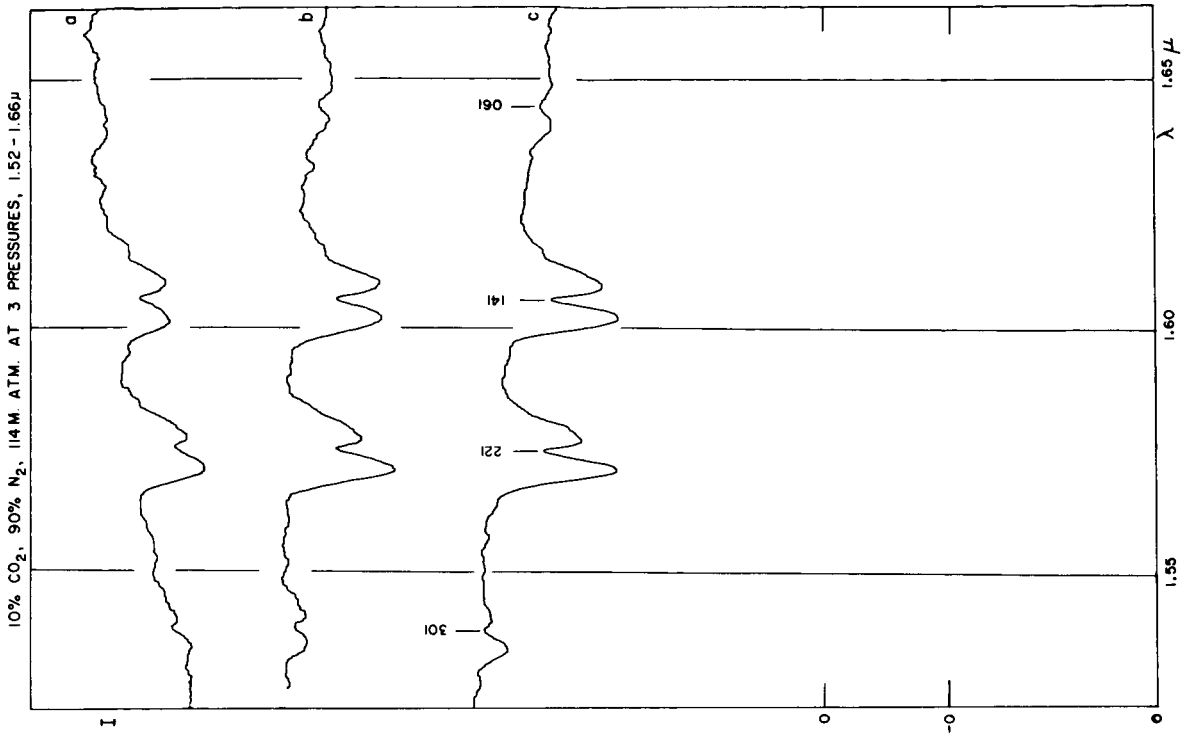

Fig. 8. Mixture as Fig. 7; (*a*) 1440 m at 6 cm; (*b*) 720 m at 12 cm; (*c*) 360 m at 24 cm.

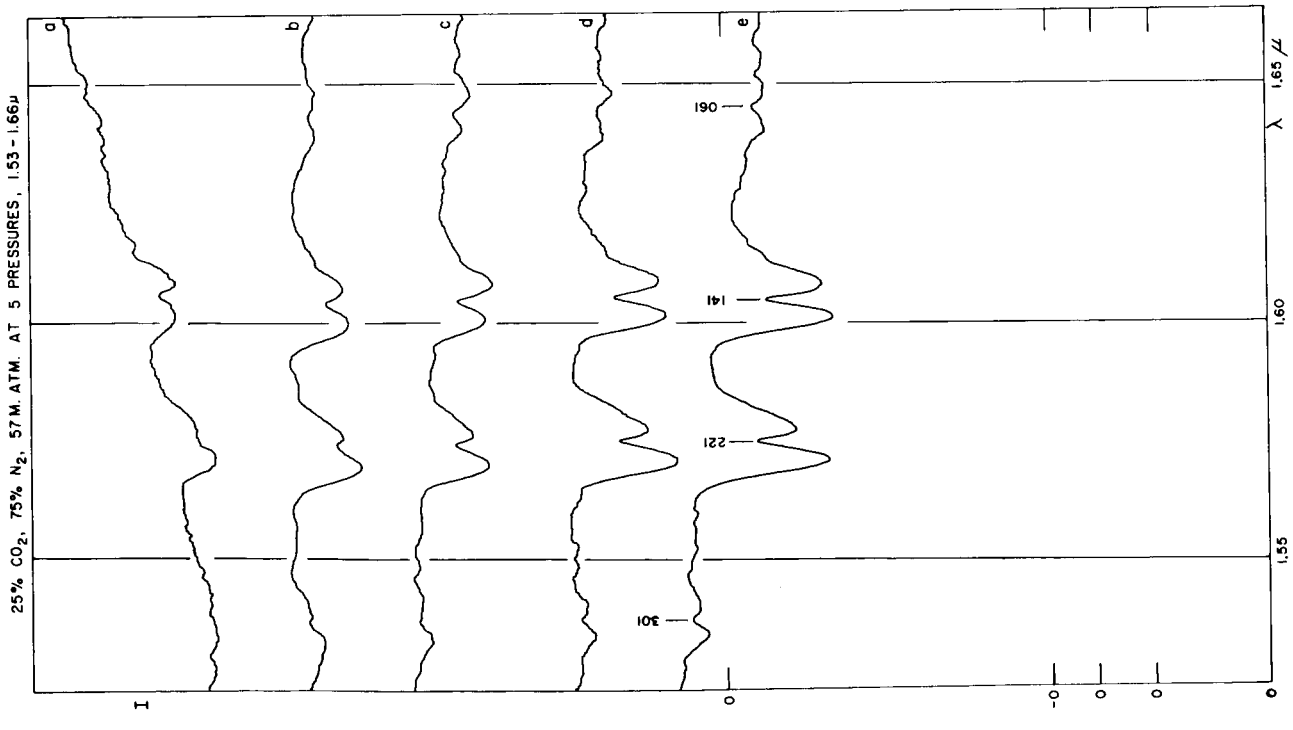

Fig. 9. Mixture 25% CO_2, 75% N_2; (*a*) 2880 m at 1.5 cm; (*b*) 1440 m at 3 cm; (*c*) 720 m at 6 cm; (*d*) 360 m at 12 cm; (*e*) 180 m at 24 cm.

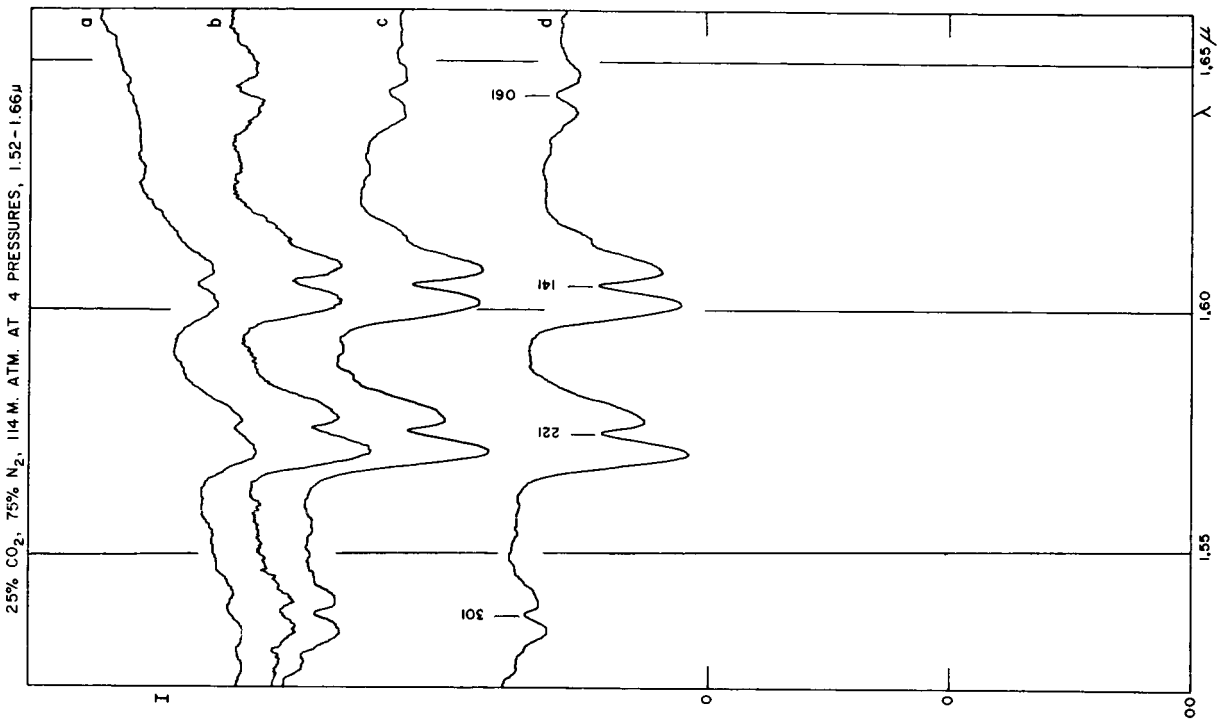

Fig. 10. Mixture as Fig. 9; (*a*), 2880 m at 3 cm; (*b*), 1440 m at 6 cm; (*c*), 720 m at 12 cm; (*d*), 360 m at 24 cm.

not precise. Weak bands for which the individual rotational lines can be observed must be used for a really good determination. This requires high-resolution spectra.

We have already noted the requirement that the pressure used in the laboratory must be consistent with the pressure exerted by a unit column of the laboratory gas mixture transferred to the surface of the planet. The appropriate relation is furnished by the Curtis-Godson approximation (Goody, 1964), which states that the mean pressure along the absorbing path in a planetary atmosphere is equal to one-half the surface pressure.

With these relationships established, the calibration is essentially defined. Using the amount of CO_2 derived from the abundance analysis, one wishes to vary the pressure and the amount of the carrier gas (N_2) until the equivalent width obtained is equal to that of the Martian absorptions. For a given CO_2/N_2 mixture, and with the amount of CO_2 fixed, only one pressure will provide a match. This pressure must then be one-half the pressure which a column of gas composed of the CO_2/N_2 mixture would exert on the surface of the planet. If the pressures do not agree, then a different mixture must be used, etc. The principle of this method is straightforward but because of the very long pathlengths required, some extrapolation must still be made based on data obtained with smaller amounts of gas at higher pressures.

We have referred to Figs. 11-13, giving plots of log EW vs. pressure for three gas mixtures. The horizontal lines show the value of the Martian absorption, with the total absorption (Mars and Earth) added for reference in Fig. 11. The curves indicate the dependence of the equivalent width on the pressure for a given amount of gas. As one would expect, the equivalent width decreases with decreasing pressure, with the decrease becoming less pronounced as lower pressures are approached or smaller amounts of gas are used. For a given pressure, doubling the amount of gas results in an increase of about 0.15 in log EW, as shown in the upper part of Fig. 11; i.e., the bands are on the square-root part of the curve of growth. In the lower left of this plot the increase is less than 0.15, indicating that the bands fall in the transition region. In the lower right corner we see that the effect of increased pressure on small amounts of gas results in a removal of saturation, with a consequently slower increase in equivalent width with increasing pressure. This same general behavior is exhibited by the other graphs.

Knowing these relations it is then possible to extrapolate on the plots to the pathlength corresponding to the Martian CO_2 abundance. This line is indicated on each figure by dots and labeled with the appropriate amount of gas. The intercepts of these lines with the horizontal line indicating the equivalent width of the Martian CO_2 absorptions, correspond to the pressures necessary for these amounts of gas to produce absorptions of the required strength.

The second method of presenting the laboratory data is shown in Figs. 15, 16, and 17. Here the abscissa is the logarithm of the product of pressure (in mb), effective air mass on Mars and amount of gas (in m atm). The ordinate is the same as that of the previous plots and the equivalent width of the Martian absorptions is again indicated by a horizontal line. Inspection of Fig. 15, which displays the data for pure CO_2, indicates that the relation

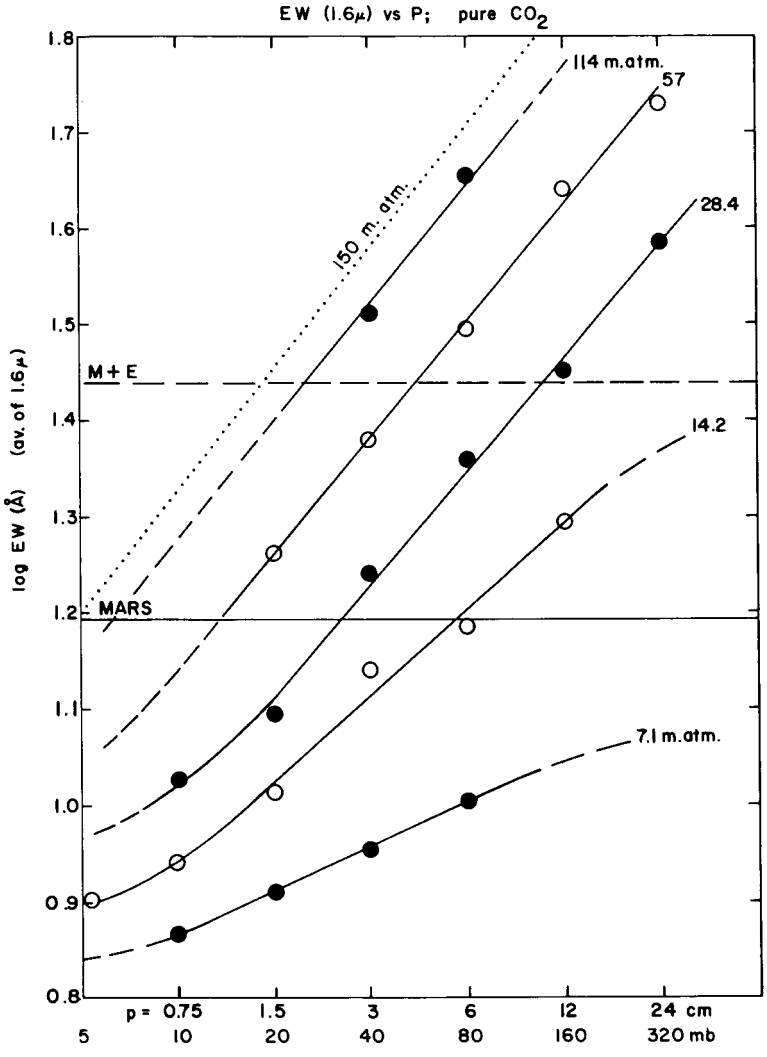

Fig. 11. Equivalent width, average of two strong 1.6 μ bands, vs. pressure, expressed both in cm Hg and mb, for pure CO_2. Points representing same total abundance are connected by solid lines, with total abundance in meter-atmospheres indicated. Dotted line represents amount seen by spectrometer in Martian spectrum. Mars absorption indicated by horizontal line near log EW = 1.2. Higher dashed line Mars + telluric bands. Empirical pressure determined from diagram is approximately 5 mb (being half of surface pressure; see Fig. 18).

between log EW and log ηpw can be represented by the following equation:

$$\log \mathrm{EW} = \frac{1}{2.32} \log \eta pw - 0.65 \qquad (1)$$

This relation holds very well for pressures from 20–40 mb over a range of log EW from 1.0 to 1.5.

At lower pressures, there is a tendency for the line defined by Equation 1 to be approached asymptotically from the left as the amount of CO_2 increases.

Fig. 11 shows that the effective pressure associated with the Martian equivalent width must be less than 10 mb. Thus the intercept with the line representing the Martian absorptions on Fig. 15 defines an upper limit to the effective pressure since it is essentially defined by the observations at 20 and 40 mb. With $w = 150$ m atm we find p (emp) $=$ 5.8 mb. A lower limit may be set by estimating where the intercept would fall at very low pressures. Fig.

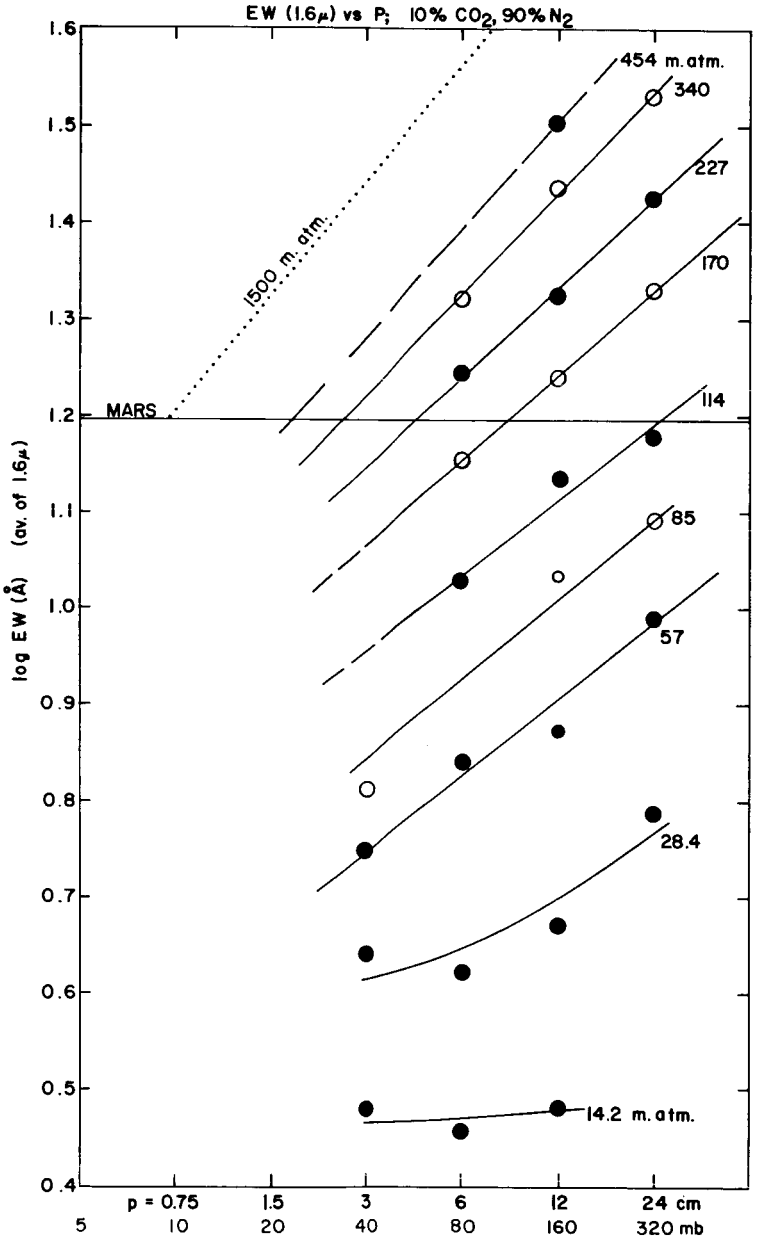

Fig. 12. As Fig. 11, for 10% CO_2, 90% N_2.

At higher pressures it is approached from the right. The factor multiplying log ηpw is slightly smaller than ½, suggesting that in this range of p and w the bands fall in the transition region of the curve of growth. This is in agreement with the conclusions derived from Fig. 11.

15 indicates that the 10 mb curve will become asymptotic well before the intercept is reached. At much lower pressures it is probable that the intercept will be further to the left on the diagram, but a limit will be approached beyond which decreasing the pressure has no effect on the equivalent width since the latter will be determined solely by Doppler broadening. This limit is difficult to define empirically since our data do not extend to low enough pressures. However, the lower left-hand corner of Fig. 15 shows that the curves, corresponding to the lowest pressures we were able to use, are beginning to crowd together indicating that the limit referred to above is being approached. This suggests an intercept no further to the left than about log $\eta pw = 2.78$ which corresponds to p (emp) $= 4$ mb.

Similar arguments may be applied to the other two figures. Fig. 16 is of particular interest since it shows the other extreme case considered, the 10% CO_2 mixture. The curves drawn in the lower left corner of this plot are tentatively based on the appearance of Fig. 15, since there are insufficient data to allow a precise representation. The region of the intercept with the equivalent width of the Martian absorption is better defined and again indicates the crowding together of the lines as lower pressures are approached. The slopes of these lines are slightly *greater* than ½, indicating that the bands are again in the transition region of the curve of growth, but closer to the linear part. Fig. 17 presents the intermediate case of the 25% CO_2 mixture.

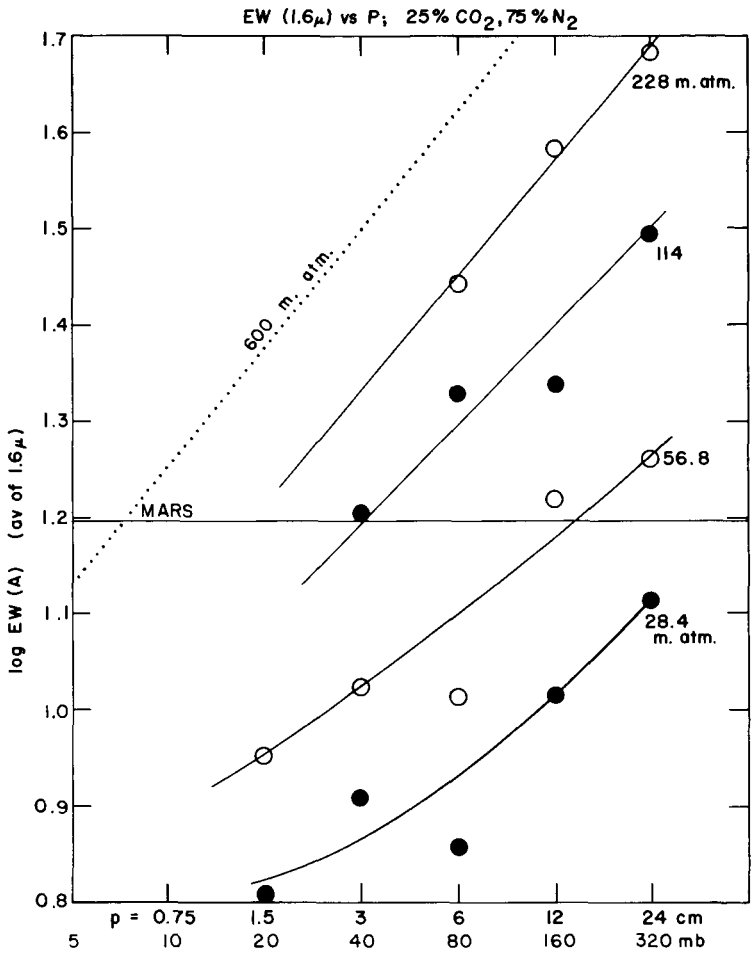

Fig. 13. As Fig. 11, for 25% CO_2, 75% N_2.

As stated above, the pressures derived empirically from the equivalent widths (p emp) are equal to ½ the surface pressure. The upper and lower limits on the surface pressure, as deduced from Figs. 15-17, are given in Table 4. The calculated

surface pressures for the three cases are also given in the table as p (cal). These values are presented graphically in Fig. 18.

The diagonal line in this illustration represents the locus of points for which the calculated and empirically determined pressures are equal. Thus the intersection of the diagonal with the region defined by the upper and lower limits derived for each gas mixture yields the range of pressures which satisfy both the laboratory observations and the constraint imposed by the Martian gravitational field. Since the lower limits are deliberately somewhat conservative, a value of 17 ± 3 (p.e.) is regarded representative of this determination. The medial dashed line in Fig. 18 corresponds to the solutions defined by the dotted lines in Figs. 11-13.

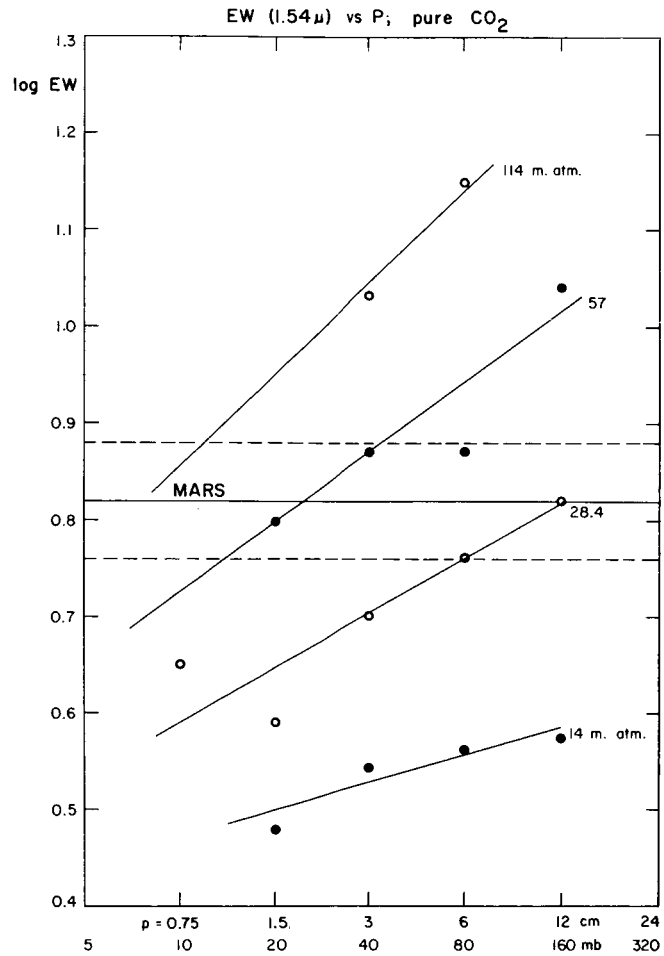

Fig. 14. As Fig. 11, pure CO_2, but for 1.54 μ CO_2 band. Dashed horizontal lines delimit area of uncertainty of Mars absorption.

TABLE 4

CALCULATED AND EMPIRICAL PRESSURES OF MIXTURES OF CO_2 AT THE SURFACE OF MARS

% CO_2	p (cal)	p (emp) Lower Limit	p (emp) Upper Limit
100	3.5	8.0	17.6
25	10.1	10.5	17.6
10	23.4	13.2	22.2

The interpretation of this result may be expressed in the following way: A pure CO_2 atmosphere consisting of the known amount of gas would not exert a high-enough surface pressure to produce the amount of broadening required to match the observed Martian equivalent width. On the other hand, a 10% CO_2 atmosphere would be too massive. For a surface pressure of 17 mb the fraction of CO_2 in a predominantly nitrogen atmosphere is 0.14, or the mixing ratio $N_2/CO_2 = 6/1$.

Up to this point, we have assumed that the broadening of the CO_2 bands is due primarily to N_2. Another gas likely to be present in the Martian atmosphere is radiogenic argon (see discussion below). It is thus of interest to investigate the effects of broadening induced by this gas. With this in mind, laboratory tracings were obtained of 57 m atm of CO_2 at a pressure of 3 cm. Argon was then added to produce a total pressure of 6 cm. The two values of log EW obtained from the 1.6 μ bands were 1.38 for pure CO_2, $p = 3$ cm and 1.44 for CO_2 + Ar, $p = 6$ cm. Reference to Fig. 11 indicates that for pure CO_2 at $p = 3$ cm, log EW = 1.38, indicating good reproducibility of the data. Fig. 13 shows that for 228 m atm of a 25% CO_2/N_2 mixture (i.e., 57 m atm of CO_2) at $p = 6$ cm, log EW = 1.45. In other words, the effect of broadening by Ar appears to be essentially the same as that produced by N_2, at least in this range of pressure. Therefore, the N_2/CO_2 ratio derived above may be regarded as actually representing the $(N_2 + Ar)/CO_2$ ratio, with the ratio Ar/N_2 left undetermined.

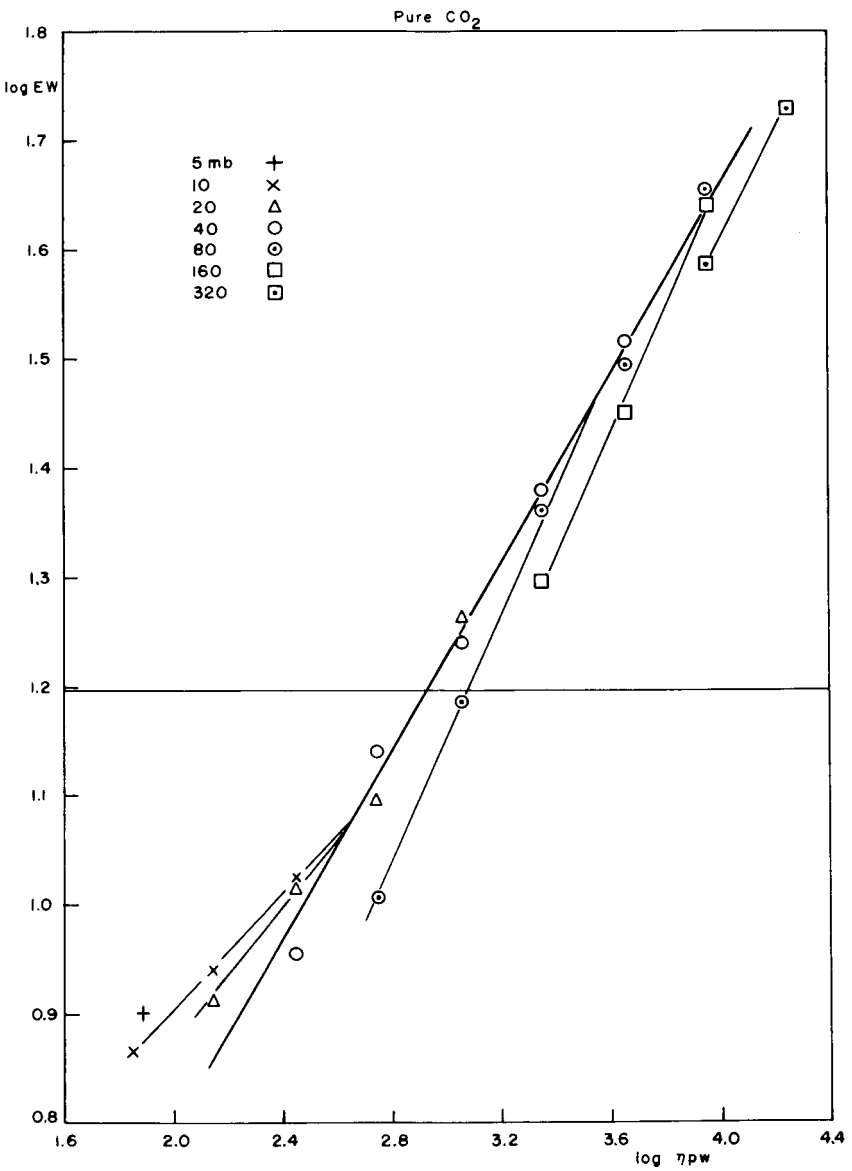

Fig. 15. Data of Fig. 11 presented with log ηpw as abscissa instead of log p.

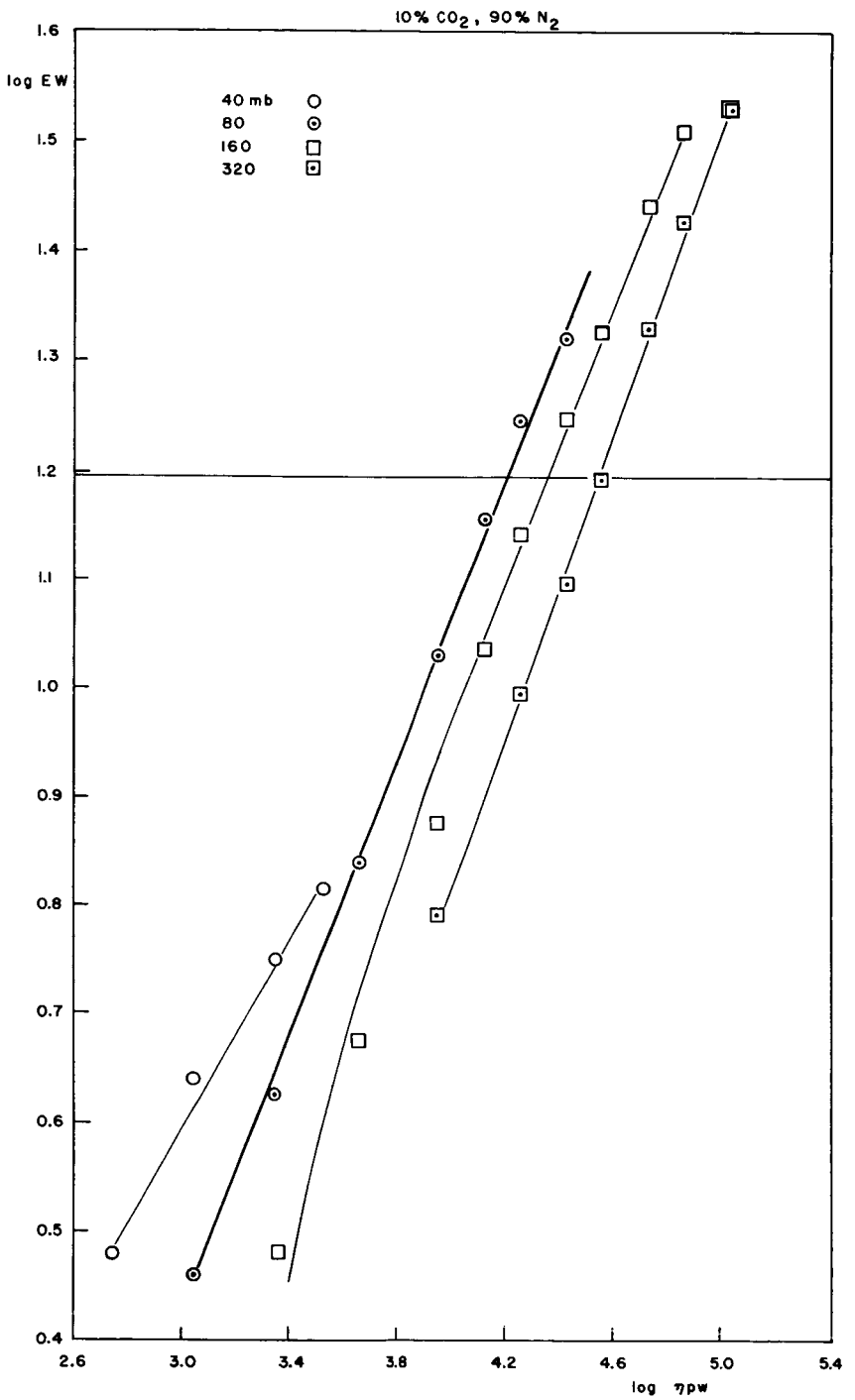

Fig. 16. Data of Fig. 12 presented with log ηpw as abscissa instead of log p.

The surface pressure can also be determined directly from the equivalent widths of the Martian and telluric 1.6 μ bands. This method was applied by Kaplan, Münch, and Spinrad (1964) to the stronger band at 2.06 μ. As we have seen from the discussion of the laboratory data,

$$W \sim (\eta pw)^n, \tag{2}$$

where the exponent can in principle be determined empirically. One can thus write:

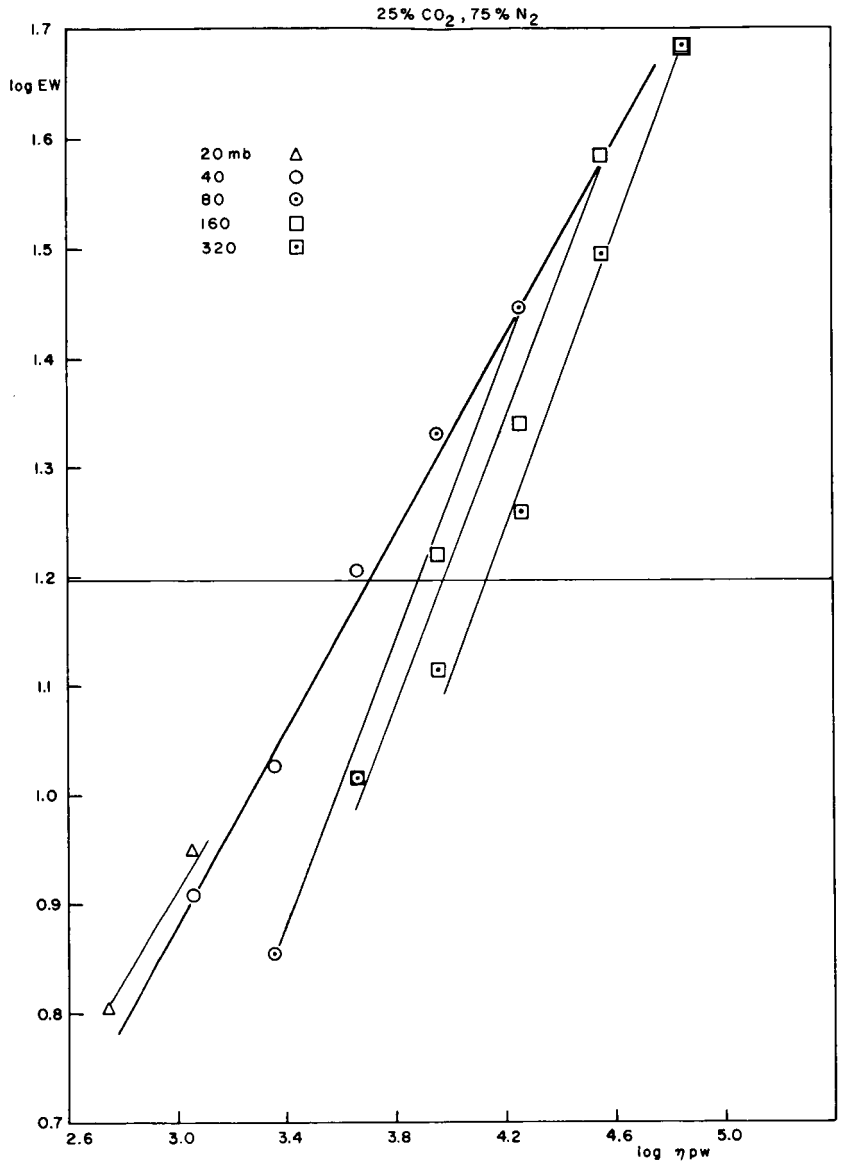

Fig. 17. Data of Fig. 13 presented with log ηpw as abscissa instead of log p.

$$P_M = \frac{\eta_E P_E w_E W_E^{-1/n_E}}{\eta_M w_M W_M^{-1/n_M}} \qquad (3)$$

where n_M and n_E represent the appropriate exponents for the Martian and telluric bands, respectively. The laboratory data indicate a value for $1/n_M$ of ~ 1.5; we shall assume $n_M = n_E$ for this discussion. The equivalent widths of the Martian and telluric 1.6 μ bands are given in *Comm.* 31. With $p_E \approx 800$ mb, $\eta_E = 1.05$, and $w_E \approx 2.1$ m atm, we find $p_M = 18$ mb. This pressure must be corrected for the difference in pressure broadening induced in a N_2/CO_2 mixture where dilution by N_2 is not infinite. This leads to the lower value of $p = 15$ mb, in good agreement with the laboratory determination. If $1/n_M = 1/n_E = 2$, this figure is increased to 16 mb.

The most important source of error associated with these determinations is the uncertainty in the Martian CO_2 abundance. If $w = 60$ m atm, the

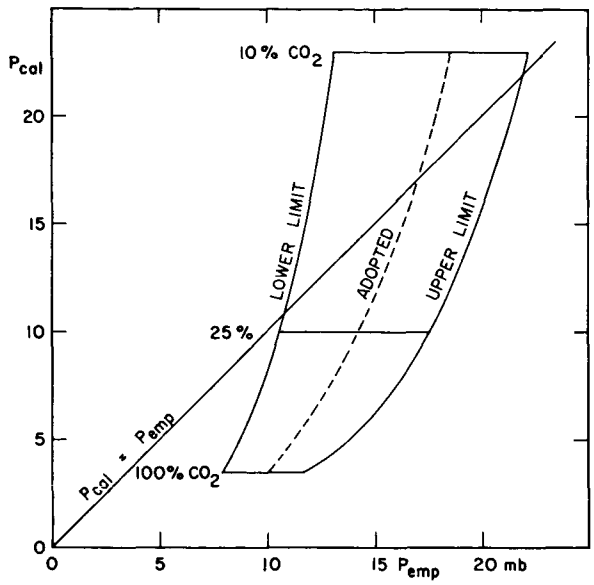

Fig. 18. Calculated pressures at Martian surface (based on weight of gas column) vs. pressures determined empirically from 1.6 μ bands, for 3 gas mixtures. Dashed median line represents adopted solution; intersect with diagonal gives derived pressure of Martian atmosphere, 17 $\pm$ 3 mb.

pressure determined from the laboratory measures is reduced to 15 mb with a concomitant decrease in the amount of N_2. Conversely, a reduction of the amount of CO_2 leads to an increase in the surface pressure and N_2 content. Including the uncertainty in the air mass, we find the results of the two approaches to the determination of the surface pressure can be summarized as:

$$p_{\text{emp}} = 17 \pm 3 \text{ mb (p.e.)}.$$

The difference between 17 and 25 $\pm$ 15 mb, obtained by Kaplan, Münch and Spinrad (1964), probably results from the fact that the 25 mb determination was made from observations of the strong bands near 2 μ where both the Martian and telluric components are saturated. The two components were not well separated by the Doppler shift and there is the additional possibility of contamination due to telluric water vapor, problems which were not encountered at 1.6 μ.

4. The Argon and Oxygen Contents

The Martian argon content will have an origin similar to that of the terrestrial atmosphere: be overwhelmingly composed of radiogenic Ar^{40} exhaled from the crust. The amount per cm^2 of surface present might therefore be as great as on the Earth *if* the enrichment of the surface layer in potassium had been the same and *if* the degassing of radiogenic argon had been equally efficient. Both assumptions are likely to be very extreme for a planet having a mass of only 10% of the Earth. The gross upper limit so obtained would cause a weight of the column of Ar on Mars of $9.3 \times (40/29) \times 0.38$ mb $= 4.8$ mb, 0.93 being the volume percentage of argon in the terrestrial atmosphere.

A fairly realistic value might be found by the assumption that the crustal exhalation process leading eventually to the formation of atmospheric N_2 would have had similar efficiency relative to the Earth as that of argon, although, admittedly, this involves an assumption about the time sequences of these events. Then one finds that the Ar/N_2 ratios on the two planets will not be grossly different, or both roughly 1.2% by volume. The fractional volume of Ar in the Mars atmosphere will then be about $0.012 \times 0.86 = 0.010$ (one per cent); and the weight of the column 0.23 mb, 20 $\times$ less than the gross upper limit mentioned above. (The ratio 20 represents, of course, essentially the abundance ratio of the two atmospheres, N_2 being the chief constituent of both).

On the basis of a diagram by Paetzold (1963), relating the computed Martian O_3 content to the assumed fractional O_2 content, and the limit of O_3 established by Kuiper (1952), the upper limit to the fractional O_2 content is found to be 0.0002.

Including the upper limits for several gases derived before (Kuiper, 1952 and *Comm.* No. 31), and Mr. Marshall's result in *Comm.* No. 35, we find the preliminary composition model of the Mars atmosphere listed in Table 5.

Acknowledgments. We are indebted to Government agencies which have made this research possible. The program in planetary spectroscopy at this Laboratory has been supported by NASA through Grants NsG 61-161 and NsG 223-61. Mr. Owen's contributions have been assisted by ONR Grants Nonr (G)-00050-62 and ONR G-00014-64.

APPENDIX

Air Mass

The equivalent width of a band will be proportional to $(\eta pw)^n$ where η is the air mass, p is the effective pressure, w is the amount of absorbing gas in a unit column, and n has a value between 0 and 1. The effective air mass η, which gives a measure of the amount of gas contributing to the absorption, is

TABLE 5
PRELIMINARY COMPOSITION MODEL OF MARTIAN ATMOSPHERE

GAS	ABUNDANCE (cm, NPT)	VOLUME FRACTION	GAS	ABUNDANCE (cm, NPT)
N_2	30000	0.85	COS	< 0.2
CO_2	5000	0.14	CH_2O	< 0.3
Ar	400	0.01	N_2O	< 0.08
H_2O	1.		NO	$<20.$
O_3	< 0.05		NO_2	< 0.0008
O_2	$< 7.$		H_2S	< 7.5
SO_2	< 0.003		CH_4	< 0.4
CO	$< 1.$		NH_3	< 0.1

obtained by averaging $\sec^n \theta$ over the equatorial strip of the planet which was accepted by the slit of the spectrometer.

$$\eta^n = \frac{\int_0^{\pi/2} \sec^n \theta \cos\theta \, d\theta}{\int_0^{\pi/2} \cos\theta \, d\theta} = \int_0^{\pi/2} \cos^{1-n}\theta \, d\theta.$$

This integral may be expressed in gamma functions:

$$\eta^n = \frac{\sqrt{\pi}}{2} \frac{\Gamma\left(1-\frac{n}{2}\right)}{\Gamma\left(\frac{3-n}{2}\right)} = \frac{\sqrt{\pi}}{2} \frac{1}{\left(1-\frac{n}{2}\right)} \frac{\Gamma\left(2-\frac{n}{2}\right)}{\Gamma\left(\frac{3-n}{2}\right)}$$

$$\eta = 2\left[\frac{\sqrt{\pi}}{2-n} \frac{\Gamma\left(\frac{4-n}{2}\right)}{\Gamma\left(\frac{3-n}{2}\right)}\right]^{\frac{1}{n}}$$

Values for η for several values of n are given in the accompanying table:

n	$1/n$	η
1.00	1.00	3.14
.80	1.25	3.00
.75	1.33	2.99
.67	1.50	2.96
.50	2.00	2.87
.40	2.50	2.84
.33	3.00	2.82
.25	4.00	2.81
.20	5.00	2.78
.10	10.00	2.74
0.02	50.00	2.21

The exponent depends on the position of the band on the curve of growth. In the case of an isolated line, the curve of growth has three principal regions: the linear part ($n = 1$, weak lines); the transition region ($n \sim 0$, saturation just beginning) and the square-root part ($n = ½$, strong lines). For an unresolved band, an average is taken over weak and strong lines and one must also contend with effects due to overlapping. Summing over weak and strong lines will simulate adding curves of growth for different amounts of gas: the linear part merges into a region where the slope n is between 1 and 0 but closer to 1, while the lower section of the square-root part will approach a slope between ½ and 0. The transition zone will thus be extended into a region of gradually-changing slope. The effect of overlapping will be most noticeable for the strongest lines where it will lead to a "rounding off" of the square-root region with increases in the amount of gas having less effect on the equivalent width.

REFERENCES

Goody, R. M. 1964, *Atmospheric Radiation I, Theoretical Basis* (Oxford: Clarendon).

Kaplan, L. D., Münch, G., and Spinrad, H., 1964, *Ap. J., 139,* 1.

Kuiper, G. P. 1952, *The Atmospheres of the Earth and Planets,* ed. G. P. Kuiper (Chicago: University of Chicago Press), p. 374, Table 9.

Paetzold, H. K. 1963, *La Physique des Planètes,* (Liège) Chap. 44, p. 452.

No. 33 A DETERMINATION OF THE MARTIAN CO_2 ABUNDANCE

by T. C. OWEN*

June 8, 1964
Revised August 26, 1964

Lunar and Planetary Laboratory
and
Kitt Peak National Observatory**

Contribution No. 66 of the Kitt Peak National Observatory

ABSTRACT

Two independent determinations are presented of the CO_2 content of the Martian atmosphere derived from the Mt. Wilson plate obtained by Kaplan, Münch, and Spinrad.

1. Introduction

The two preceding papers (*Comm. LPL* 31 and 32) present new spectra of the planet Mars in the 1.0–2.5 μ region and their laboratory calibration with a long absorption tube. This calibration leads to a relationship between total atmospheric pressure and CO_2 abundance. Before the atmospheric pressure (and, by inference, an approximate composition) can be found, independent data on the Martian CO_2 abundance are required. The best source of this information at present is the Martian λ 8689Å CO_2 band observed by Kaplan, Münch, and Spinrad (1964) (referred to hereafter as KMS). These authors themselves calibrated this CO_2 band from laboratory observations supplied by Rank, but because of the peculiar role played in this band by the effects of blending by solar Fraunhofer lines it appeared important to recalibrate the spectrum in such a manner that the effects of solar blending would be accurately allowed for. The interest in the λ 8689Å band stems from the fact that the lines in this band are very weak so there is almost no saturation. Thus they are on the linear part of the curve of growth and their intensities are directly proportional to the abundance.

After calculating the effective air mass corresponding to the Martian observation and making slight corrections for collisional broadening and saturation effects due to the narrowness of the lines, KMS derived a value of 55 $\pm$ 20 m atm for the CO_2 abundance. This value corresponds to an assumed temperature of 230°K in the Martian atmosphere. For 200°K, the corresponding value was 50 $\pm$ 20 m atm. The reason cited for the large probable error associated with these values was the difficulty in determining the equivalent widths of the weak CO_2 lines.

The new calibration of the Mt. Wilson spectrogram was done in two steps. A preliminary calibration was made prior to the completion of our high-dispersion laboratory spectrograph by means of observations of the 8689Å band of CO_2 in the

*Graduate Research Student, 1963, Kitt Peak National Observatory.

**Operated by the Association of Universities for Research in Astronomy, Inc., under contract with the National Science Foundation.

solar spectrum at sunrise. When the spectrograph was finished, laboratory spectra of CO_2 were obtained from which a more precise value for the Martian abundance could be derived. For the sake of completeness and because of the intrinsic interest in the solar observation, both of these techniques are described below.

2. *Observations and Experimental Procedure*

The observations of the Sun were made with the McMath Solar Telescope of the Kitt Peak National Observatory. The 30-foot spectrograph employed with this instrument gives a dispersion of 1Å/mm when the grating is used in the first order (blaze at 8000Å). The solar spectrum was obtained by setting up the image of the eastern horizon on the spectrograph with the slit oriented parallel to the horizon and just above it, slightly southwest of the sunrise point. The Sun was allowed to drift past the slit during the course of the exposure, which was made at a fixed zenith angle. The heliostat was then moved to position the slit ahead of the Sun and the procedure was repeated. In this way a series of exposures corresponding to decreasing values of zenith angle could be obtained within a few minutes while conditions were optimum.

The laboratory work was carried out with the help of a 72-foot multiple path absorption tube. The aim of the program was the acquisition of a series of spectra of different amounts of CO_2 that could be compared directly with the Mt. Wilson spectrogram of Mars. To achieve this end, spectra were obtained at a range of pressures between 10 and 20 cm Hg and a corresponding range of pathlengths using the Sun as a light source. The laboratory spectrograph is of the Czerny-Turner type and has a 10-foot focal length. A 600 line/mm grating blazed at 1.6 μ was used in the second order to produce a dispersion of 2.5Å/mm. This configuration matched the resolution of the Mt. Wilson spectrogram rather well when the slit was opened to 100 μ. As a final precaution, hypersensitized IV-N, the type of emulsion that recorded the spectrum of Mars, was employed for the laboratory work.

3. *The Martian CO_2 Abundance*

(a) The Solar Observations

The most suitable solar spectra for the present purpose were obtained on November 12, 1963. A reproduction of the spectrum corresponding to the largest zenith angle is given in Figure 1 together with a comparison spectrum taken with the Sun two hours past the meridian. These spectra indicate one of the problems encountered in the calibration of the intensities of the Martian CO_2 lines by revealing the large number of faint solar lines which occur in this spectral region. Nevertheless, the interval between the two lines at 8689.79Å and 8692.34Å is clear, and on the spectrum obtained with the Sun at the horizon, the $J = 8$, 10, and 12 lines of the R branch of the $5\nu_3$ band of CO_2 are faintly visible. The presence of R(4) is revealed by the enhancement of the solar line at 8693.15Å. The many weak solar absorptions in this region essentially exclude the P branch lines of the CO_2 band from consideration in the abundance determination.

A comparison of these spectra with the spectrum of Mars, reproduced in Figure 2, reveals that the resolution of the former is considerably higher (the group of lines at 8680Å is a good indicator). It is evident that the telluric CO_2 lines are considerably weaker than those in the spectrum of Mars, even at this large zenith angle. This difference is easily seen by comparing the intensity of R(10) with the solar lines at 8682.99Å and 8728.60Å on each spectrum. From such a comparison it is possible to estimate that the telluric lines are weaker by a factor of about 4. This indicates that at normal air paths the Martian CO_2 lines will be roughly 100 times stronger than the telluric equivalents. Thus there should be no problem due to blending with the telluric features.

To proceed from these observations to a rough estimate of the Martian CO_2 abundance, it is necessary to know the air mass through which the observations were made. For such large zenith angles it is no longer possible to use the customary approximations employed in calculating air masses for use in photometric extinction determinations. Instead, a graphical interpolation method was employed, based on data tabulated by Allen (1963). The zenith angles were computed from readings of the setting circles and verified by calculation of the position of the center of the Sun's disc from the recorded times (correcting for refraction). The air mass was then read from a plot of zenith angle vs air mass constructed from Allen's data and corrected for the local temperature and pressure. This led to a value of 30 ± 3 air masses which corresponds to roughly 66 m atm of CO_2. Thus the Martian CO_2 lines would require about 264 m atm or roughly 73 m atm of CO_2 in the atmosphere of Mars when account is

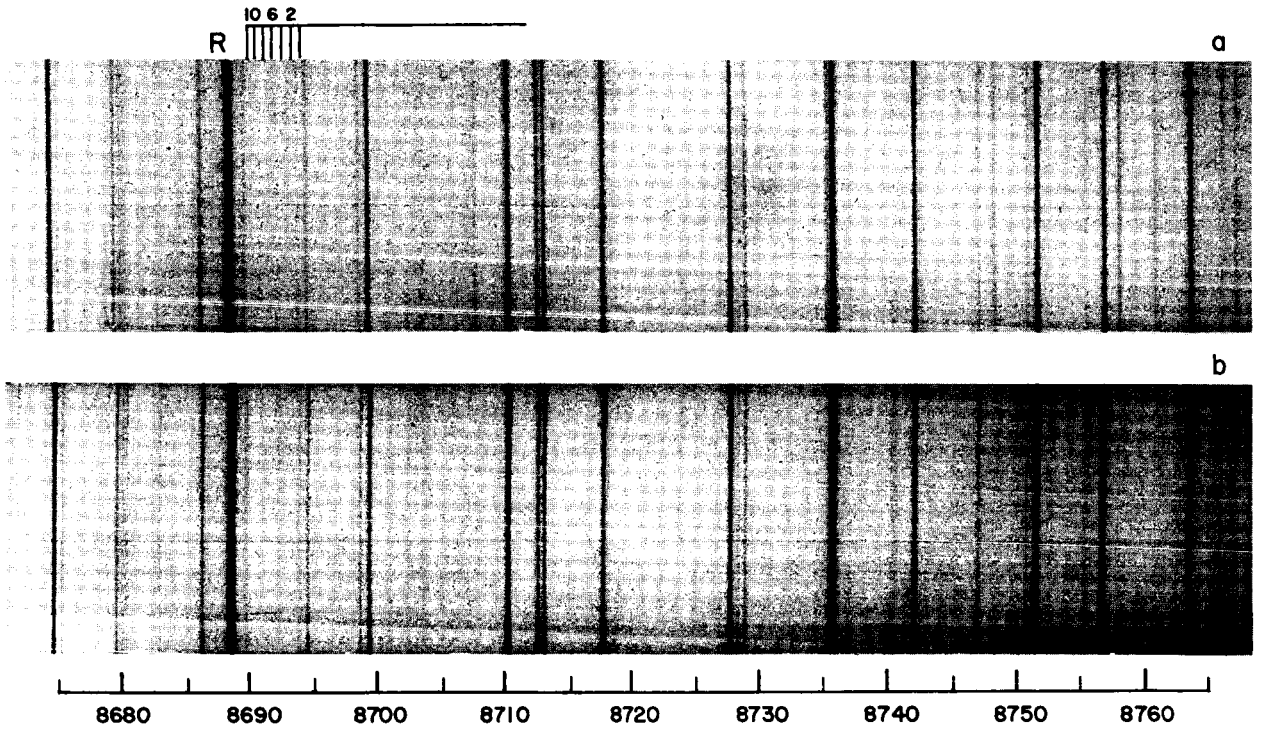

Fig. 1. Spectra of the Sun with McMath Solar Telescope at two zenith angles to show the presence of telluric absorption of $5\nu_3$ (λ8696) of CO_2 with a large air mass: (*a*) Z = 89°57′; (*b*) Z = 32°30′.

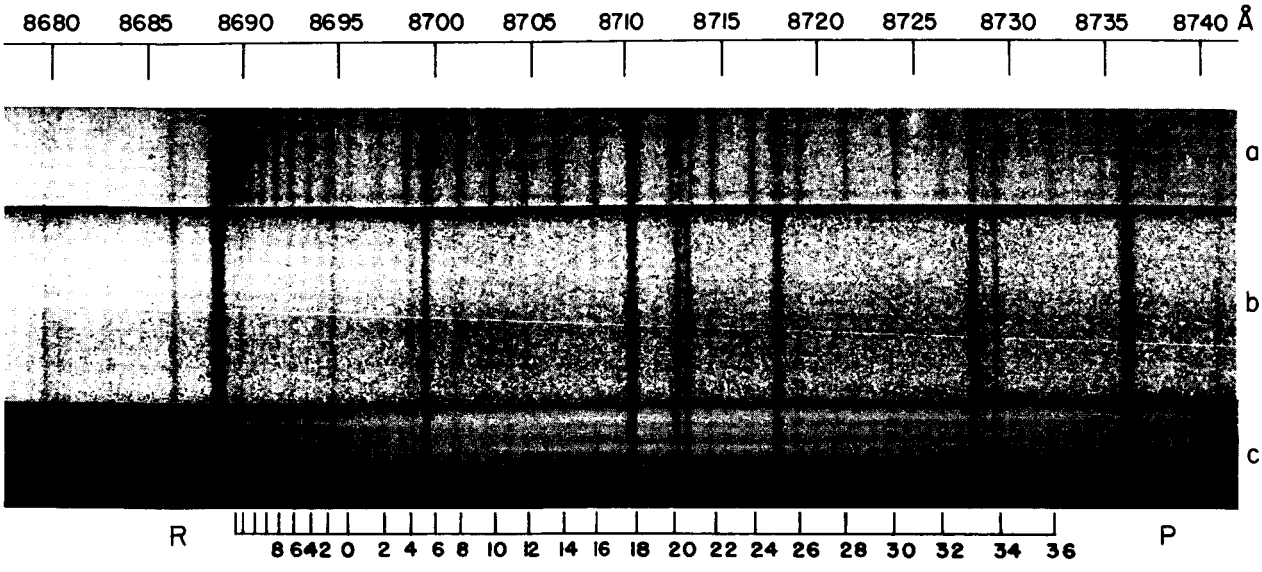

Fig. 2. Spectra of: (*a*) Venus; (*b*) Mars, and (*c*) a laboratory pathlength of 223 m atm (NTP) of CO_2 with the Sun as light source. The *J* numbers of R and P branch lines of the $5\nu_3$ band are shown at the bottom.

taken of the geometry of the Mars observation (see below). This admittedly crude determination served to verify the result of KMS to the extent that it supports the requirement for a larger amount of Martian CO_2 than previously expected.

(b) The Laboratory Calibration

After the amount of gas needed to reproduce the Martian line intensities was roughly known, a series of laboratory spectra was obtained with a range in equivalent pathlength from 85 to 350 m atm. Several combinations of pressure and optical path were used in order to test for pressure-broadening effects, which were found to be negligible within the accuracy of the determination. In an effort to avoid the uncertainty that KMS found to be associated with measurements of the equivalent widths of such weak lines as these, an initial attempt was made to compare the line intensities visually. For this purpose, four solar lines were chosen to serve as standards on each plate: λ8667.37 (Si, −1); λ8668.46 (⊙, −2d?); λ8680.41 (S, 0); and λ8728.60 (Si, −2) (identifications and intensities from Babcock and Moore [1947]). On reproductions of the Mars spectrogram kindly made available by Dr. Spinrad, it is evident that the Martian CO_2 lines exhibit intensities intermediate between that of λ8667.37 and λ8668.46 or λ8728.60. Of the latter two lines, the last one is barely indicated on the reproductions, the other line is not visible. This difference in intensity is also apparent on the laboratory plates. On this basis, it was found necessary for the laboratory pathlengths to lie within the range 241 ± 44 m atm in order to give intensities comparable with the Martian CO_2 lines. The laboratory plate giving the closest match is reproduced with a copy of the Martian spectrogram in Figure 2. As a further check, densitometer tracings were made of the plates corresponding to the indicated range in pathlength and the relative intensities of the solar and CO_2 lines were measured. The difficulties experienced in making these measurements corroborated the remarks of KMS, but the results served to confirm the visual estimate. The ratio of the mean intensity of the three CO_2 lines to that of the solar line at 8667.37Å was .4, .6, and .9 for pathlengths of 197, 241, and 289 m atm, respectively. KMS derive a mean equivalent width of 3.8 mÅ for the CO_2 lines and give the corresponding value for the solar line as 7 mÅ. On this basis they conclude that an upper limit for the CO_2 equivalent width lies between 5 and 6 mÅ. Taking ratios, this implies $.4 \leq W\ CO_2/W_\odot \leq .8$, in good agreement with the result derived above. A densitometer tracing of the 241 m atm laboratory plate is presented for comparison with a similar tracing of the Martian spectrogram in Figure 3. A high-resolution solar trace is added for comparison.

In order to convert the equivalent pathlength derived above into an abundance of CO_2 in the atmosphere of Mars, it is necessary to know the effective air mass and temperature at which the Martian spectrogram was obtained. KMS have calculated that for the geometry at which their observation was made, and with the smearing effects of seeing and guiding errors, the effective air mass is 3.6*. Use of this air mass leads to a value of 67 ± 15 m atm. It remains to correct this figure for the difference in temperature between the laboratory and the Martian atmosphere. From a rough analysis of the relative intensities of the Martian CO_2 lines, KMS conclude that "the apparent positions of the band maxima are consistent with an atmospheric temperature of about 230°K." They note that the blending with solar lines and the uncertainty of their measures makes this an unreliable value. In view of the fact that the mean Martian surface temperature at aphelion is roughly 240°K (Pettit, 1961), an atmospheric temperature of 230°K seems rather high. Perhaps with this in mind, KMS also use a value of 200°K, which would appear to be more reasonable. It would be highly desirable to obtain observations of an unblended CO_2 band (e.g., $\nu_1 + 2\nu_2 + 3\nu_3$ at 1.05 μ), the rotational structure of which could be analyzed less ambiguously. For the present we will use the same two values for the temperature as KMS (cf. Appendix).

For a linear molecule such as CO_2 the intensity of a rotational line in absorption is given by the expression (R branch lines)

*In computing this air mass, KMS restricted themselves to the southern third of the planet. The present comparison was made using both the upper and lower thirds of the reproduced spectrum, although the densitometer tracings were compared to the tracing of the southern third prepared by KMS. As shown in *Comm.* 32, the air mass corresponding to a slit placed pole to pole on the planet is 3.14 for weak lines. For a "polar" third of the disk this would be increased to 4.18. The reduction to the cited value of 3.6 presumably comes about as a result of the seeing and guiding errors the authors estimate to be present. These two effects will cause an apparent motion of the slit with respect to the disk of the planet and will diminish the correspondence between a given position on the planet and a given part of the spectrum. We assume a probable error of ± 0.4 in this value.

$$I_{abs} = \frac{S_{abs}}{Q_r} 2(J+1) \exp\left[\frac{-BJ(J+1)hc}{kT}\right]. \quad (1)$$

The intensity ratio of a line at temperatures T_1 and T_2 is then

$$\frac{I_1}{I_2} = \frac{T_2}{T_1} \exp\left[-BJ(J+1)\frac{hc}{k}\left(\frac{1}{T_1} - \frac{1}{T_2}\right)\right], \quad (2)$$

in which the rotational state sum Q_r has been approximated by an integral:

$$Q_r \approx \int_0^\infty (2J+1) \exp\left[\frac{-hcBJ(J+1)}{kT}\right] dJ = \frac{kT}{hcB} \quad (3)$$

The latter should be a close approximation owing to the small value of B for CO_2 (Herzberg, 1950). For J = 10, $B = 0.3866$, $T_1 = 297°K$, and $T_2 = 230°K$, 200°K we obtain

$$\frac{I_1}{I_2} = .82\ (T_2 = 230°K), .74\ (T_2 = 200°K).$$

Reducing the laboratory abundance to NTP, we obtain 62 ± 11 m atm. If this figure is now multiplied by the factors derived above, the Martian CO_2 abundance is found to be 51 ± 15 m atm (T = 230°K) or 46 ± 15 m atm (T = 200°K). These figures represent the amount of gas at NTP which would give the intensities observed in the Martian spectrum if the gas were cooled to the assumed mean atmospheric temperature of Mars.

It is evident that the agreement with the results of KMS is quite good. Although the abundances reported here are somewhat lower than theirs, each set of figures falls well within the range of error corresponding to the other set. The agreement may even be better than it appears, since it is not clear what

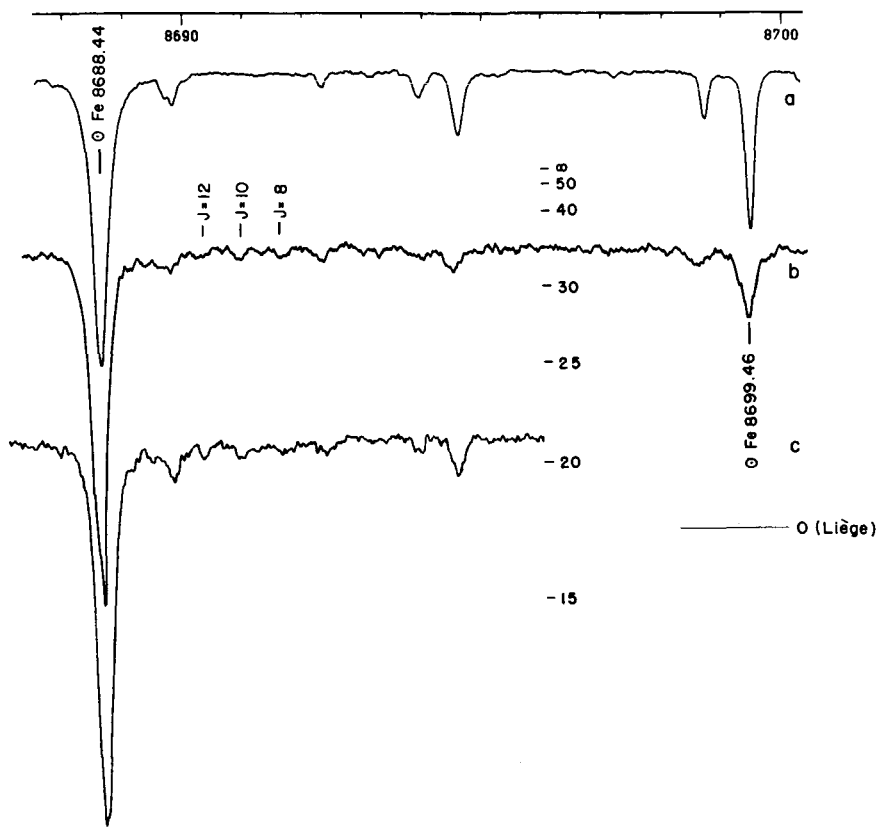

Fig. 3. Solar spectrum (Liège, 1963), Mt. Wilson Mars spectrum, and laboratory comparison (Sun + CO_2). Last two show three rotational lines of CO_2.

temperature has been used by KMS to standardize their meter atmosphere. It has not been possible to reduce the probable error as much as had been hoped, but the accordance of the two sets of values strengthens the validity of each. It appears that additional observations of Mars are needed to increase the accuracy of the determination.

Acknowledgments. The author is grateful to Dr. Hyron Spinrad for providing copies of the Mt.

Wilson spectrogram and for helpful discussions. The Kitt Peak Solar Telescope was made available for the solar observations through the courtesy of Dr. Keith Pierce, who also provided a batch of photographic plates for the laboratory work at a crucial moment. Advice and encouragement were given throughout the course of this study by Dr. Gerard Kuiper. The laboratory program was supported by the Office of Naval Research under contract NR046-791.

APPENDIX

Atmospheric Temperature and the 1.05μ CO_2 Bands

As a first approximation, we can assume that the atmosphere is adiabatic to the height above the surface corresponding to the mean level at which the CO_2 absorption occurs. At this level, the pressure is equal to one-half that at the surface (*Comm.* 32). If we adopt the atmospheric mixture derived in the previous paper, the adiabatic lapse rate for the Martian atmosphere is 3.7°C/km. (It is noted that a considerable range in proportions of CO_2 and N_2 results in roughly the same lapse rate.) The adiabatic assumption then leads to the relation $T_M = 0.833T_S$ where T_M is the temperature at the mean absorbing level and T_S is the surface temperature. Using Pettit's value for $T_S = 240°K$, one finds $T_M = 200°K$. It should be pointed out that since the abundance determination is essentially restricted to the polar thirds of the planet, an even lower mean surface temperature than that assumed here is probably appropriate, so 200°K may be an upper limit.

Ideally, of course, one would like to determine the atmospheric temperature from the same bands used for the abundance analysis. This is not possible in the case of the 8689Å band, since only three rotational lines are unblended and these are very weak. One is thus led to an investigation of the stronger bands near 1.05 μ. These bands are described in Table 1, which is based on a similar table prepared by Herzberg and Herzberg (1953). On the intensity scale in this table, the $5\nu_3$ band at 8689Å has the value unity. Figure 4 shows the appearance of the bands at 1.036 μ and 1.049 μ at three pathlengths which bracket the equivalent optical path for absorption in the Martian atmosphere, as deduced in this paper. All three spectra were obtained at atmospheric pressure (~ 700 mb). The Sun is again used as a light source, so these spectra are very similar to what one would actually observe when obtaining spectra of Mars. It is apparent that even at the smallest observed pathlengths, the 1.048 μ band is much stronger than $5\nu_3$ and both P and R branch lines are easily visible. The strongest of these lines may be slightly saturated at the low pressure of the Martian atmosphere, but the presence of the weaker band at 1.036 μ allows an empirical evaluation of this possibility. There is a still weaker band at 1.063 μ (not shown), which is barely visible at the intermediate pathlength and relatively easy to discern at the maximum pathlength. Thus the three bands taken together should provide a valuable independent check on both the CO_2 abundance and the mean atmospheric temperature.

Such a study would not be free of observational difficulties, however. This region of the spectrum requires the use of the I-Z emulsion which is notoriously slow and grainy. It is doubtful that the resolution illustrated in Figure 4 could be achieved on Martian spectrograms, but a considerable sacrifice can be afforded. As an illustration, we can consider the lines in the P branch of the 1.049 μ band. The original dispersion of the laboratory plate was 5Å/mm and the spacing of these lines is roughly 2.4Å. Thus a dispersion of 15Å/mm would leave the lines separated by .16 mm. This is slightly greater than the separation of the last resolvable lines of the R branch on the present plates and would therefore be acceptable if the projected slit width remains the same. This is not a prohibitive assignment for a suitably designed spectrograph.

The remaining difficulty is the problem of blending with solar features. Inspection of Figure 4 indicates that several such blends occur, but there are a

TABLE 1
CO_2 BANDS NEAR 1.05 μ

λ_h (air)	ν_h (vac)	INTENSITY	ν_0 (vac)	ASSIGNMENT	λ_0 (air)
10626.7	9407.7	4	9389.0	$4\nu_2 + 3\nu_3$	10647.8
10487.6	9532.3	20	9517.0	$\nu_1 + 2\nu_2 + 3\nu_3$	10504.6
10361.8	9648.2	8	9631.4	$2\nu_1 + 3\nu_3$	10381.0

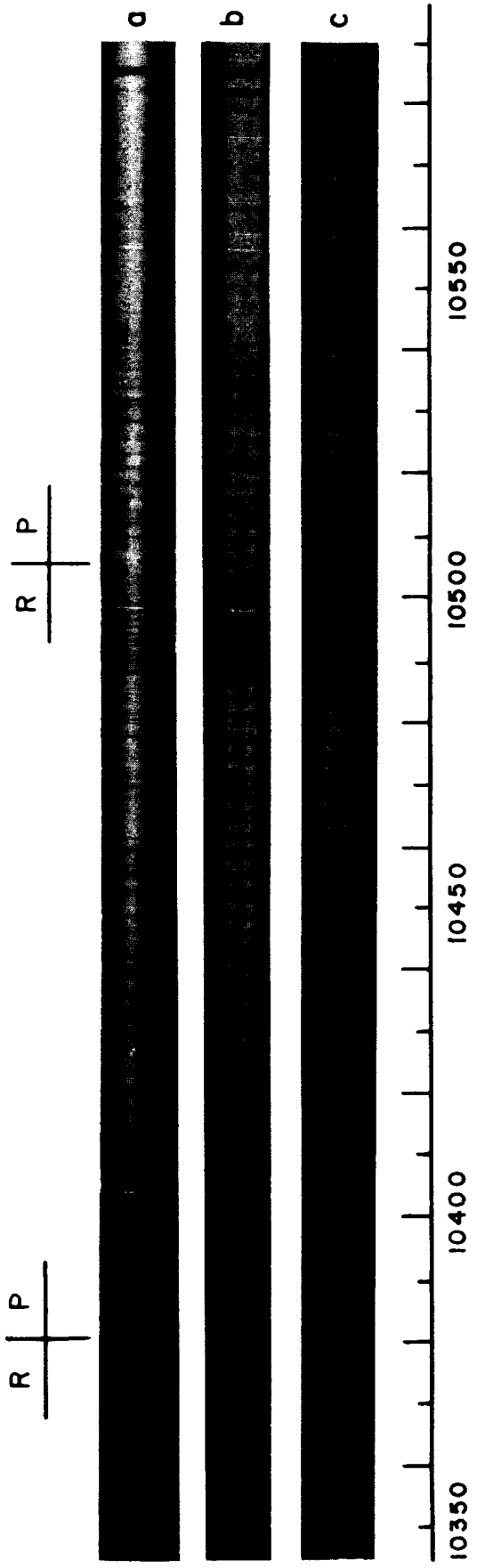

Fig. 4. Laboratory spectra of $2\nu_1 + 2\nu_3$ and $\nu_1 + 2\nu_2 + 3\nu_3$ of CO_2 at three pathlengths (NTP). The Sun was again used as light source. (*a*) 333 m atm; (*b*) 250 m atm; (*c*) 166 m atm.

sufficient number of unblended lines to give reliable results, particularly if all three bands are used.

Note added in proof. After the above was written, Dr. J. Chamberlain suggested to the writer that one might expect overlapping in the R branch of the 8689Å band of CO_2 due to doubling back of the rotational lines after formation of the band head. This will complicate the analysis because the temperature dependence of the lines with high J numbers will be different from that of the rotational lines considered here (mean $J = 10$).The writer was unable to find accurate observed wavelengths of the higher rotational lines reported in the literature and could not resolve them on the plates discussed above. Therefore the rotational constants given by Herzberg and Herzberg (1953) were used to predict the positions of these lines according to the approximate relation

$$\nu_J = \nu_0 + 2B' + (3B' - B'')\,J + (B' - B'')\,J^2. \quad (4)$$

The line $J = 40$ was subsequently chosen as having a position close to that of $J = 10$ and thus being representative of the problem. Using equation (1), we find the relative intensities of $J = 40$ and $J = 10$ are as follows:

$$T = 297°\text{K}, \frac{I_{10}}{I_{40}} = 4.85$$

$$T = 200°\text{K}, \frac{I_{10}}{I_{40}} = 20.$$

If we now express the observed intensity as a simple sum of the intensities of $J = 10$ and $J = 40$ we have

$$\frac{I_{\text{lab}}}{I_{\text{Mars}}} = \frac{I_{10}\left(1 + \frac{1}{4.85}\right)}{I_{10'}\left(1 + \frac{1}{20}\right)} = 0.85$$

where

$$\frac{I_{10}}{I_{10'}} \equiv \frac{I_1}{I_2} = 0.74 \text{ for } T_1 = 297°\text{K}, T_2 = 200°\text{K}.$$

In other words, the fact that we are dealing with a blend of two lines whose intensities change in opposite ways with a decrease in temperature implies that the amount of gas required in the Martian atmosphere to reproduce the observed intensities is somewhat greater than it would be otherwise. Using the NTP laboratory value derived above, we find 53 ± 15 m atm for the Martian CO_2 abundance with an assumed atmospheric temperature of 200°K.

This correction is obviously very rough and is intended primarily as an indication of another kind of uncertainty which is present in the abundance determination. It suggests that the latter is probably better expressed as 50 ± 20 m atm to incorporate the full range of uncertainty, and thus brings the present work into exact agreement with the result of KMS. The added difficulty in correcting for the doubling back of the rotational lines represents an additional argument for attempting to observe the 1.05 μ bands, described in the Appendix, where the P branches (which have no overlapping) are relatively free from solar blends.

Brooks (unpublished) has shown that the air mass corresponding to the KMS observation of Mars should be $\eta = 3.9$. His corrections include a more exact expression for the variation of air mass with zenith angle, a greater smearing effect due to seeing and the use of the proper value for the angular separation of the earth and sun as seen from Mars. Considering both the correction for doubling back and the new value for the air mass, the CO_2 abundance remains the same as that given previously, but the uncertainty must be increased. The revised value is then 46 ± 20 m atm.

REFERENCES

Allen, C. 1963, *Astrophysical Quantities* (2nd ed.; London: Athlone Press).

Babcock, H. D. and Moore, C. E. 1947, *The Solar Spectrum, λ6600 to λ13495* (Washington, D.C.: Carnegie Institution of Washington).

Delbouille, L. and Roland, G. 1963, *Photometric Atlas of the Solar Spectrum from λ7498 to 12016* (Liège, Belgium).

Herzberg, G. 1950, *Spectra of Diatomic Molecules* (Princeton, Toronto, London, and New York: Van Nostrand Co., Inc.).

Herzberg, G. and Herzberg, L. 1953, *J. Opt. Soc. Am. 43,* 1037.

Kaplan, L., Münch, G., and Spinrad, H. 1964, *Ap. J., 139,* 1.

Pettit, E. 1961, *Planets and Satellites,* ed. G. P. Kuiper and B. M. Middlehurst (Chicago: University of Chicago Press), Chapter 10.

No. 34 LABORATORY SPECTRA FOR TESTING THE PRESENCE OF MINOR CONSTITUENTS IN PLANETARY ATMOSPHERES, I: CH_4, NH_3, N_2O, CO, COS, REGION 1–2.5 μ

by GERARD P. KUIPER AND DALE P. CRUIKSHANK

September 10, 1964

As the power of spectrometric devices for the observation of IR planetary spectra increases, new opportunities arise for testing these spectra for the presence of hitherto undetected minor constituents. For most common gases the sensitivity of such tests is minimal in the ordinary photographic range, and increases both for $\lambda << 0.3\ \mu$, where the electronic bands appear, and $\lambda >> 1\ \mu$, where the rotation-vibration bands occur. This paper is concerned with part of the second region, 1–2.5 μ, which is readily observed with a PbS spectrometer. The tests become sharper with still longer wavelengths, where the fundamentals and low overtones occur, but the difficulty of obtaining planetary spectra with adequate resolution also increases there, so that criteria must be developed for each spectral region separately. Further reasons for this are that the atmospheric windows in the IR spectrum are limited so that otherwise favorable criteria may be unavailable, and that strong masking absorptions may be present in the planetary atmospheres obscuring large regions altogether. Multiple test criteria are therefore required.

The laboratory spectra here presented were made with the PbS spectrometer described by Kuiper *et al.* (*LPL Comm. 1,* 119). Absorption cells of various lengths were used made of glass tubing since some of the gases would react with galvanized iron. The light source used was an incandescent laboratory lamp. The windows of the cells were either glass or Suprasil (Englehard Industries, Inc.), and glass lenses (total thickness up to 3 cm) were used in the optical system. In the spectral region covered these lenses had no appreciable selective absorptions.

The spectra show, in addition to the absorptions of the gases under study, absorptions caused by CO_2 and H_2O in the spectrometer and the laboratory (with some enrichment of CO_2 due to evaporating dry ice). The total path in the spectrometer and laboratory was about 3 meters.

The present paper is limited to the gases listed in the title. CO as a minor constituent has been treated previously (Kuiper, *LPL Comm. 1,* 114–115). The tests for NO_2 are insensitive in the region considered here and are no match for the very rich photographic spectrum. The latter is considered in *Communication* No. 35.

The records in the present paper have been used in *Communication* No. 31 and will be referred to in other studies in preparation.

Acknowledgments. The program of infrared planetary spectroscopy is supported by the National Aeronautics and Space Administration through Grant No. NsG 161-61.

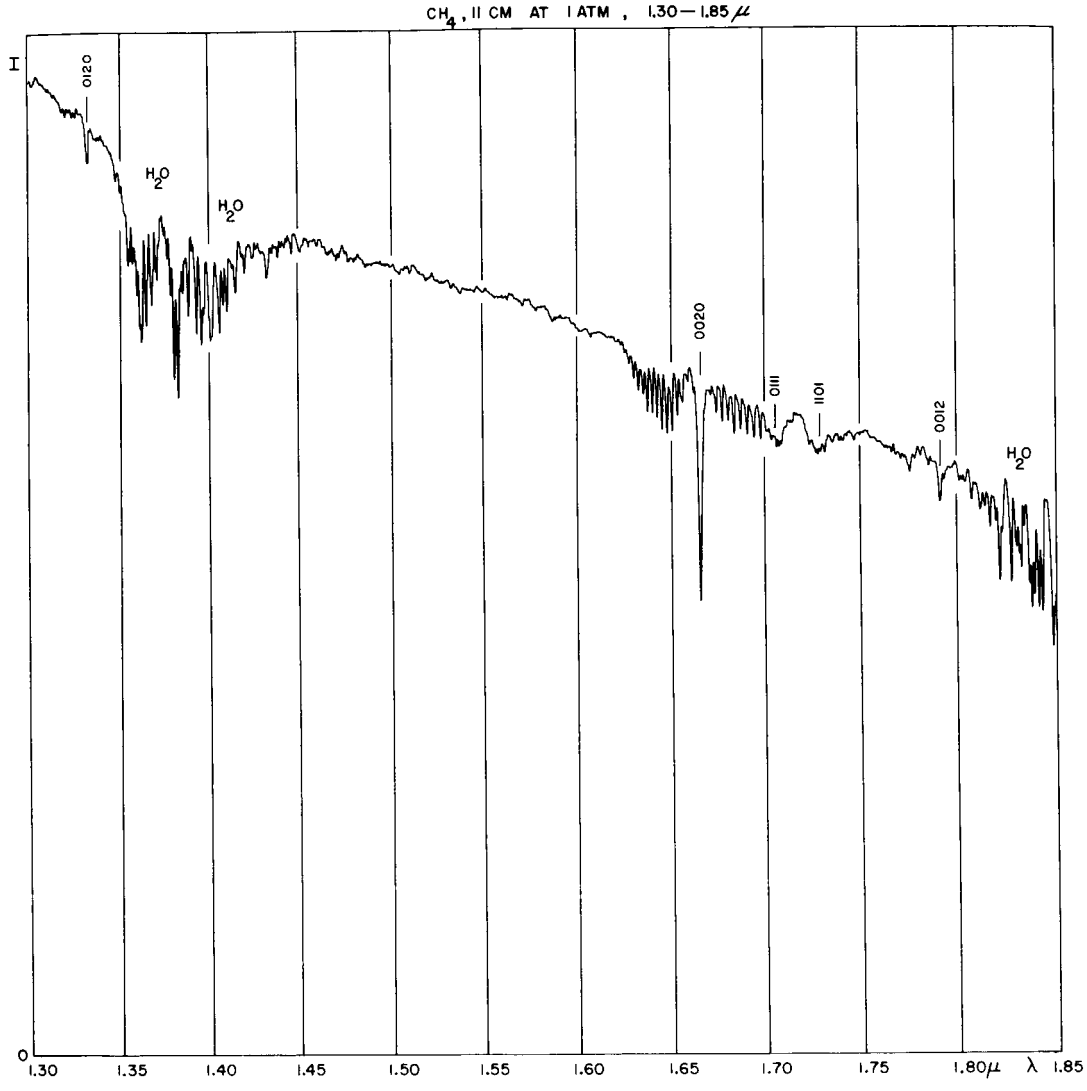

Fig. 1. CH_4, 11 cm at $p = 1$ atm, 1.30–1.85 μ, 1.6 μ grating, Corning 2540 filter, detector cell 0.1 mm, slit 0.18 mm, scan 5/1 (i.e. 0.2 μ scanned in 5 min. and chart speed *1* inch per minute), $\tau = 1$ sec. (i.e. the record is time-constant limited).

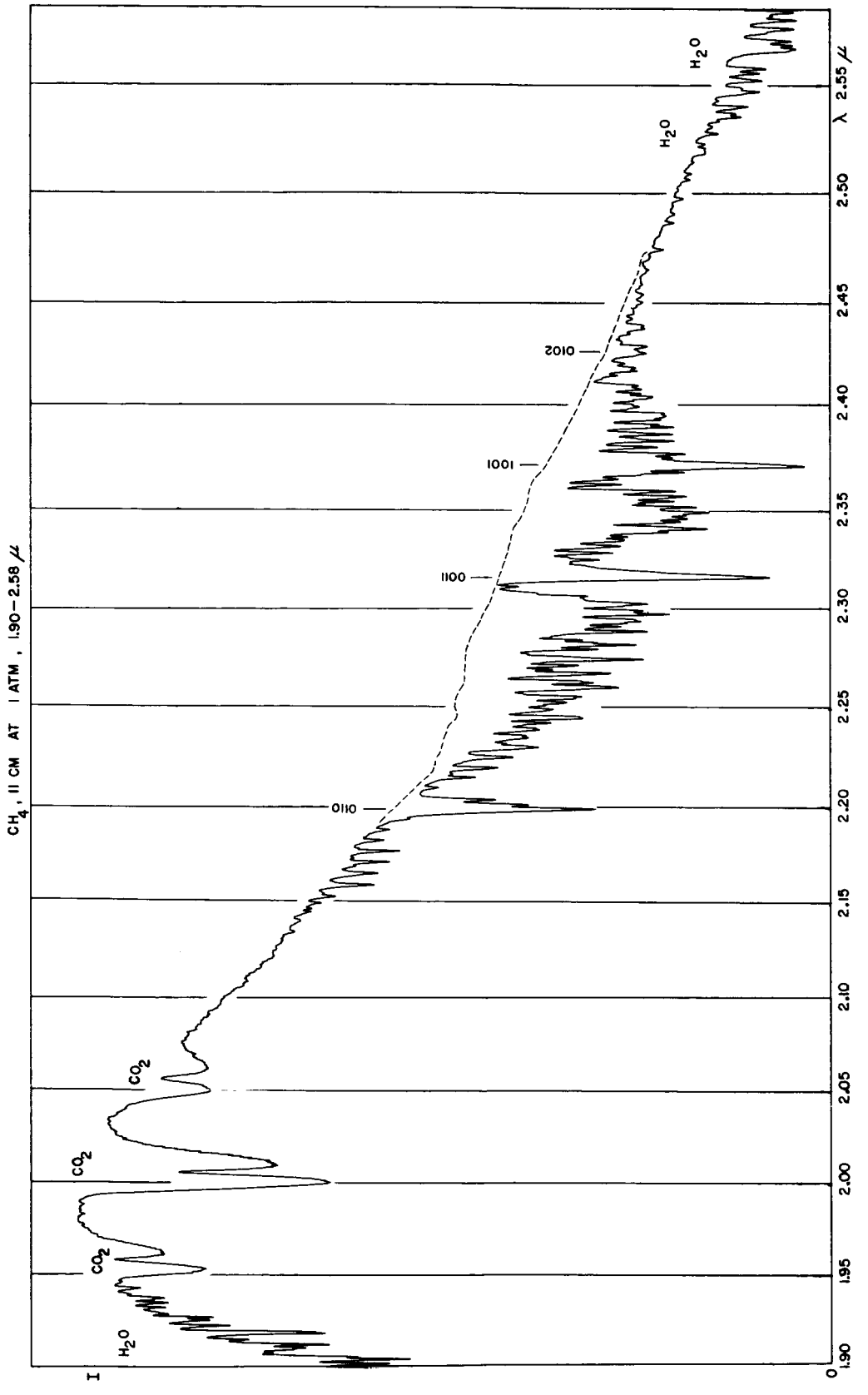

Fig. 2. CH_4, 11 cm at $p = 1$ atm, 1.90–2.58 μ, 1.6 μ grating, 2 μ filter, cell 0.1 mm, slit 0.18 mm, scan 5/1, $\tau = 1$ sec. Undisturbed continuum indicated by dashed line.

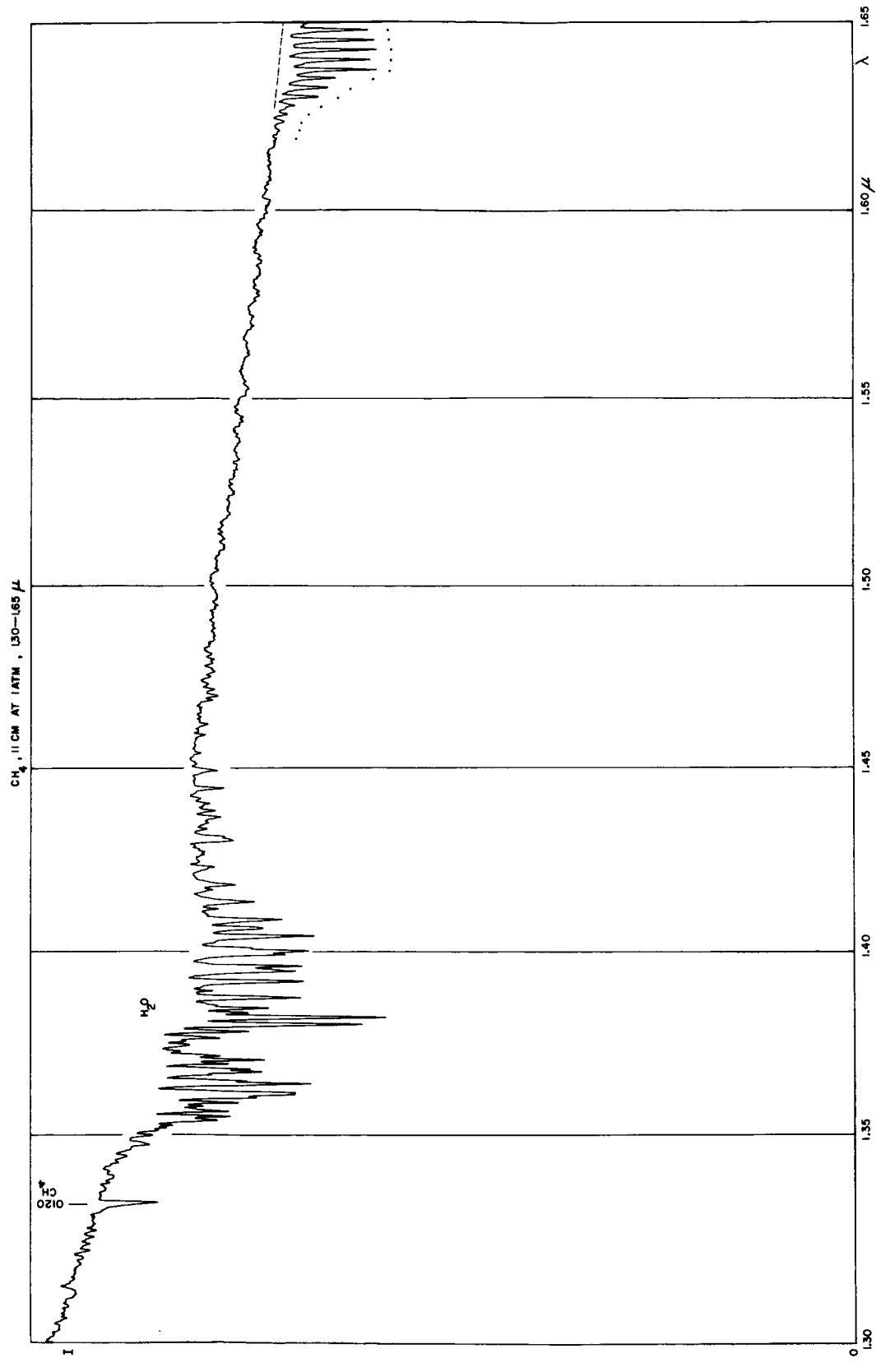

Fig. 3, Part 1. CH_4, 1.30–1.65 μ, as Fig. 1, but scan 12.5/1 (resolution increased over Fig. 1 because of longer scanning time).

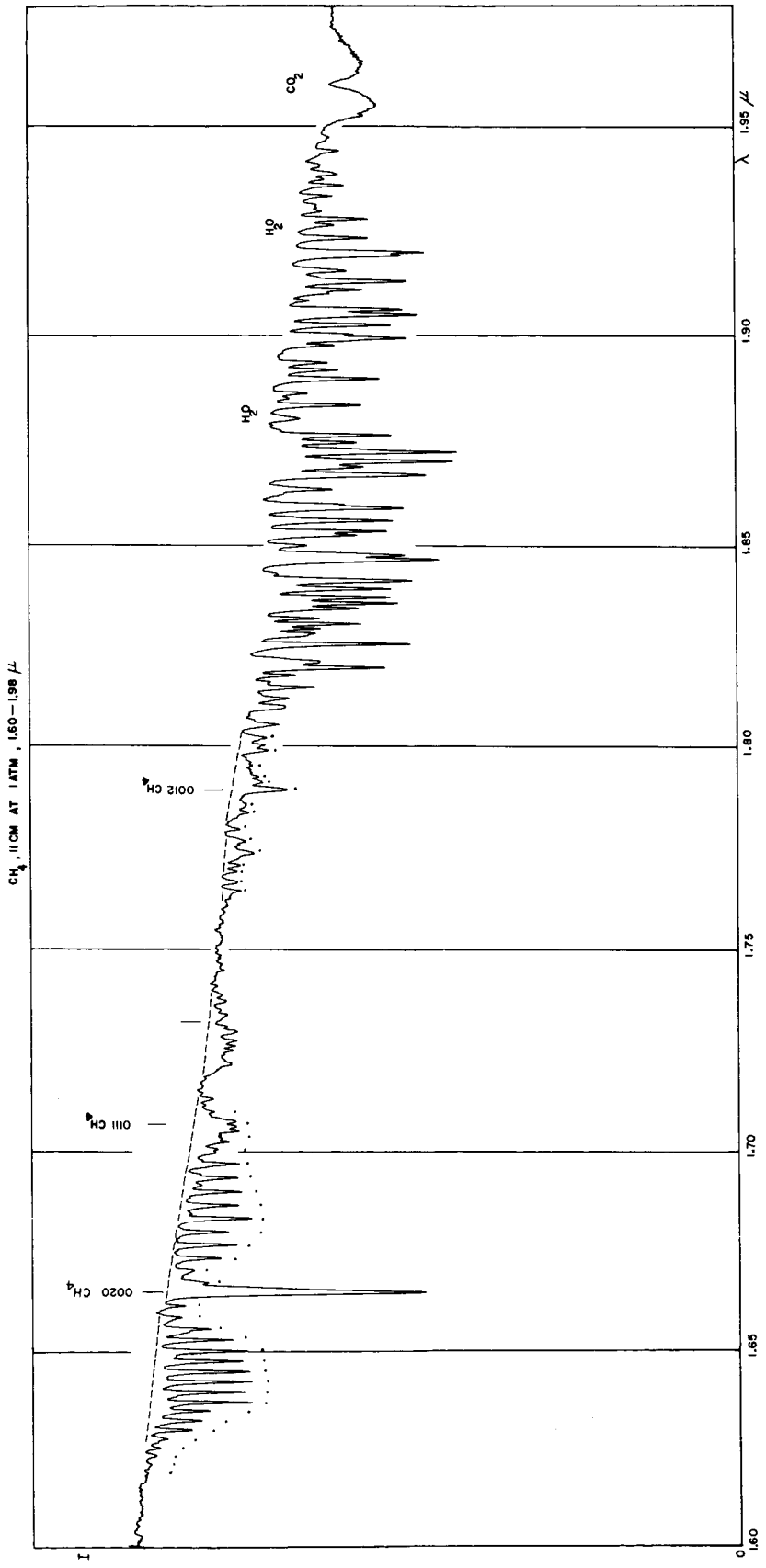

Fig. 3, Part 2. CH_4, 1.60–1.98 μ. *Dashed line,* undisturbed continuum. *Dots,* rotational lines.

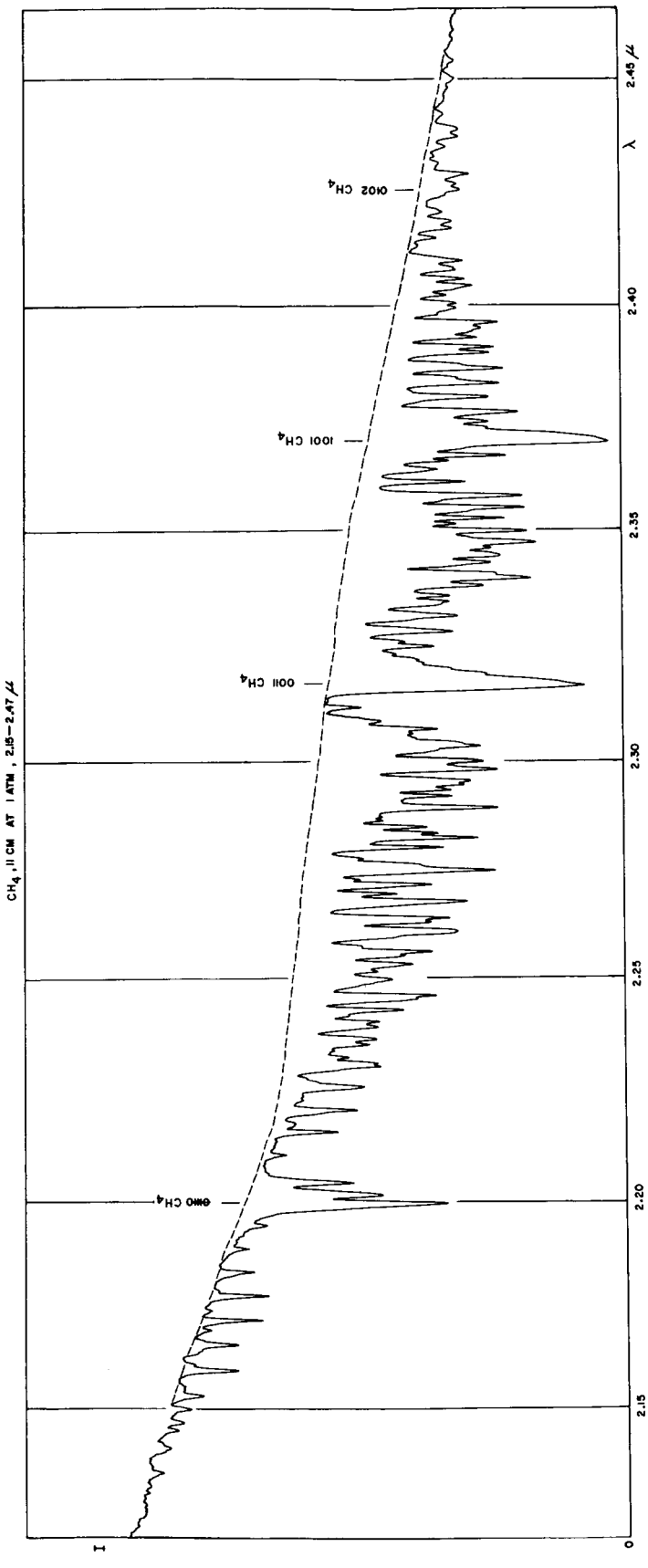

Fig. 4. CH_4, 11 cm at $p = 1$ atm, 2.12–2.46 μ and scan 12.5/1; cf. Fig. 2.

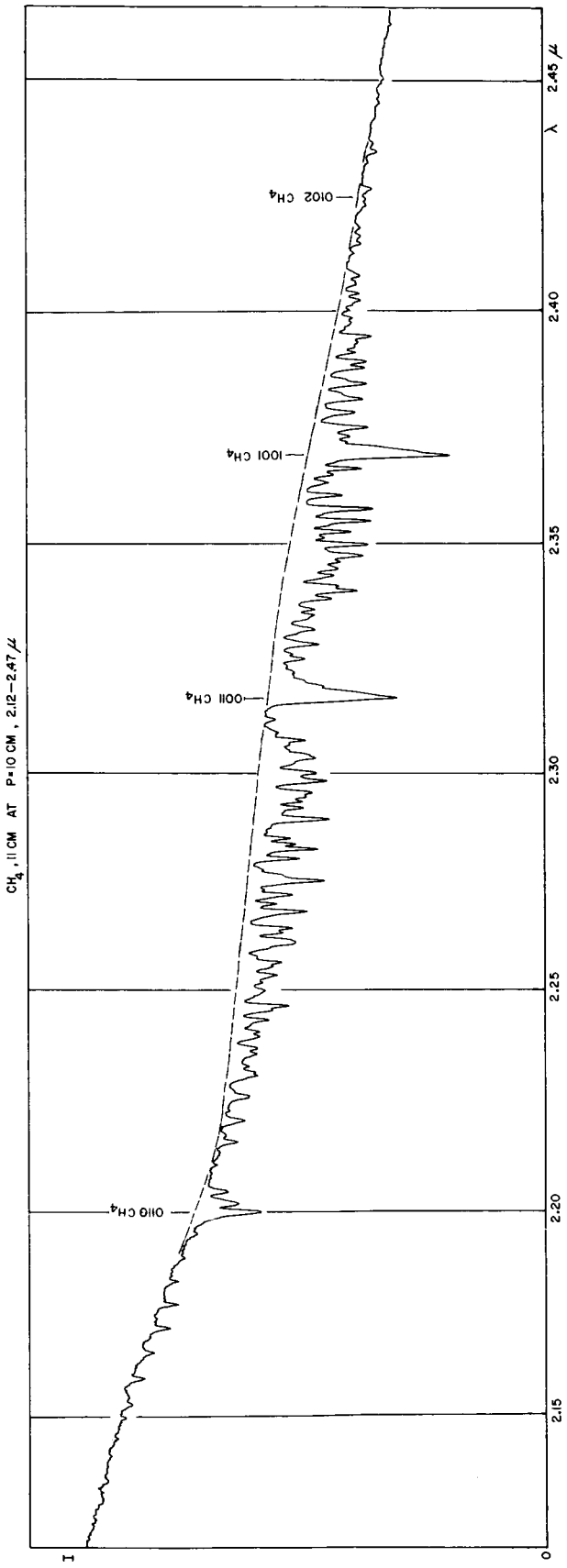

Fig. 5. CH_4, 11 cm at $p = 10$ cm, 2.12–2.47 μ, scan 12.5/1; cf. Fig. 4.

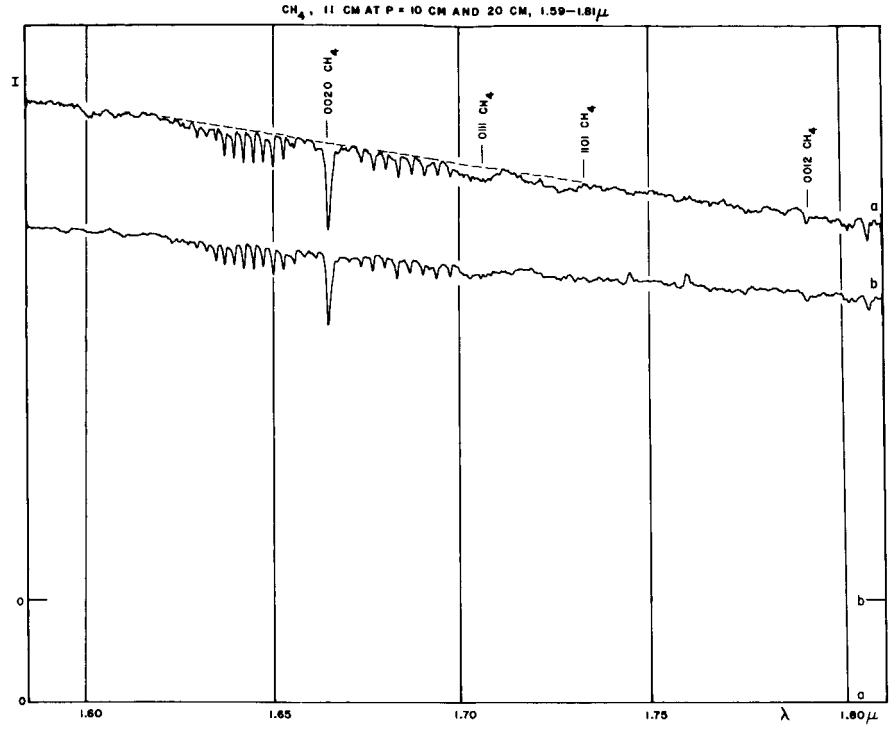

Fig. 6. CH_4, 1.59–1.81 μ; 11 cm at $p = 10$ cm (a), and 20 cm (b); scan 12.5/1; cf. Fig. 3. The zero levels are here in *reverse* order from the graphs, so that amplitude of curve a is 1.6 $\times$ larger than of curve b, more than compensating for intensity difference of band.

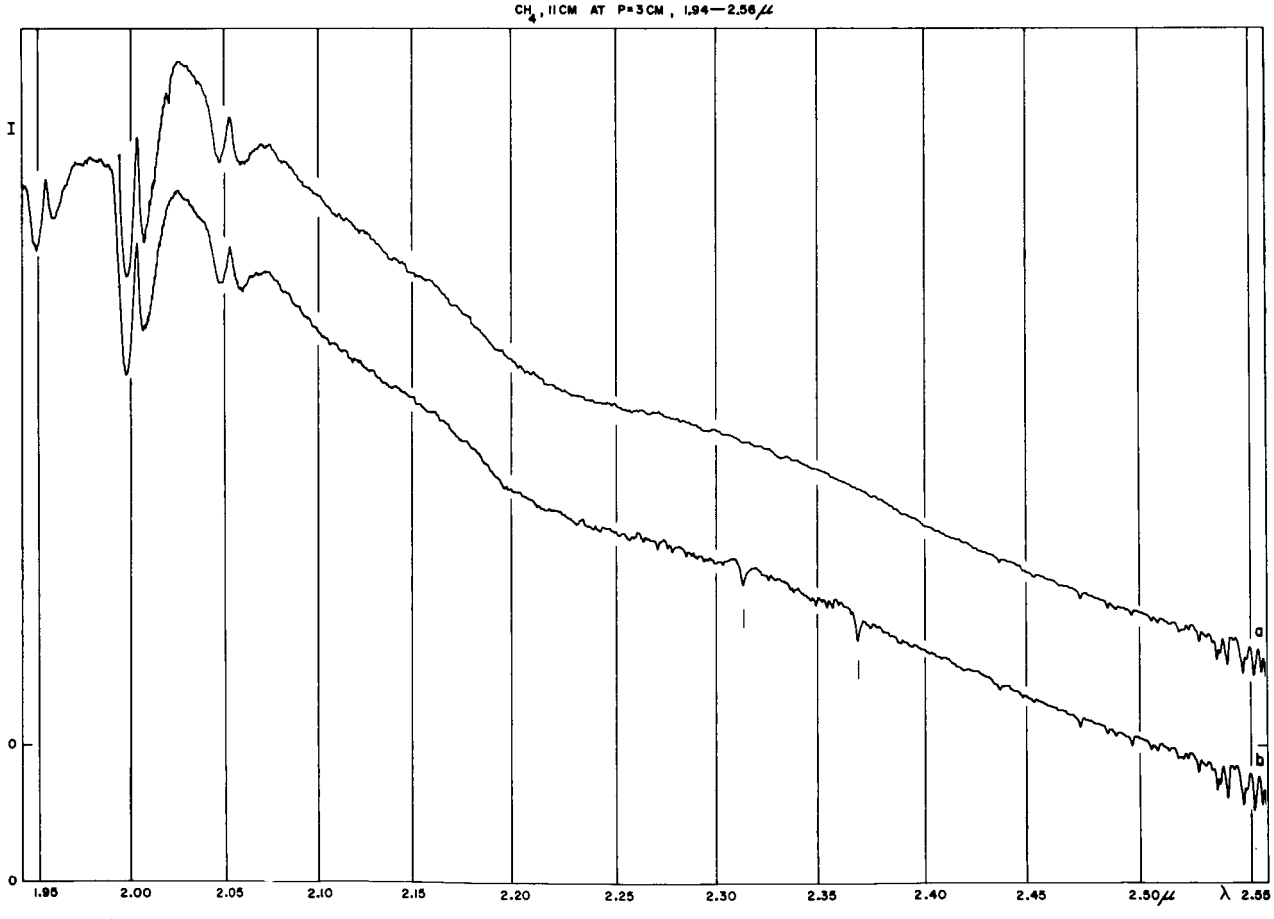

Fig. 7. CH_4, 11 cm at $p = 3$ cm (b) and blank run (a), 1.90–2.58 μ, 1.6 μ grating, 2 μ filter, cell 0.1 mm, slit 0.18 mm, scan 5/1, $\tau = 1$ sec.

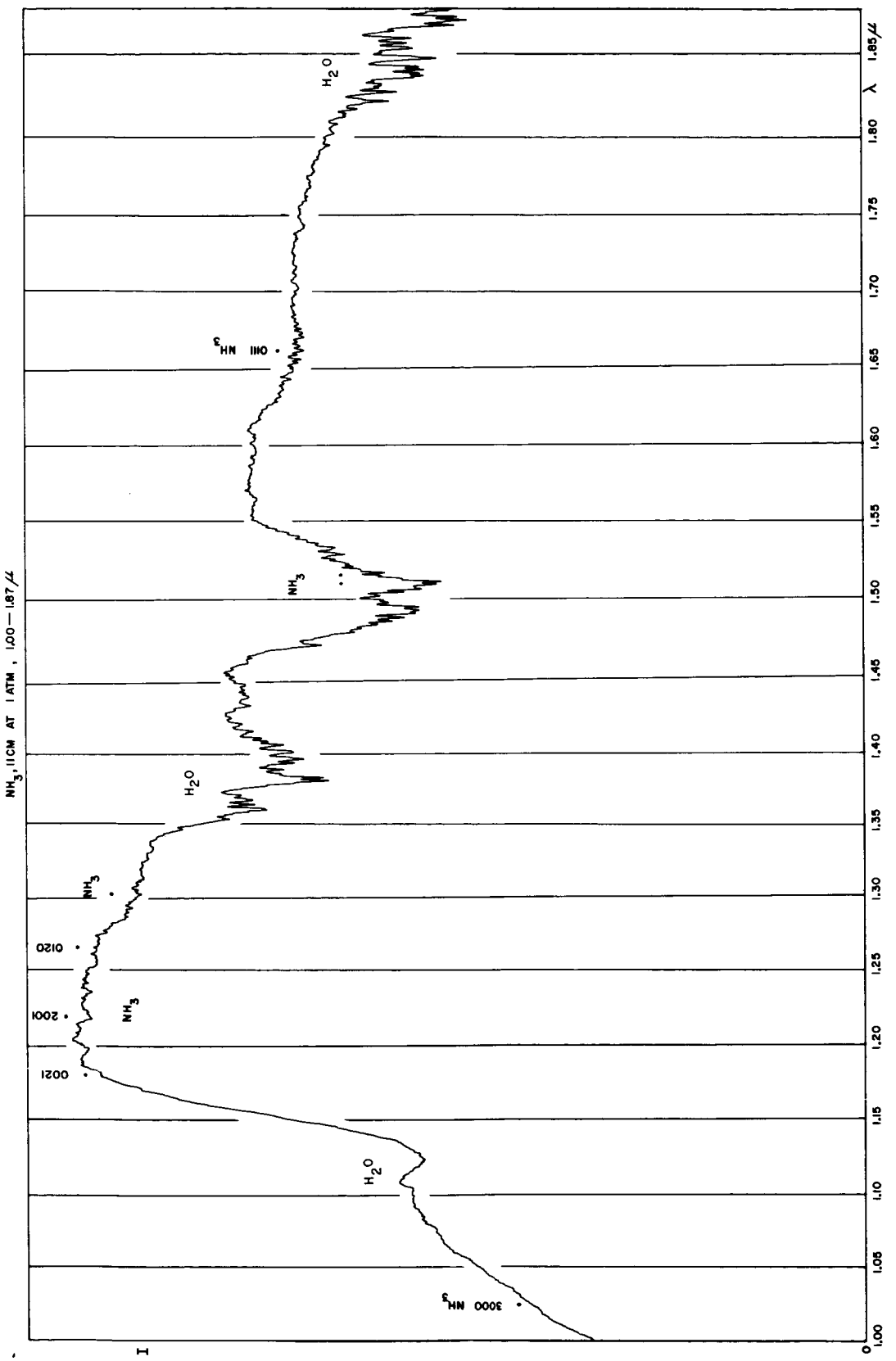

Fig. 8. NH_3, 11 cm at $p = 1$ atm, 1.00–1.87 μ, otherwise as Fig. 1. Dots signify weak NH_3 bands (G. Herzberg, *Infrared and Raman Spectra*, New York, Van Nostrand, 1945, p. 296).

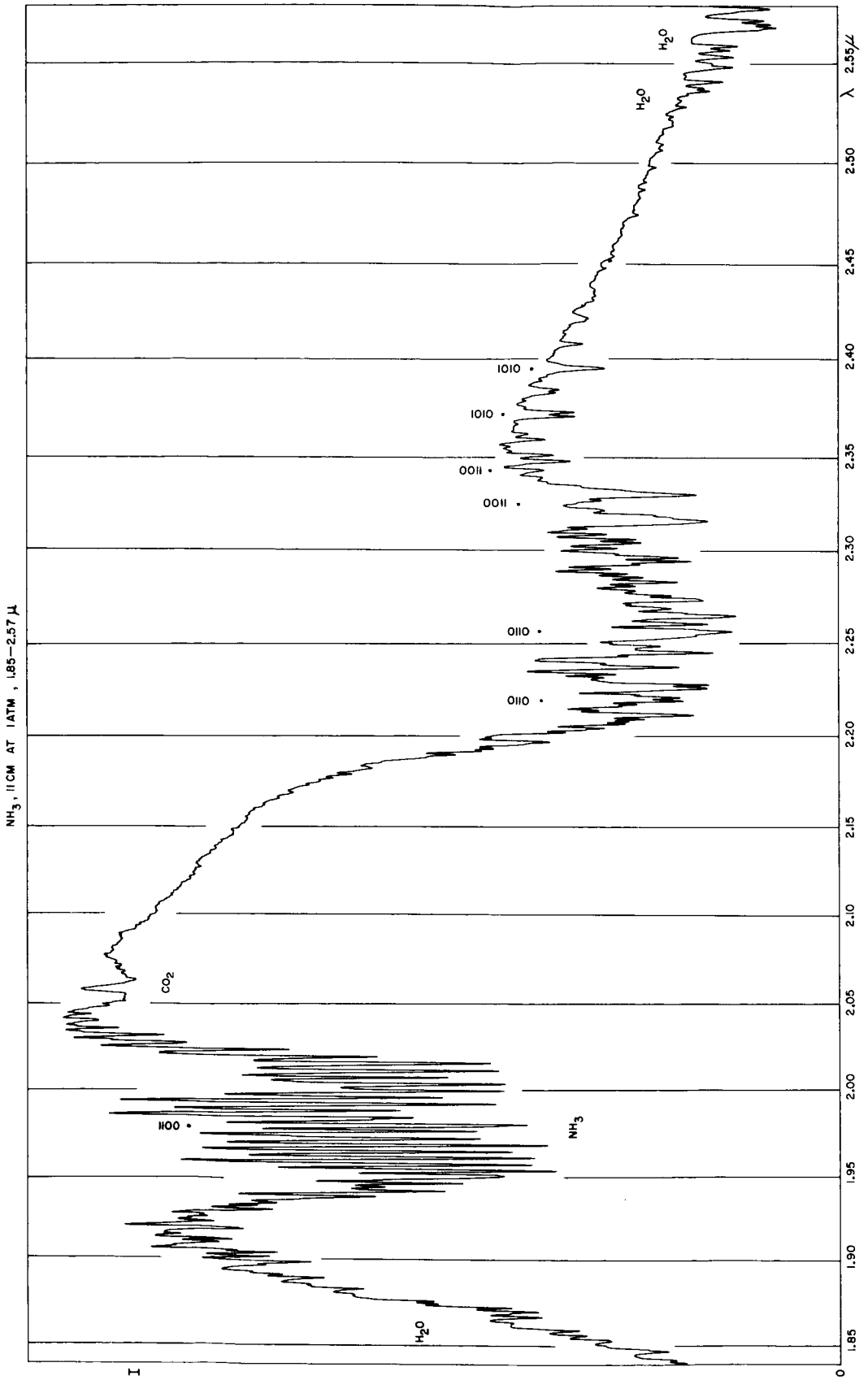

Fig. 9. NH_3, 11 cm at $p = 1$ atm, 1.85–2.57 μ, otherwise as Fig. 2.

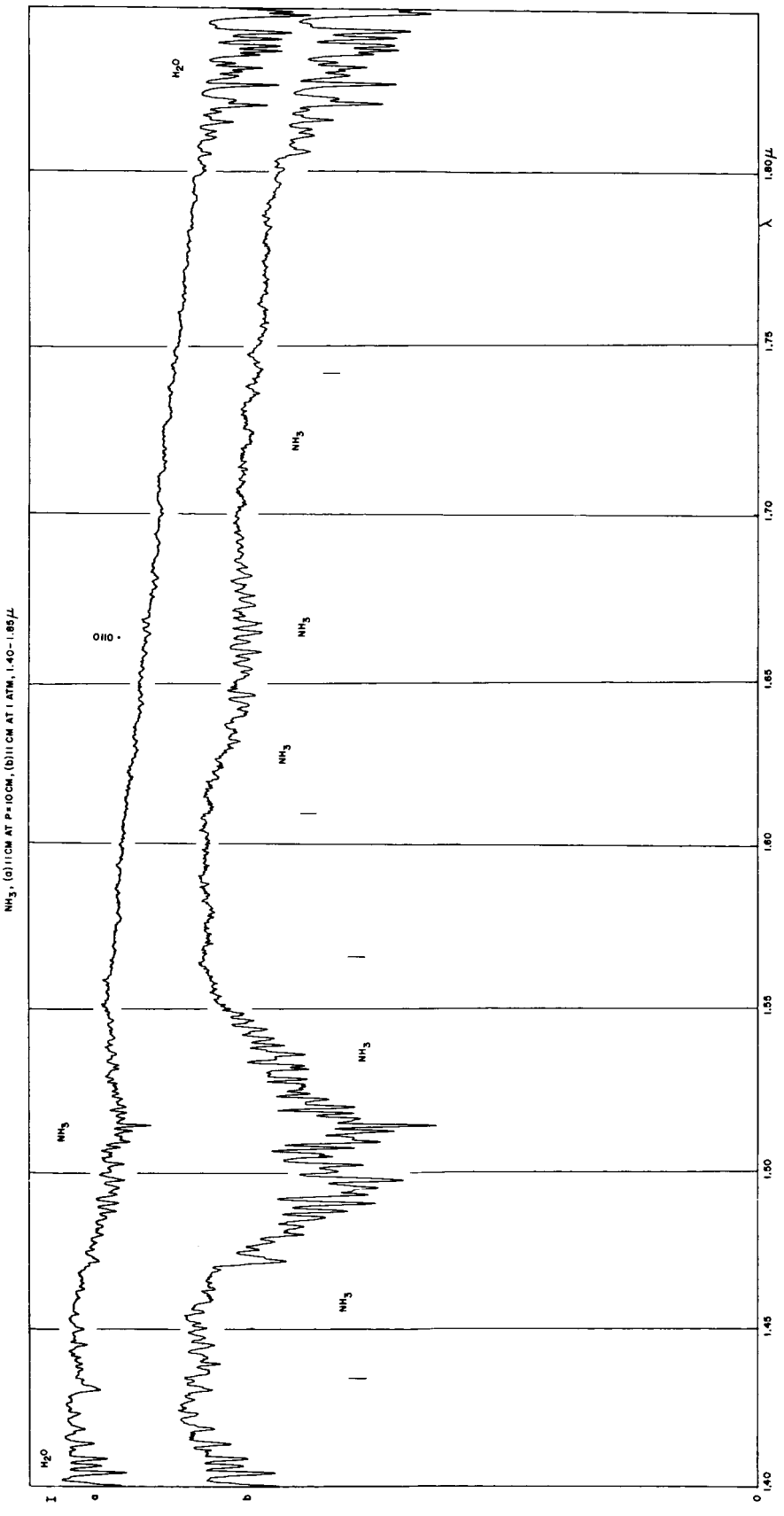

Fig. 10. NH_3, 11 cm at $p = 10$ cm and 1 atm, 1.40–1.85 μ, scan 12.5/1; cf. Fig. 8.

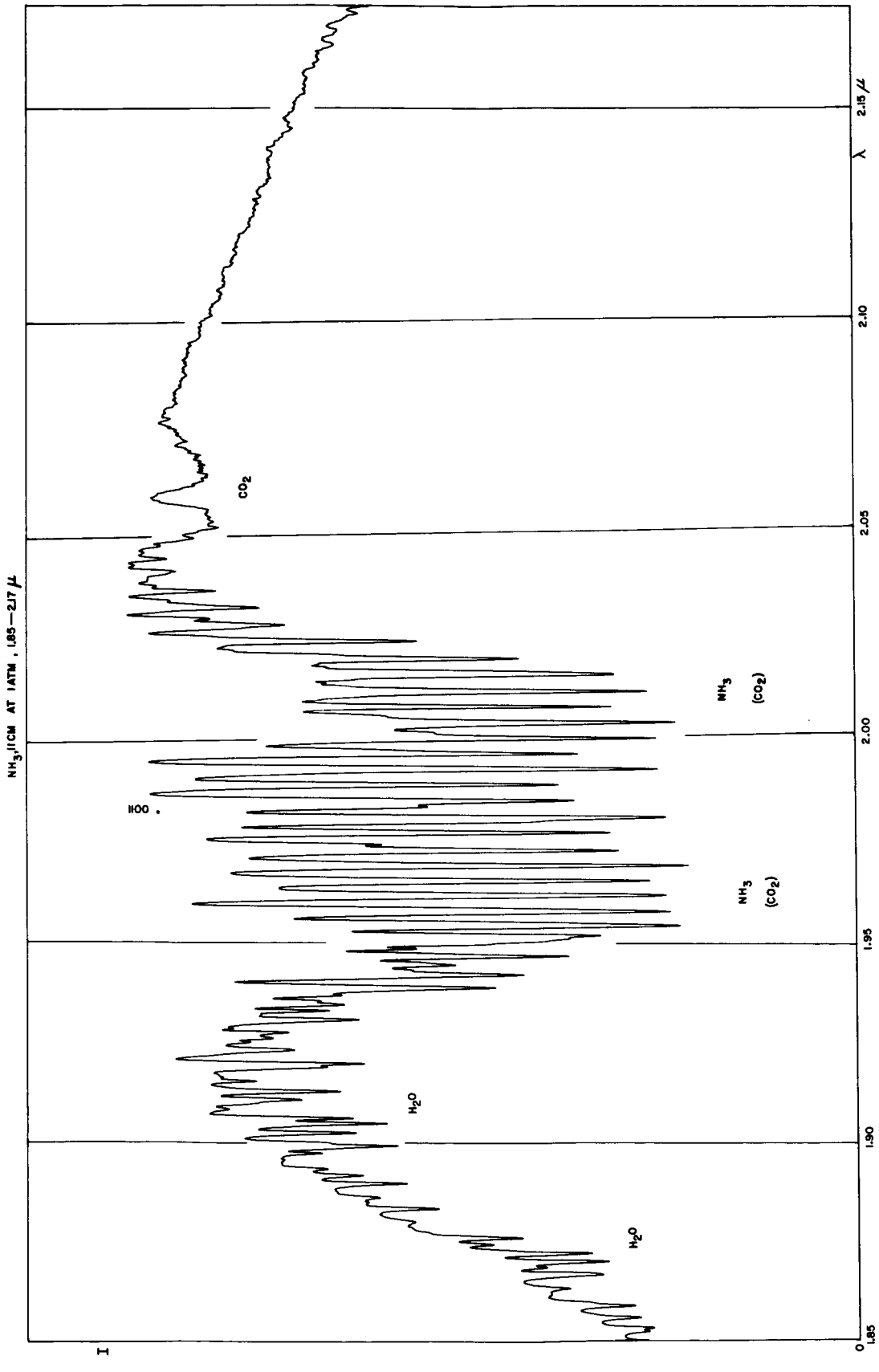

Fig. 11. NH_3, 11 cm at $p = 1$ atm, 1.85–2.17 μ, scan 12.5/1; cf. Figs. 7, 14.

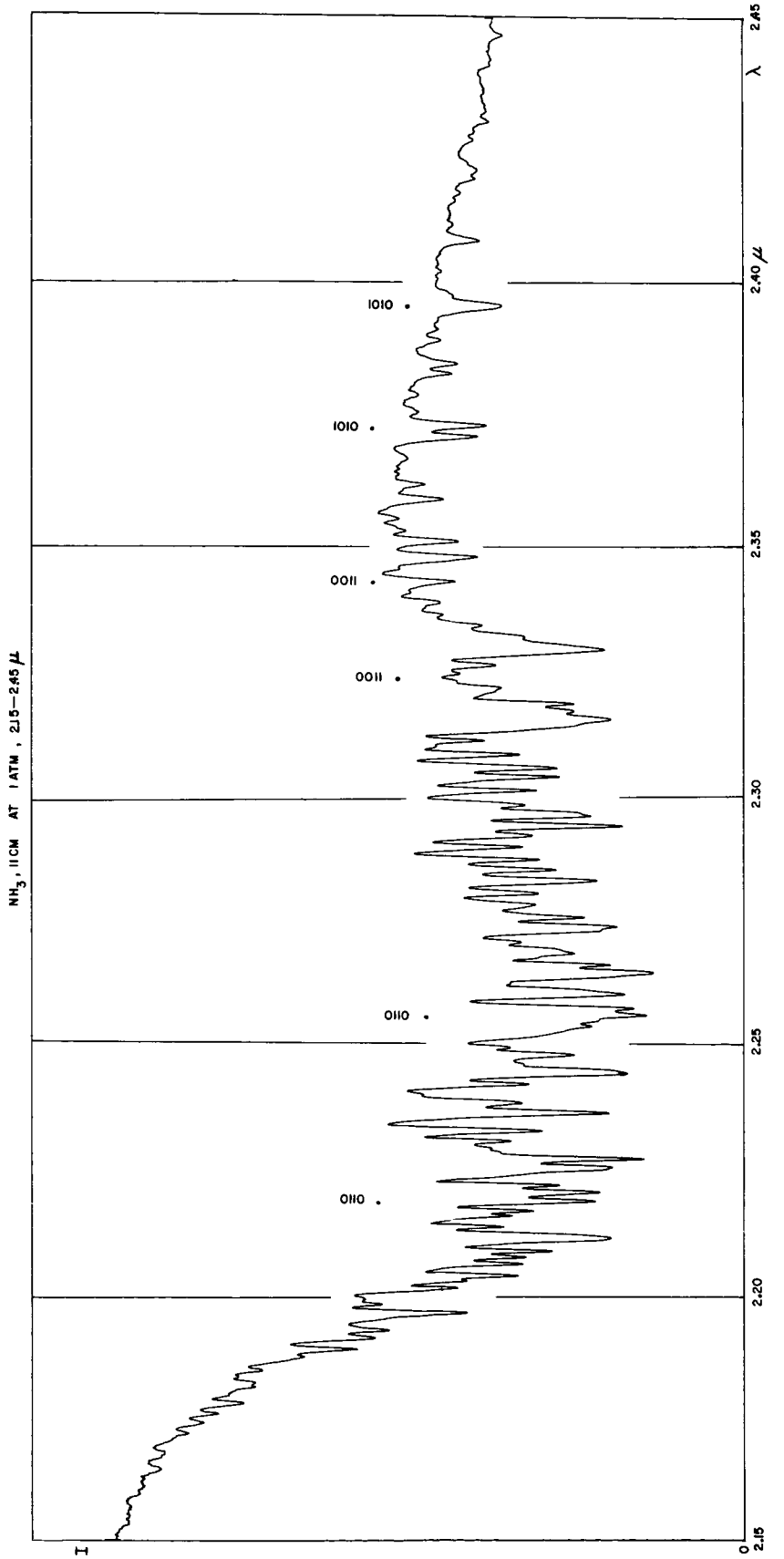

Fig. 12. NH_3, 11 cm at $p = 1$ atm, 2.15–2.45 μ, scan 12.5/1; cf. Figs. 7, 15.

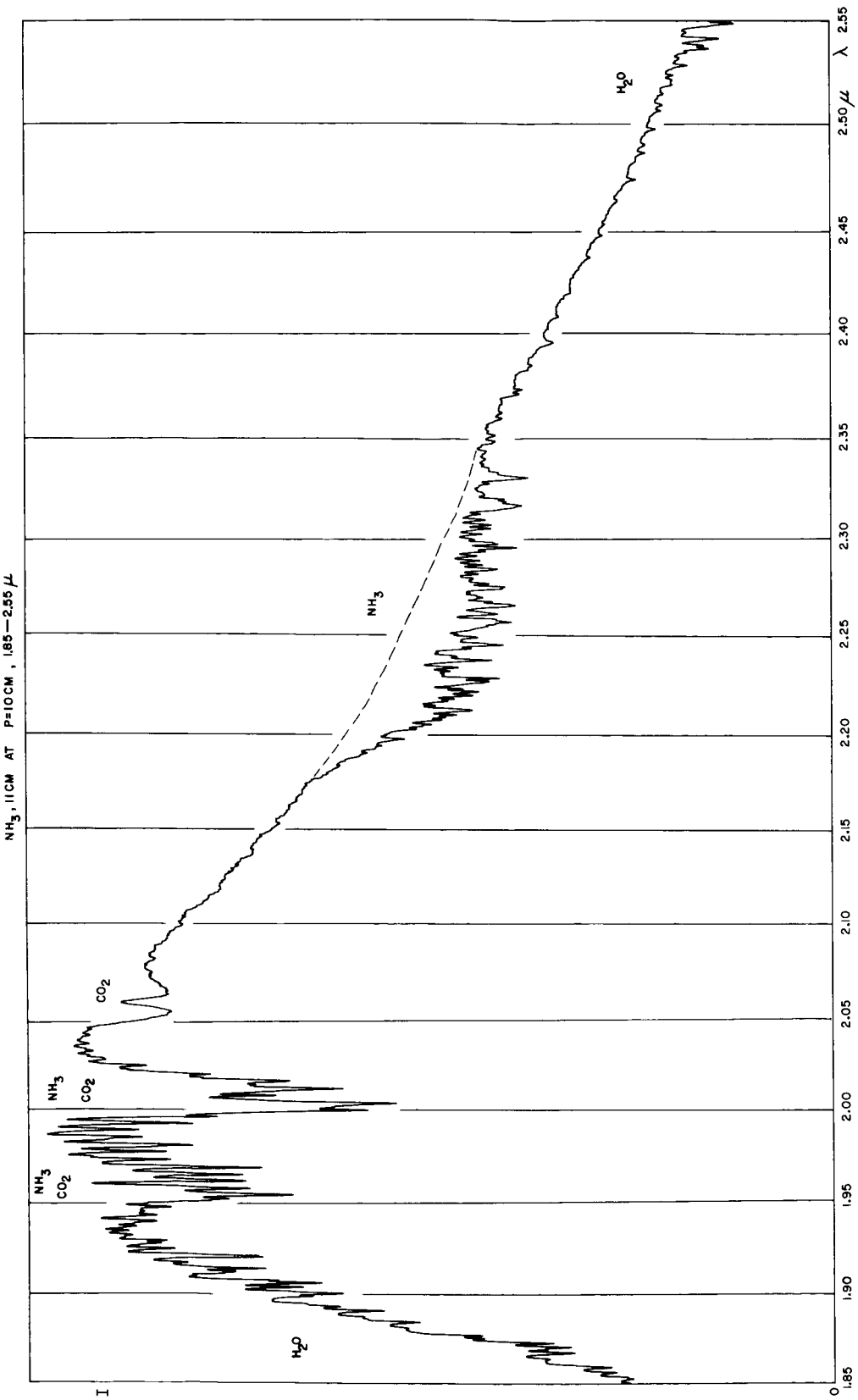

Fig. 13. NH_3, 11 cm at $p = 10$ cm, 1.85–2.55 μ, scan 5/1; cf. Fig. 7.

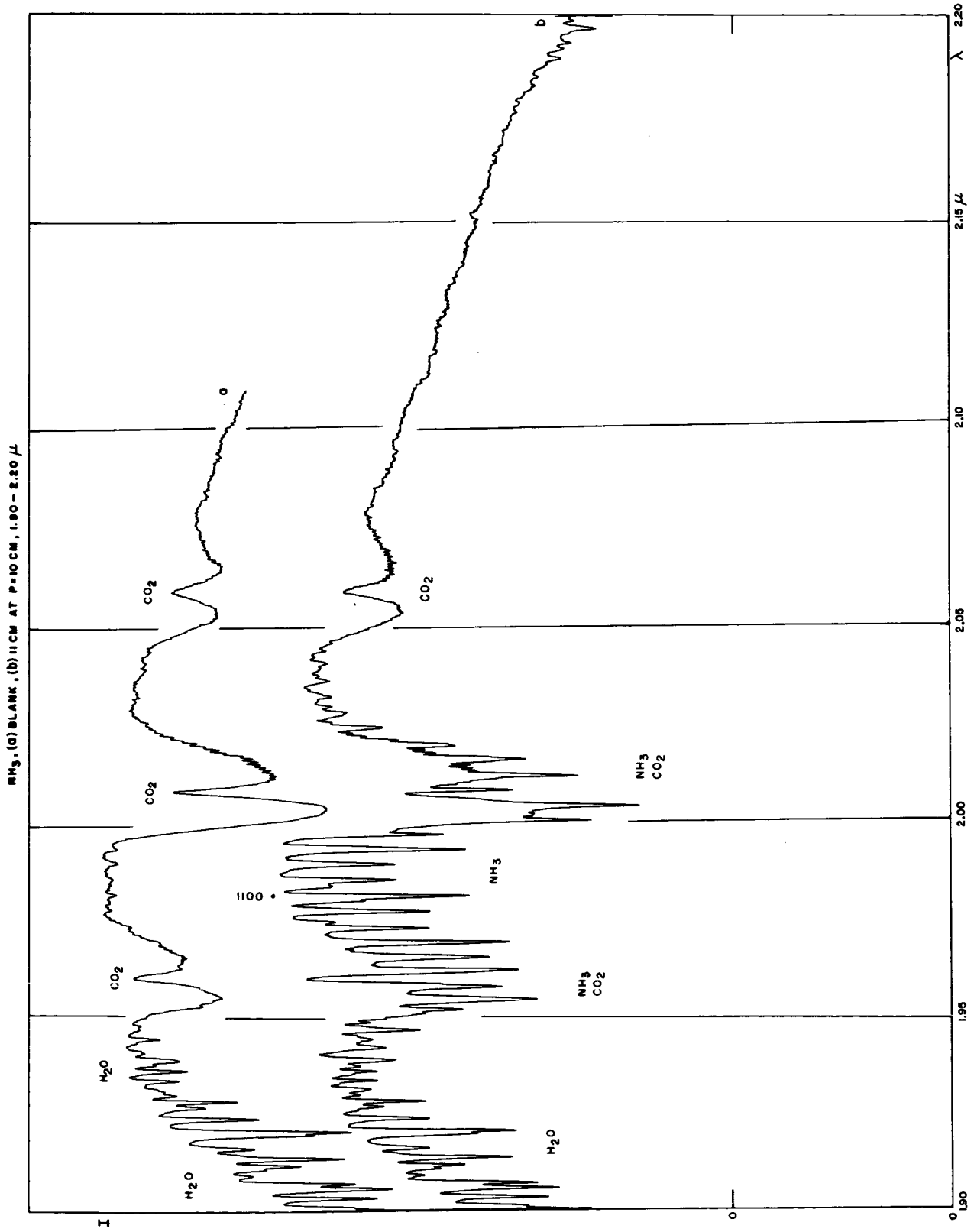

Fig. 14. Blank run and NH_3, 11 cm at $p = 10$ cm, 1.90–2.20 μ, scan 12.5/1; cf. Fig. 11.

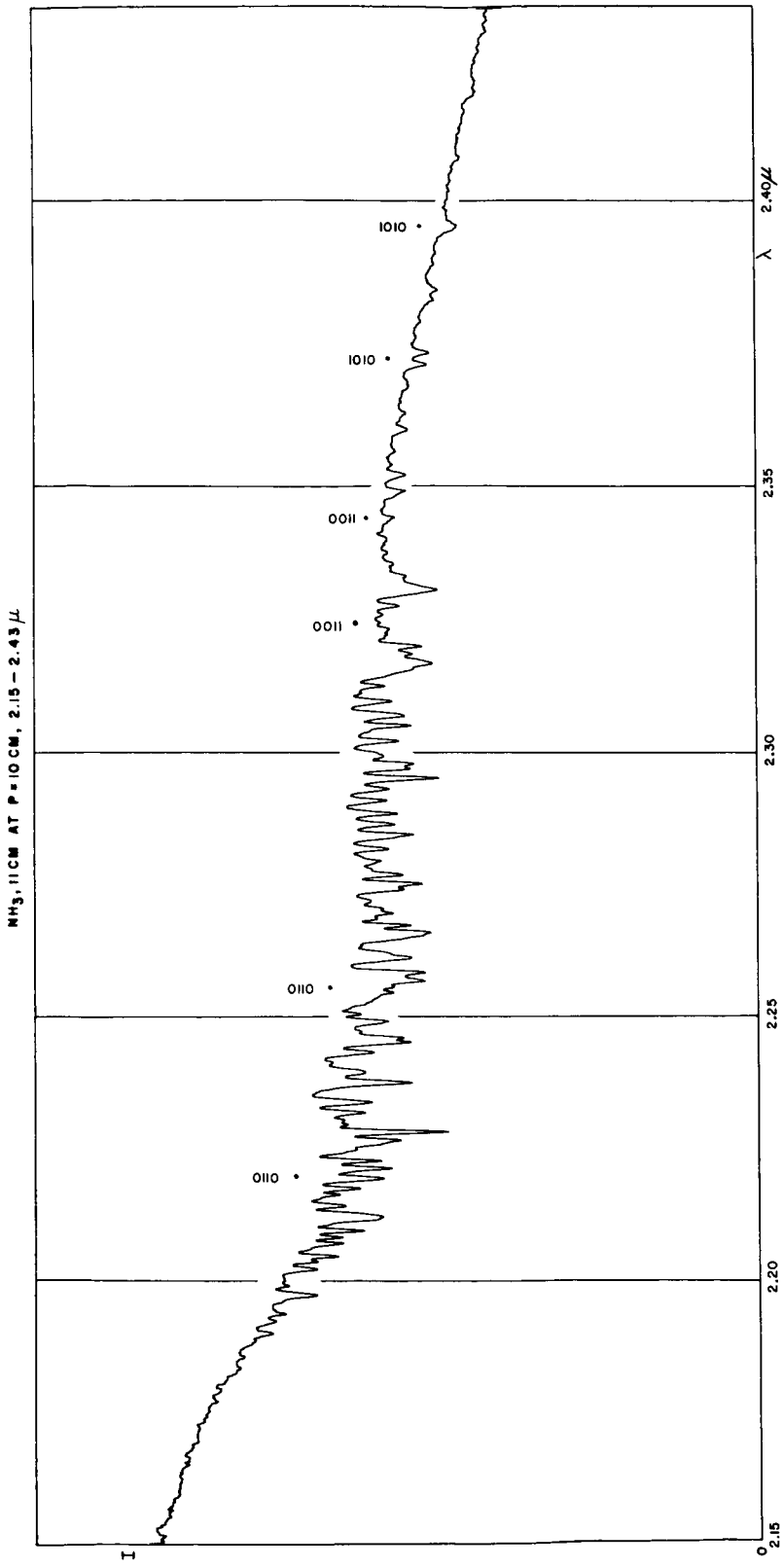

Fig. 15. NH_3, 11 cm at $p = 10$ cm, 2.15–2.43 μ, scan 12.5/1; cf. Figs. 12 and 13.

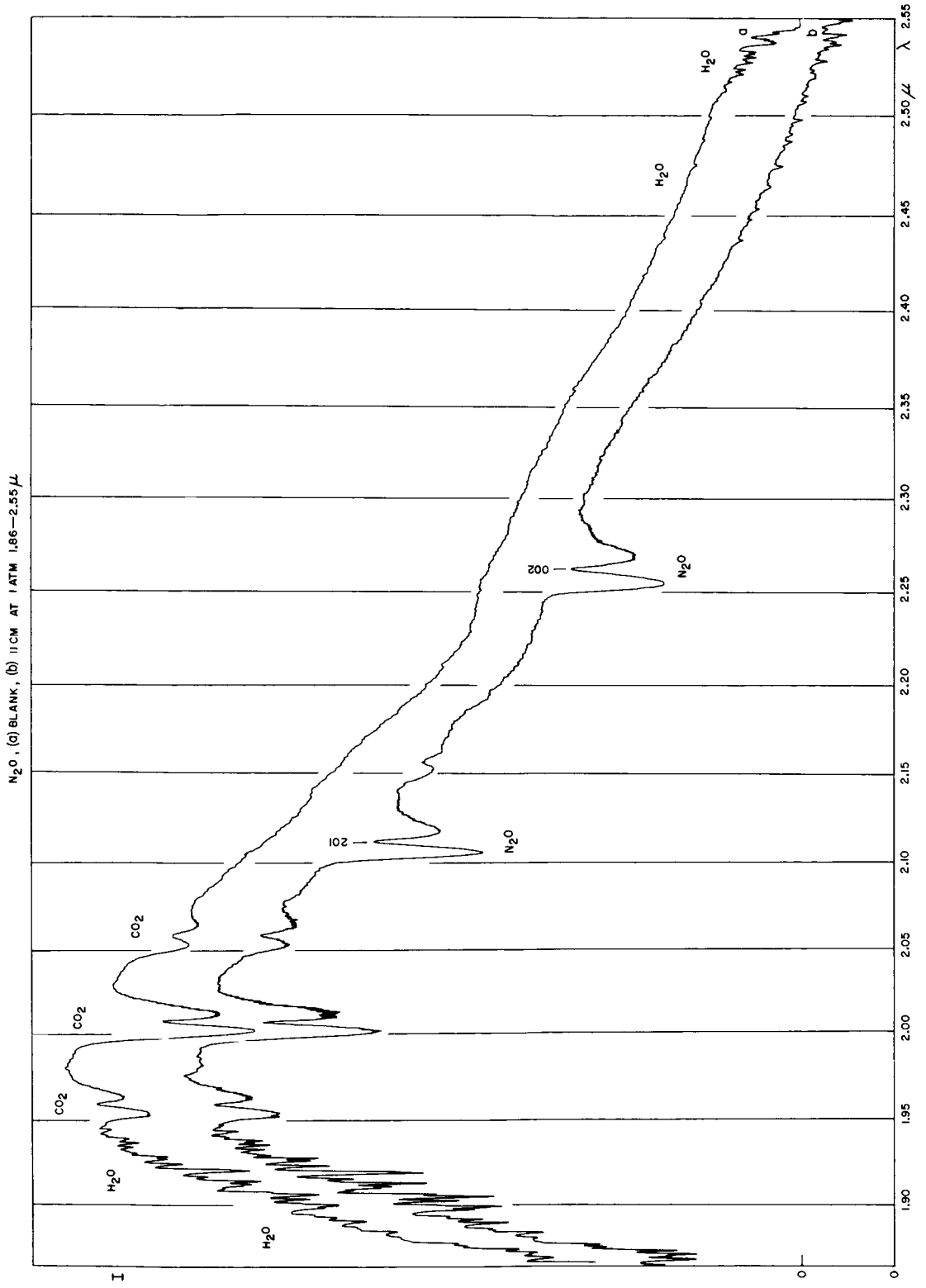

Fig. 16. Blank run and N_2O, 11 cm at $p = 1$ atm, 1.86–2.55 μ, scan 5/1. As Fig. 2.

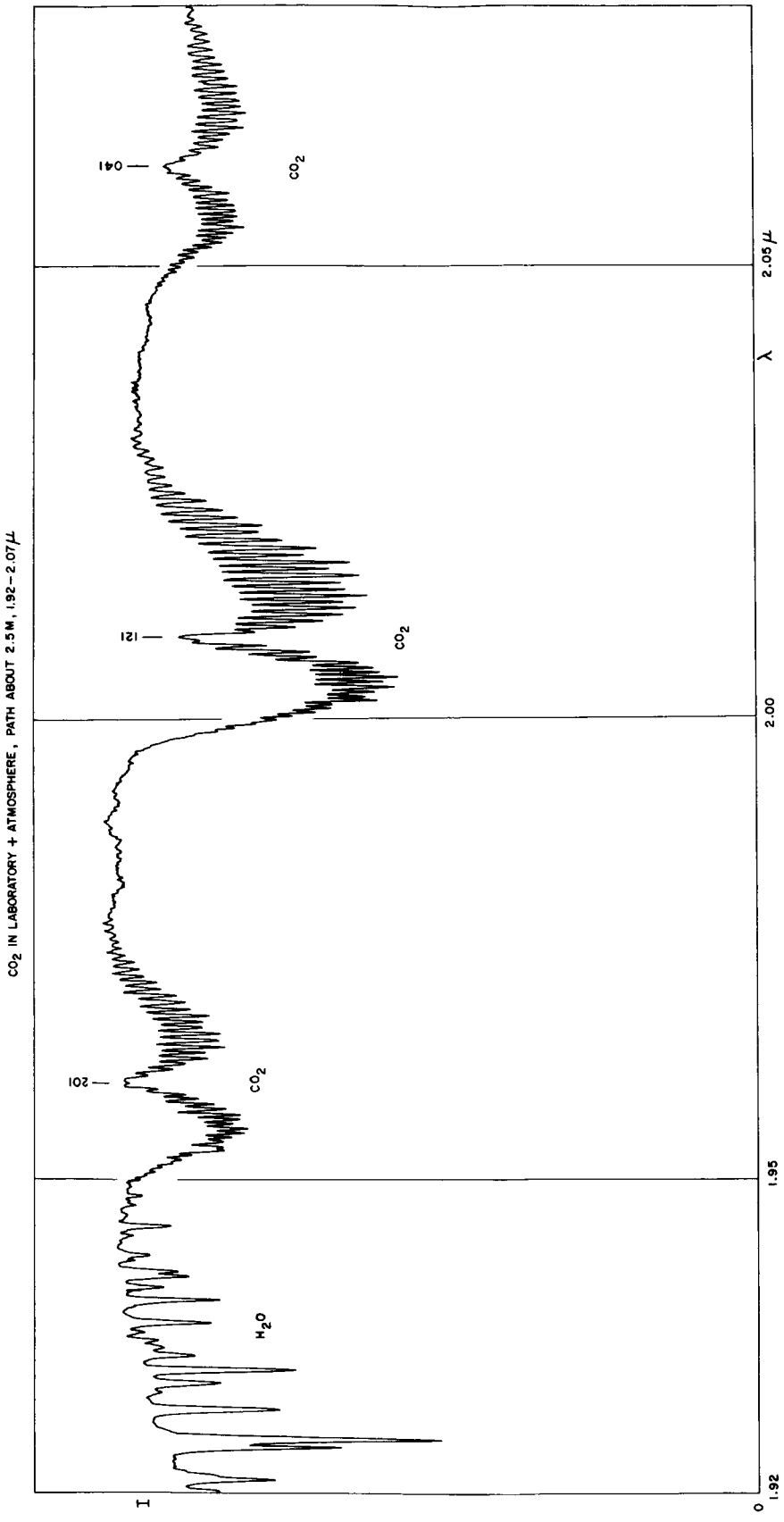

Fig. 17. CO_2 and H_2O, laboratory path of about 2.5 m, scan 25/1; for comparison with N_2O in Fig. 18.

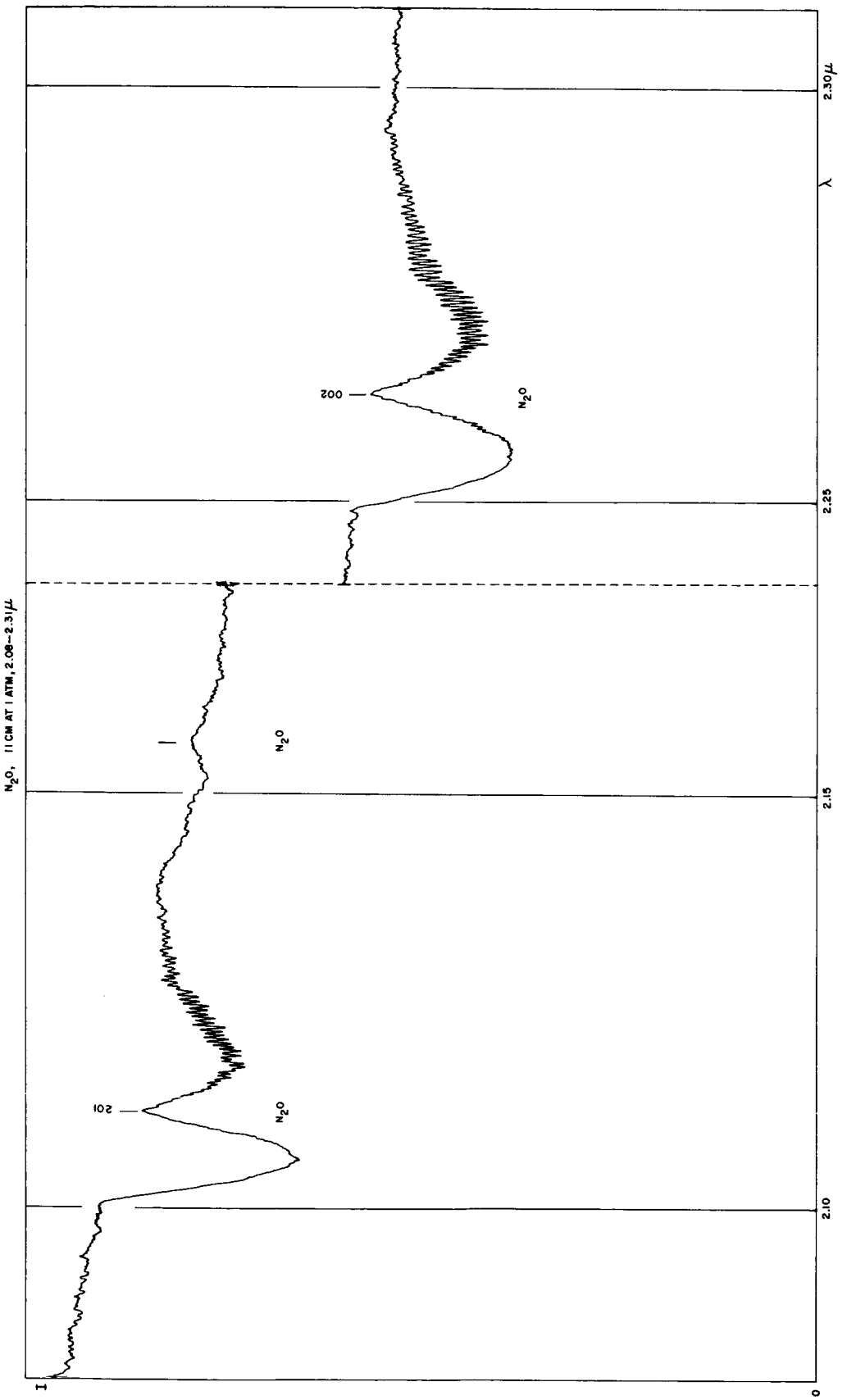

Fig. 18. N_2O, 11 cm at $p = 1$ atm, scan 25/1. Bands (201) and (002) compared to (201), (121), (041) of CO_2 in Fig. 17.

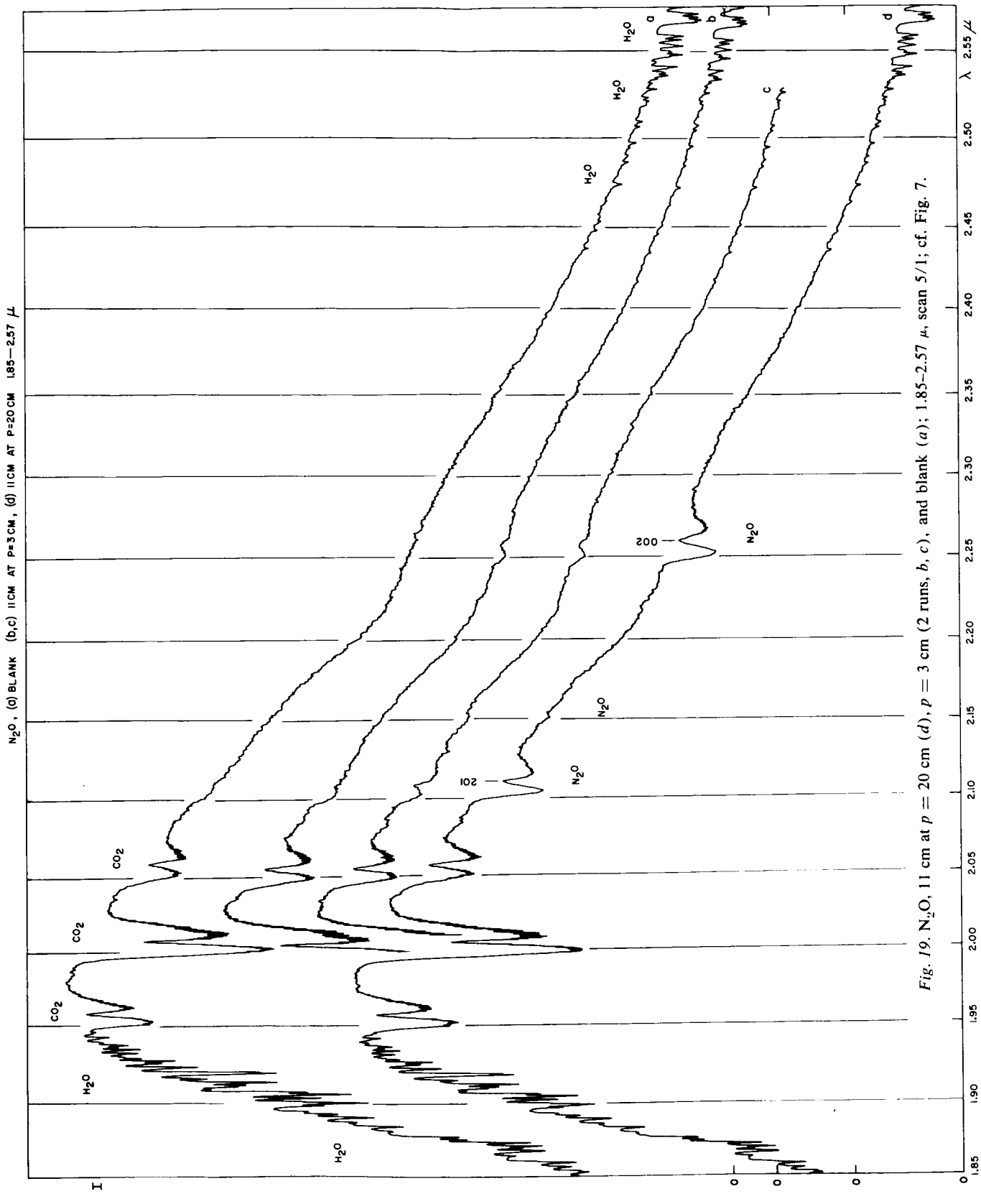

Fig. 19. N_2O, 11 cm at $p = 20$ cm (d), $p = 3$ cm (2 runs, b, c), and blank (a); 1.85–2.57 μ, scan 5/1; cf. Fig. 7.

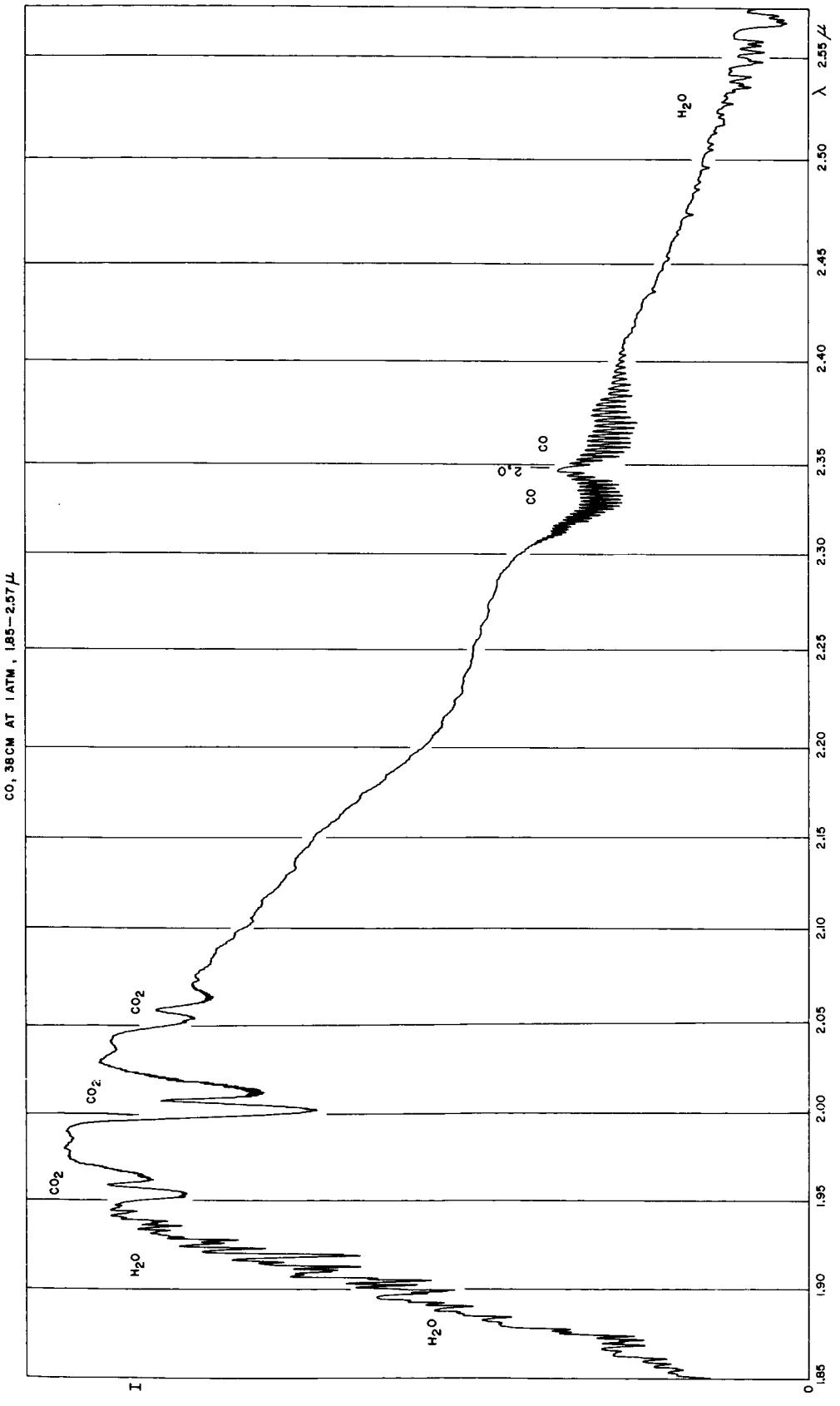

Fig. 20. CO, 38 cm at $p = 1$ atm, 1.85–2.57 μ, scan 5/1. The (2, 0) band is shown in different amounts and with more resolution in Fig. 21.

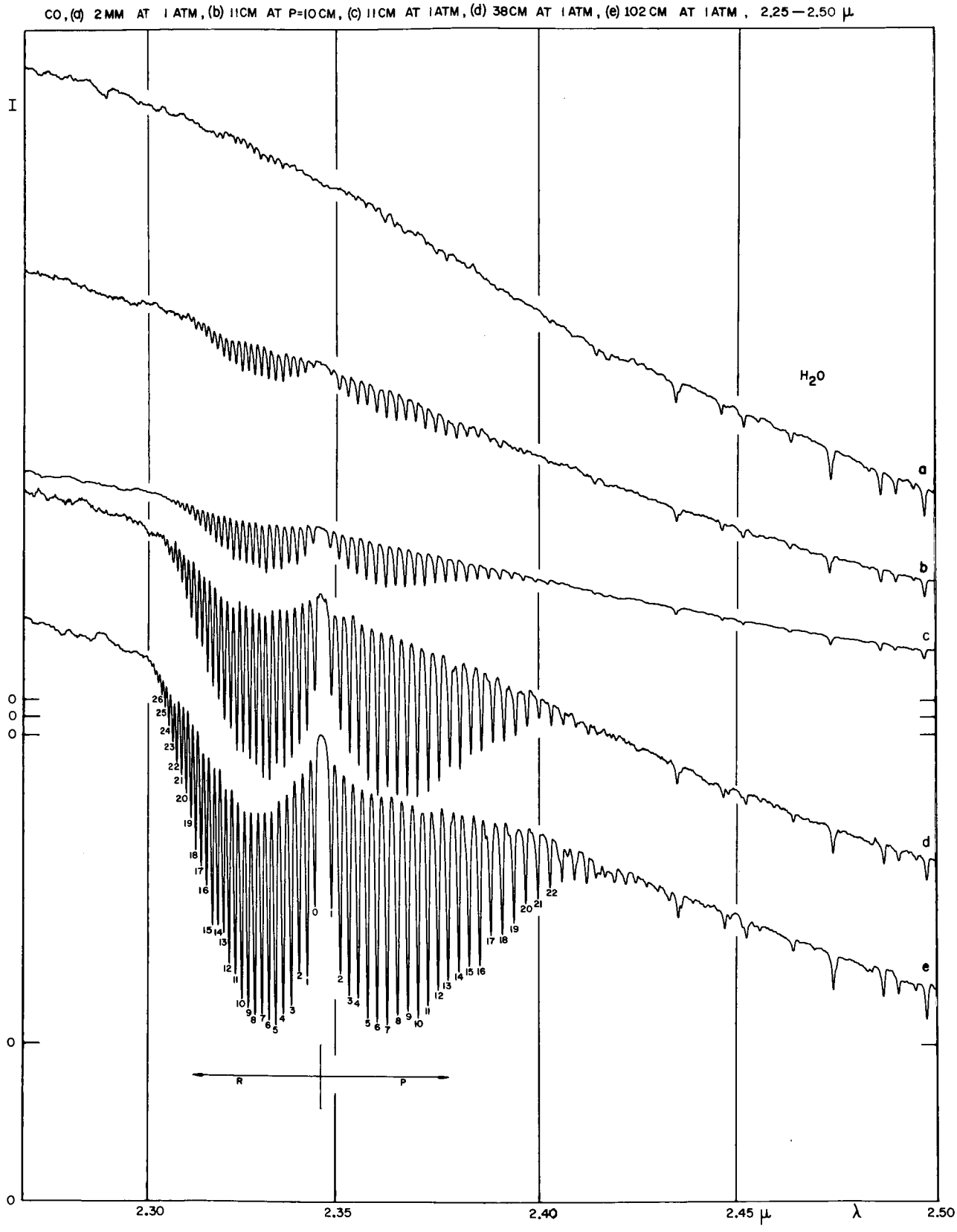

Fig. 21. The (2, 0) band of CO at various pathlengths and pressures, as indicated. Scan 12.5/1.

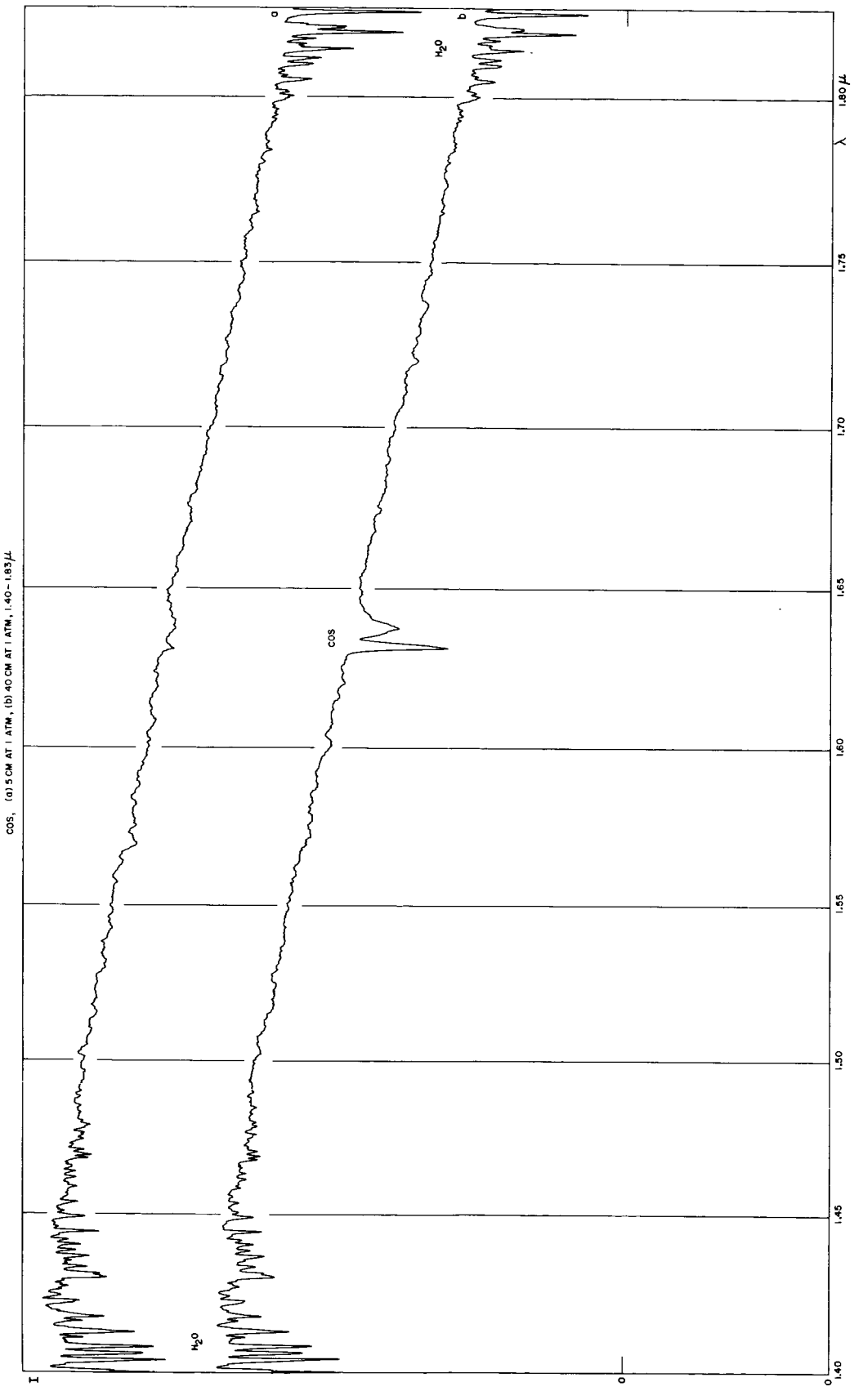

Fig. 22. COS, 5 and 40 cm at $p = 1$ atm, 1.40–1.82 μ, scan 12.5/1.

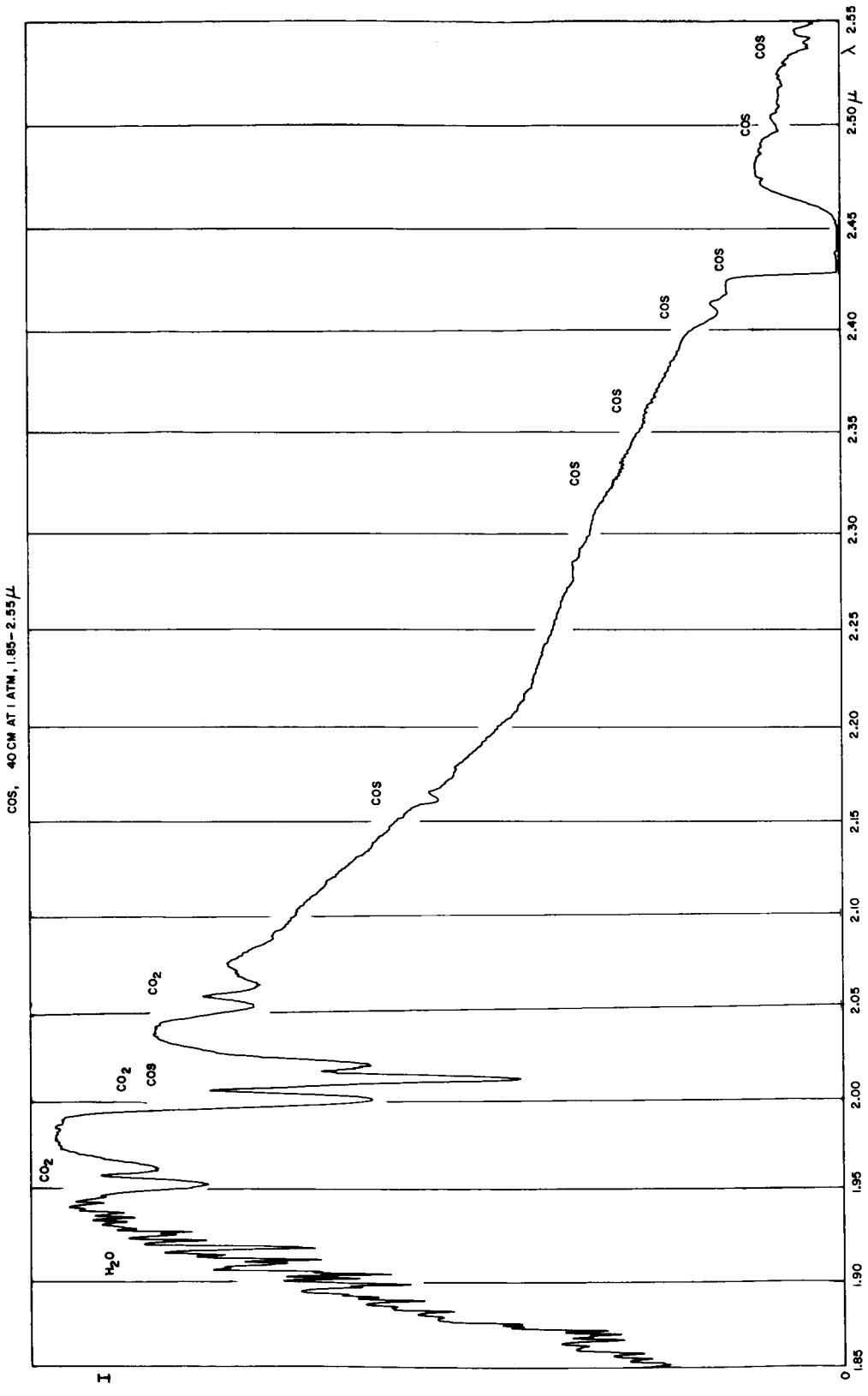

Fig. 23. COS, 40 cm at $p = 1$ atm, 1.85–2.55 μ, scan 5/1.

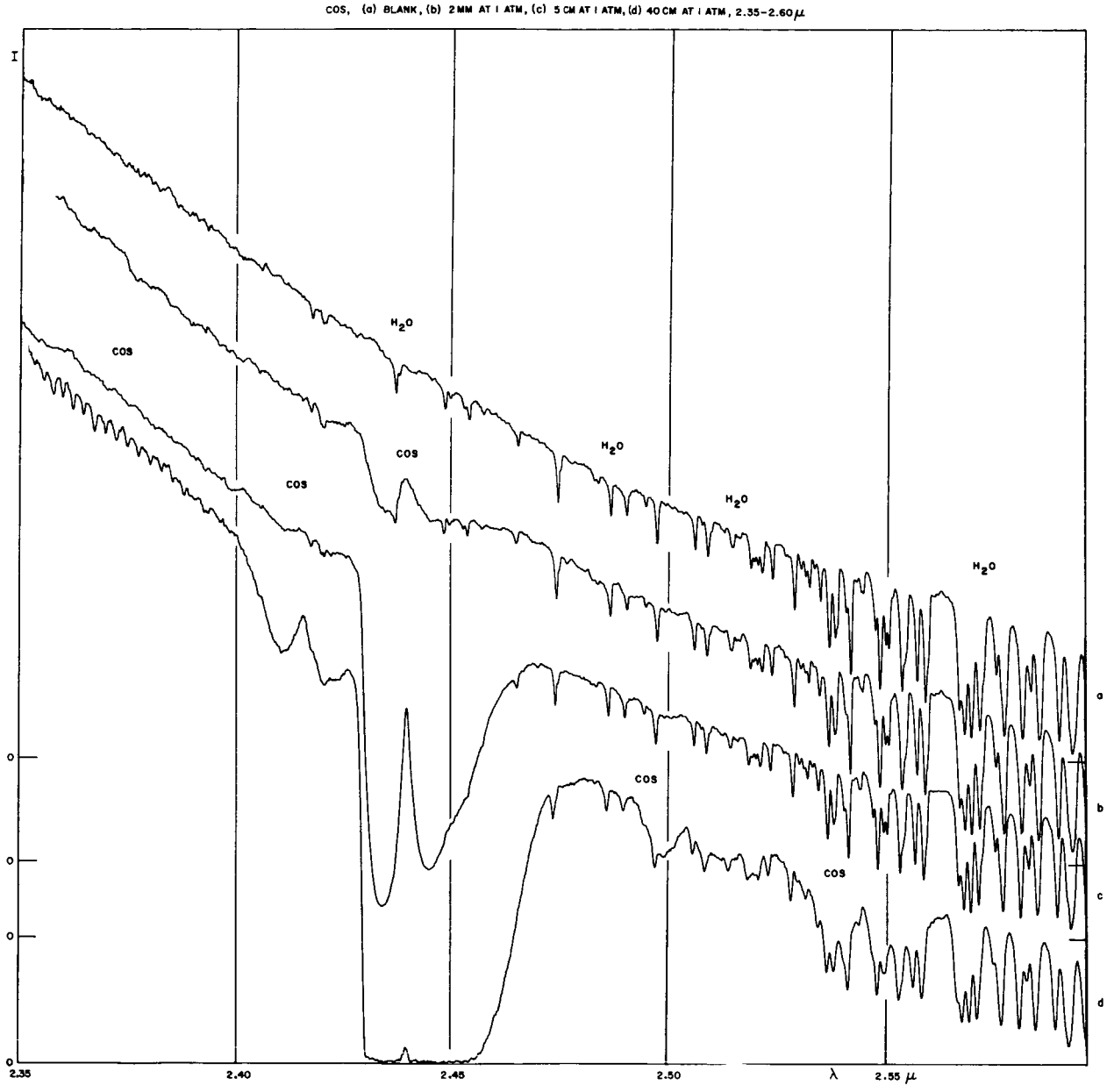

Fig. 24. COS in region 2.35–2.60 μ, with various pathlengths and gas pressures, as indicated. Scan 12.5/1.

No. 35 IMPROVED TEST FOR NO_2 ON MARS

by JAMES V. MARSHALL*

September 10, 1964

ABSTRACT

On the basis of new laboratory tests and microphotometer traces of Mt. Wilson coudé spectra, an upper limit of 8 micron-atm of NO_2 in a vertical column of the Mars atmosphere has been derived. This is two orders of magnitude less than the previous limit and appears to remove empirical arguments for the presence of this gas in the (normal) Martian atmosphere.

Following the announcements by Kiess *et al* (1960, 1963) of their detection of NO_2 in Martian spectra taken in 1956 and 1960–61, several authors have disputed these claims and have set upper limits on the presence of NO_2 in the Mars atmosphere. Sinton and Strong (1960) obtained $<$ 50 mm atm for the planet using the 10 μ region; Sinton (1961a, 1961b) from the 3.34 μ band set the upper limit at 4 mm atm and later 2 mm atm; Kiess *et al* (1963) stated that their plates in the region 0.61–0.63 μ indicate the presence of the gas in the amount of about 1 mm atm; while Spinrad (1963) from the 0.57–0.60 μ region derived 1 mm atm as an upper limit.

Rev. G. T. Sill and the author have photographed the entire NO_2 absorption spectrum between 0.35–1.2 μ with various dispersions averaging about 5Å/mm, with the author continuing the program after Rev. Sill's departure on August 8. The plates discussed here were made more recently. The laboratory runs are absorption spectra with both an incandescent light (0.35–1.2 μ) and the sun as a source (regions of special interest from 0.40–0.46 μ).

The NO_2 absorptions in the blue and violet are the strongest in the accessible photographic region and therefore this paper deals with these bands only. A reproduction of the 4300–4500Å interval, containing the strongest NO_2 bands of the entire region examined, is found in Figure 1; the amount used was about 2 mm atm. A solar spectrum is added for comparison purposes. It is noted that much weaker NO_2 absorptions will be detectable. Reference is made to a low-dispersion absorption spectrum, 4200–4800Å, by Pearse and Gaydon (1950).

The NO_2 band centered on 4482Å occurs in a region of the solar spectrum that is fairly free from prominent Fraunhofer lines. For this reason the interval 4475–4495Å was selected for further analysis. Figure 2 shows two microphotometer traces; *above,* ⅛ mm atm of NO_2, *below,* the solar spectrum recorded through 1 mm atm of NO_2. Figure 3 is similar to Figure 2, *below,* except that the amount of NO_2 is ⅛ mm atm. (The cell used was 2 mm long, the pressure 1/16 atm.) The depression near 4482Å is now considerably reduced, but still visible as indi-

*The laboratory program here described was begun jointly by Mr. Marshall and Rev. Godfrey T. Sill, O. Carm, about July 1, 1964 and continued until Rev. Sill's departure on August 8. Mr. Marshall then continued the program alone, and the results reported here are largely his.

The Editor

cated by the straight envelopes drawn in both figures.

Figures 4 and 5 show microphotometer traces for two of seven Mt. Wilson spectra of Mars, loaned to this Laboratory, courtesy of Dr. Babcock. Their dispersion is 2.84Å/mm, and that of the laboratory comparison spectra 5Å/mm. The microphotometer tracings of comparable scale were made by using different scan rates. The record shown in Figure 5 was of a somewhat lighter exposure than that of Figure 4. Approximate intensity scales were derived from comparisons with the *Photometric Atlas of the Solar Spectrum* (Minnaert *et al*, 1940), making allowance for the moderate difference in spectral resolution. These scales are intended only for purposes of orientation and rough calibration.

Comparison of Figures 4 and 5 with Figure 3 establishes at once the extraordinary sensitivity of an NO_2 test in this spectral region. The upper limit that could be present on Mars at the time of the two 1956 Mt. Wilson plates mentioned is, at most, 1/5 of the amount present in Figure 3, or 25 micron-atmospheres. The upper limit in a vertical column of the Martian atmosphere is therefore $25/\pi = 8$ micron-atmospheres.

In addition, a number of other Mt. Wilson spectra of Mars have been examined visually. Plates Ce 39 (Oct. 16, 1926), Ce 73 (March 24, 1927), Ce 10654a (Aug. 24, 1956), Ce 10657 (Aug. 25, 1956), Ce 10658 (Aug. 26, 1956) were borrowed for study in Tucson, in addition to Ce 10655 and Ce 10662, reproduced in Figures 4 and 5. Several other plates were examined during a visit to the Mt. Wilson Observatory office on August 25, 1964. The plates examined with the microphotometer are considered representative of the available collection. The previous position tests of NO_2 two orders of magnitude greater than the upper limit set here are therefore not supported.

The question as to whether the 4482Å band might be temperature-sensitive and therefore of much-reduced intensity on Mars ($T \simeq 200°K$ vs. 295°K in the laboratory) has been discussed by Dr. Kuiper and Dr. Herzberg. Dr. Herzberg concluded that temperature effects on the 4482 NO_2 band would be small; work on the classification of the photographic spectrum of NO_2 is currently in progress in his laboratory.

Acknowledgments. I am indebted to Dr. G. P. Kuiper for his aid in the preparation of this article, to the Mt. Wilson Observatory for the loan of the Mars spectra, and to the Kitt Peak National Observatory for the use of the microphotometer. I have benefited from inspection of a prepublication copy of a review article by Drs. Carl Sagan, Philip T. Hanst, and Andrew T. Young.

The program of infrared planetary spectroscopy is supported by the National Aeronautics and Space Administration through Grant No. NsG 161-61.

Note added in proof. After the above was written the author had the opportunity to visit Dr. Kiess at his laboratory and inspect his original spectra. The author was unable to detect visually the 4480Å band of NO_2 on the Kiess spectra. The author is indebted to Dr. Kiess for his courteous reception and for the opportunity to review his material.

REFERENCES

Kiess, C. C., Karrer, S., and Kiess, H. K. 1960, "A New Interpretation of Martian Phenomena," *Publ. A.S.P. 72,* 256.

Kiess, C. C., Karrer, S., and Kiess, H. K. 1963, "Oxides of Nitrogen in the Martian Atmosphere," *Publ. A.S.P. 75,* 50.

Minnaert, M., Mulders, G. F. W., and Houtgast, J. 1940, *Photometric Atlas of the Solar Spectrum* (Amsterdam).

Pearse, R. W. B. and Gaydon, A. G. 1950, *The Identification of Molecular Spectra* (London: Chapman and Hall Ltd.), plate 8.

Sinton, W. M. 1961a, *Science 132,* 529, letter.

Sinton, W. M. 1961b, "An Upper Limit to the Concentration of NO_2 and N_2O_4 in the Martian Atmosphere," *Publ. A.S.P. 73,* 125.

Sinton, W. M. and Strong, J. 1960, "Radiometric Observations of Mars," *Ap. J. 131,* 459.

Spinrad, H. 1963, "The NO_2 Content of the Martian Atmosphere," *Publ. A.S.P. 75,* 190.

Fig. 1. The Spectrum of NO_2, 4300–4500Å, with solar comparison.

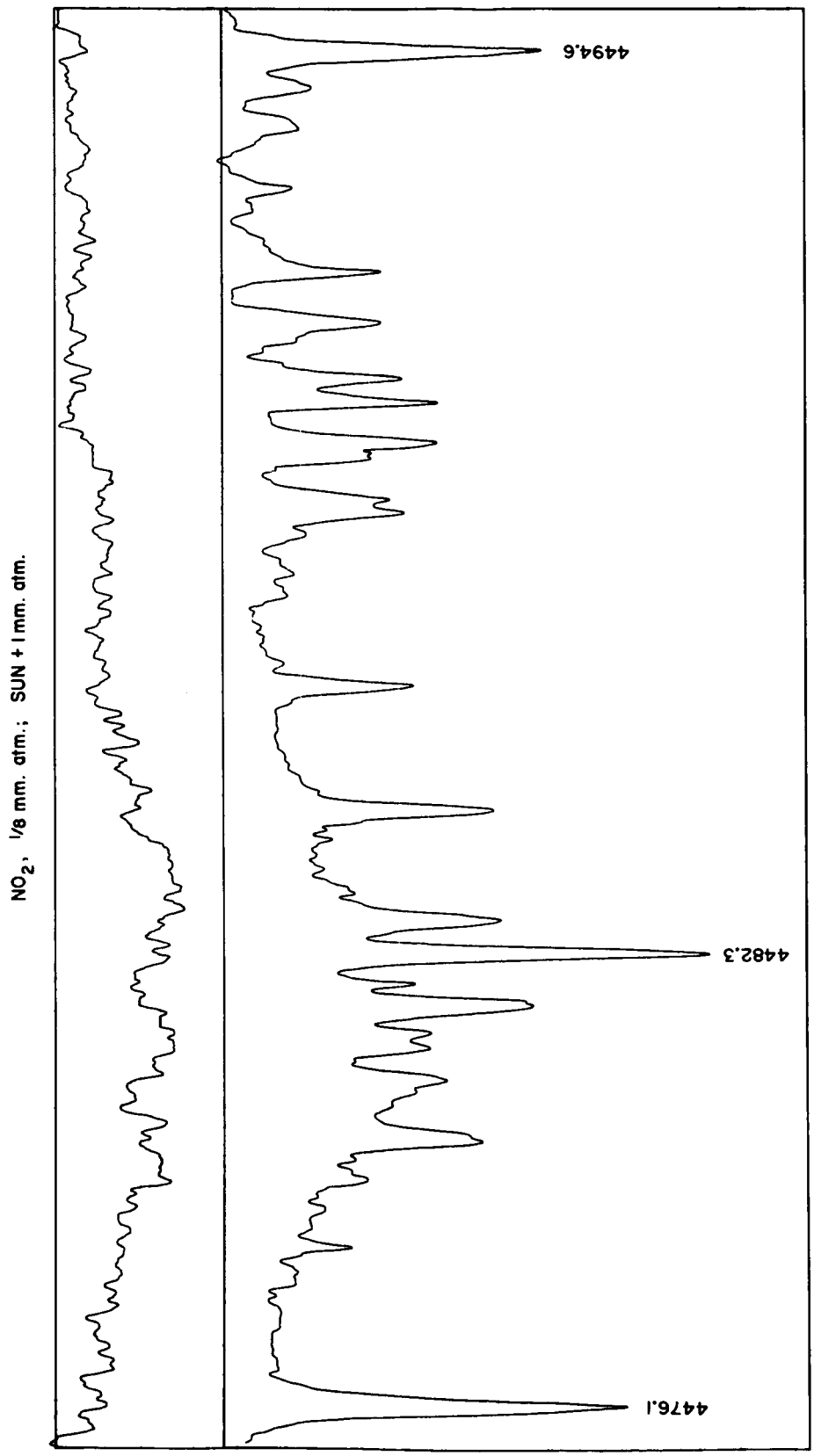

Fig. 2. Microphotometer tracings of spectra, 4475–4495Å. *Above:* NO_2 1/8 mm atm; *below*, Sun + 1 mm atm of NO_2. Undisturbed continuum indicated by straight line on top.

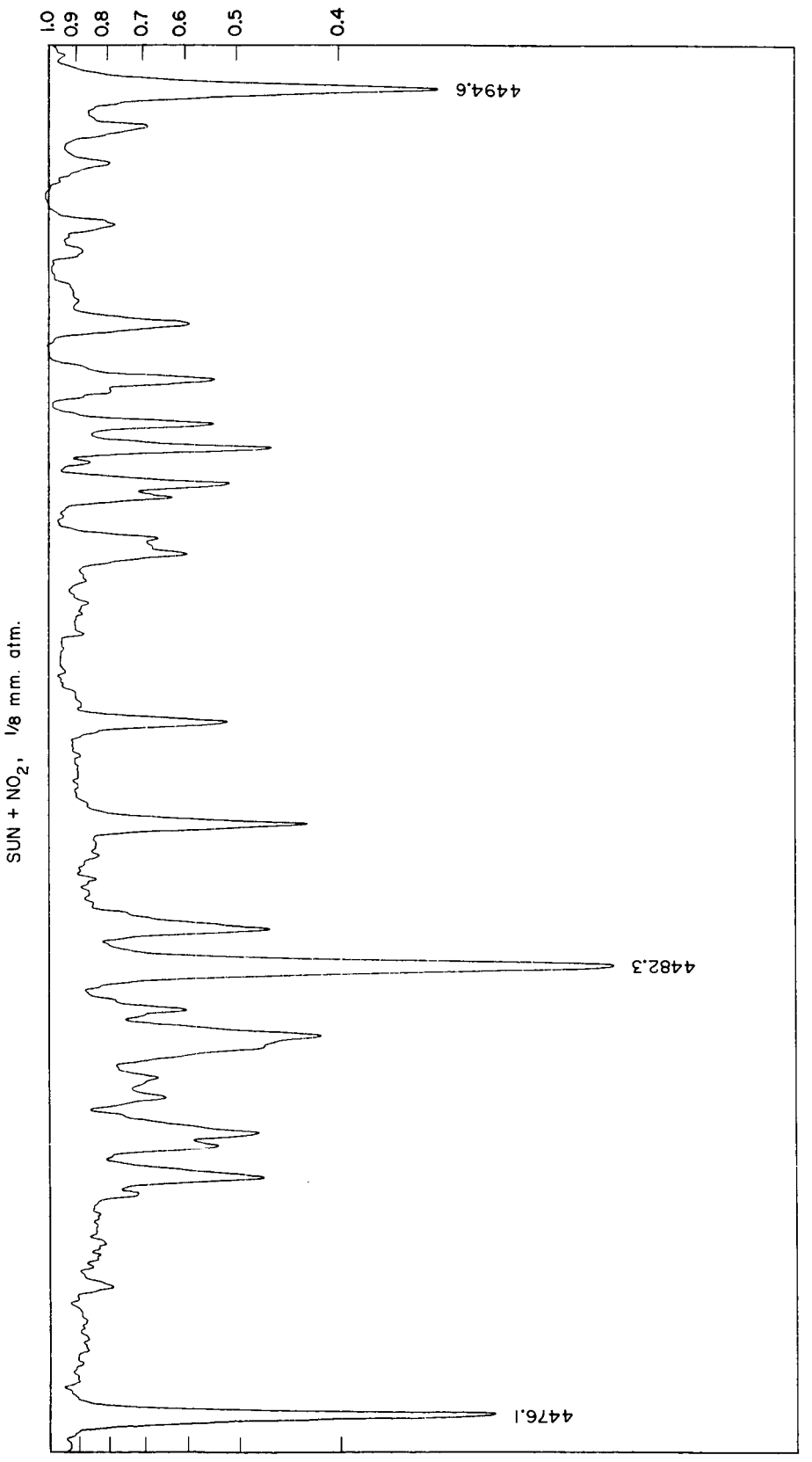

Fig. 3. Microphotometer tracing of spectrum, 4475–4495Å of Sun + 1/8 mm atm of NO_2, cf. Fig. 2.

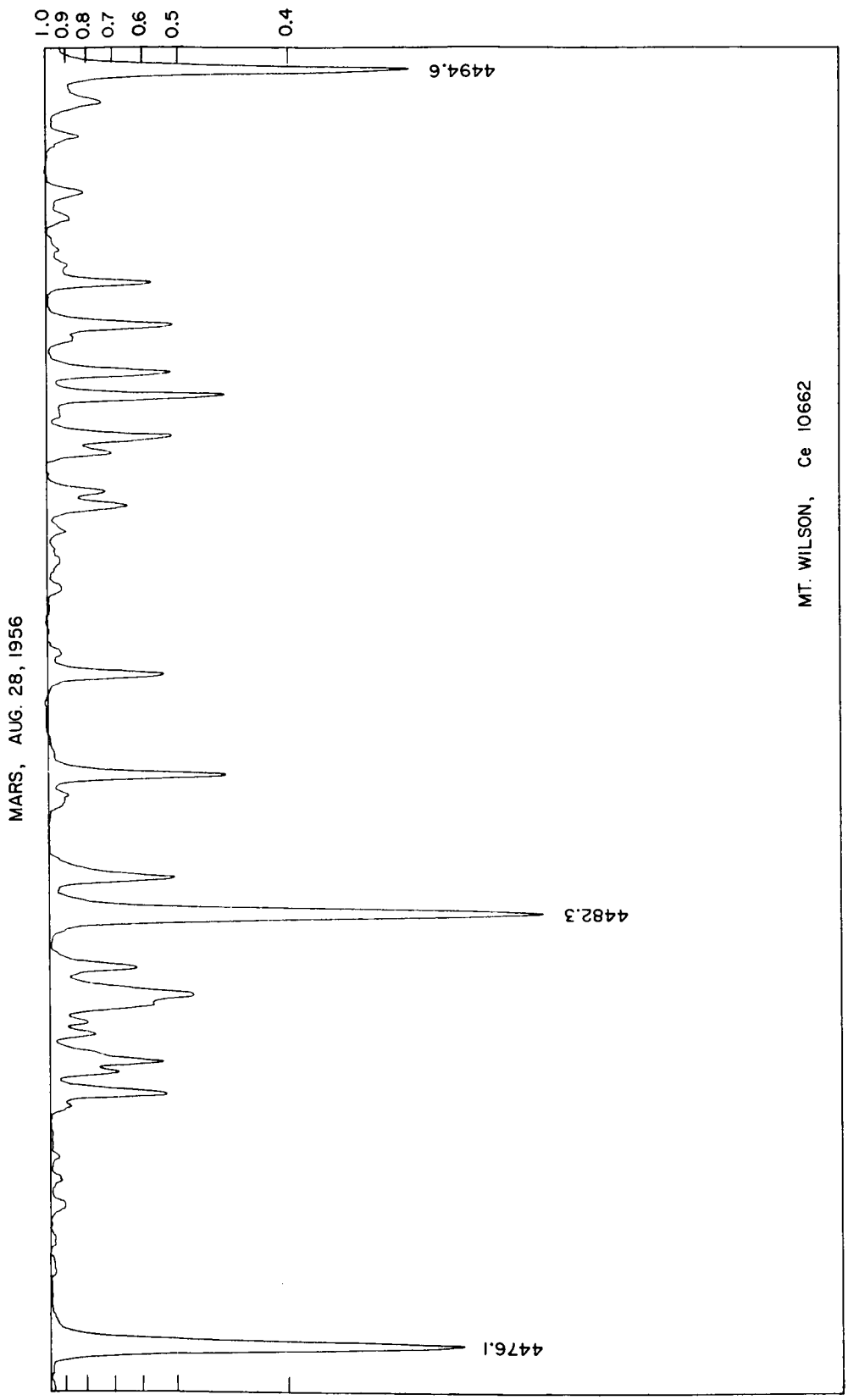

Fig. 4. Microphotometer tracing of Mars spectrum, August 28, 1956 (Mt. Wilson plate Ce 10662) 4475–4495Å. Undisturbed continuum indicated by straight line on top. Approximate intensity scale at right.

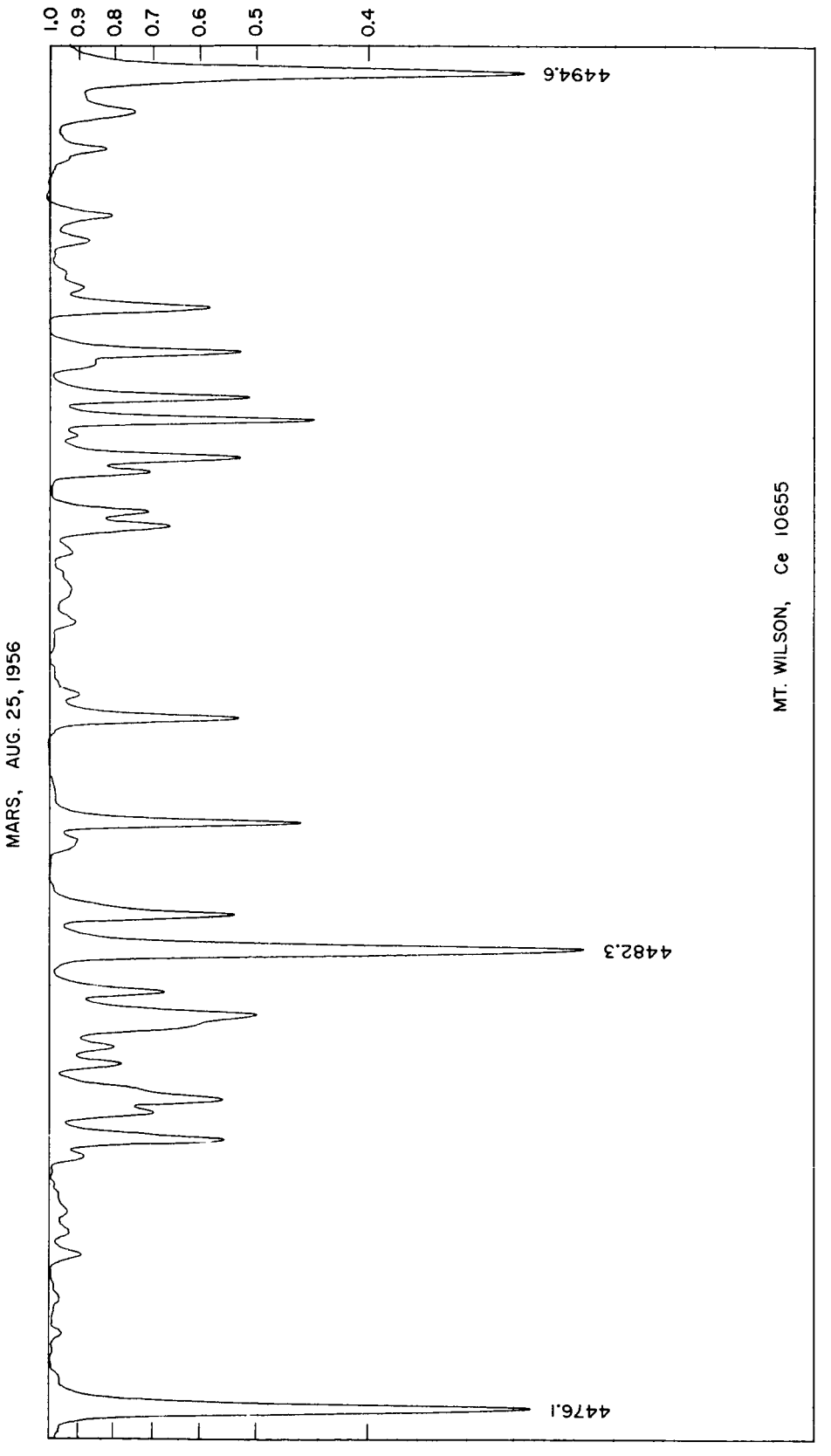

Fig. 5. Microphotometer tracing of Mars spectrum, August 25, 1956 (Mt. Wilson plate Ce 10655).